NTNU – Trondheim
Norwegian University of
Science and Technology

Dynamic Response of Floating Wind Turbines

Sjur Neuenkirchen Godø

Marine Technology
Submission date: June 2013
Supervisor: Bernt Johan Leira, IMT
Co-supervisor: Tor David Hanson, Statoil

Norwegian University of Science and Technology
Department of Marine Technology

Master's Thesis

for

Stud. Techn. Sjur Neuenkirchen Godø

Spring 2013

Dynamic Response of Floating Wind Turbines

Dynamisk respons av flytende vindturbiner

Offshore wind energy is at the threshold of large-scale application throughout Europe, followed by the US and Canada. After a series of demonstration projects up to 40 MW installed capacity, mainly at benign sites, the first large offshore wind farm of 160 MW was built at the North Sea site "Horns Rev" off the west coast of Denmark.

Right from the beginning of the exploration of offshore wind energy, the importance of dynamic behavior for the design was well recognized. In contrast with common practice in the offshore industry, frequency domain analysis of dynamic response is seldom used for wind turbines, even for the fatigue load cases. Due to the highly non-linear behavior of aerodynamic loading of the rotor, time domain simulations are required for accurate assessment of both fatigue and ultimate limit states. The consequential high computational burden necessitates simple structural models that capture the most important characteristics of dynamic behavior.

Floating wind turbines are increasingly of interest in relation to deep-water sites. These structures represent significant challenges with respect to adequate analysis tools, design procedures and design codes. Assessment of inherent model uncertainties associated with computation of load and response will be of particular importance. Within such a framework, results from model tests and full-scale measurements become crucial in order to compare observed and computed response levels.

The scope of the present study is accordingly to compare results from numerical response analysis with those from full-scale measurements.

The following subjects are to be addressed as part of this work:

1. Description of different types of offshore wind turbines with focus on floating concepts.

2. An overview of different types of load models and methods of response analysis for offshore wind turbines also considering existing (and possibly future) design guidelines and rules.

3. A description of the key structural properties of Hywind Demo is to be given. Including a discussion of the control system and a summary of the full-scale measurements associated with the Hywind-concept.

4. Establishment of an environmental model for the wave and wind environment at the Hywind Demo location.

5. Performing a long term analysis of the mooring line tension on Hywind Demo, considering the environmental parameters mean wind, significant wave height and peak period.

6. Investigating the application of the contour line method as a simplified method to estimate design loads on Hywind Demo.

The work scope may prove to be larger than initially anticipated. Subject to approval from the supervisor, topics may be deleted from the list above or reduced in extent.

In the thesis the candidate shall present his personal contribution to the resolution of problems within the scope of the thesis work.

Theories and conclusions should be based on mathematical derivations and/or logic reasoning identifying the various steps in the deduction.

The candidate should utilise the existing possibilities for obtaining relevant literature.

The thesis should be organised in a rational manner to give a clear exposition of results, assessments, and conclusions. The text should be brief and to the point, with a clear language. Telegraphic language should be avoided.

The thesis shall contain the following elements: A text defining the scope, preface, list of contents, summary, main body of thesis, conclusions with recommendations for further work, list of symbols and acronyms, references and (optional) appendices. All figures, tables and equations shall be numbered.

The supervisor may require that the candidate, in an early stage of the work, presents a written plan for the completion of the work. The plan should include a budget for the use of computer and laboratory resources which will be charged to the department. Overruns shall be reported to the supervisor.

The original contribution of the candidate and material taken from other sources shall be clearly defined. Work from other sources shall be properly referenced using an acknowledged referencing system.

The thesis shall be submitted in 3 copies:

- Signed by the candidate
- The text defining the scope included
- In bound volume(s)
- Drawings and/or computer prints which cannot be bound should be organised in a separate folder.

Supervisor: Professor Bernt J. Leira

Deadline: June 10th 2013

Trondheim, January 15th, 2013

Bernt J. Leira

Abstract

Hywind Demo is a floating wind turbine developed by Statoil ASA. In this thesis the extreme values of tension in the mooring lines on Hywind Demo are investigated. The aim of the study is to evaluate the application of the environmental contour line method on the wind turbine. The environmental contour line method will be compared to a full long term analysis of the extreme values of tension. It is expected that a full long term analysis will give good estimates of the design loads and can be used to calibrate the contour line method. Three parameters will be included in the analyses. They are significant wave height, peak period and one-hour mean wind velocity.

Since the long term analysis is particularly time consuming for complex non-linear systems, it will be beneficial if good estimates of the design loads can be found with the environmental contour line method. Both methods require a rather refined formulation of the environment in case of a joint probability model. This has been solved by adapting an existing environmental model so that it fits measurements obtained at the Hywind Demo location.

In total are 2580, three-hour time-domain simulations executed as part of the long term analysis. From each time-domain simulation, extreme values of the response are collected. Response surfaces are so fitted for the extreme values and the Gumbel coefficients. Based on the response surfaces the design loads can be calculated in two ways, with a long term formulation and by the inverse first order reliability method.

The established environmental model is used to form contour surfaces corresponding to given return periods. By evaluation of the extreme values on the contour surface, a design point can be defined for each case. The short term variation of the response is examined in detail at the design point and a design point distribution can be obtained. Then the percentile level in the design point distribution, corresponding to the design load, can be identified.

It is found that the long term formulation and the first order reliability method give agreeing results. In addition, short term variation seems to be small for the tension extremes in the mooring lines. This implies that the design load could be properly estimated by the median value in the short term extreme distribution at the design point. On the other hand, by inspecting the mooring line tension's dependence on the wind parameter it is found that the mooring line tension is not monotonically increasing. Consequently, important principles of the contour line method are violated. This violation is blamed on the active control system regulating the rotor speed of the turbine. This leads to the conclusion that the contour line method is unsuitable for application on Hywind Demo.

Sammendrag

Hywind Demo er en flytende vindturbin utviklet av Statoil ASA. I denne masteroppgaven vil ekstremverdiene av strekk i ankerlinene på Hywind Demo bli undersøkt. Målet med oppgaven er å undersøke muligheten for bruk av konturlinjemetoden til dette formålet. Konturlinjemetoden vil bli sammenlignet med en langtidsanalyse av de ekstreme strekkverdiene. Det er forventet at langtidsanalysen vil gi gode estimater av designlastene og kan bli brukt til å kalibrere konturlinjemetoden. Tre parametere vil bli inkludert i analysene. De er, signifikant bølgehøyde, topp periode og en times gjennomsnittsvind.

Langtidsanalysen kan være svært tidkrevende for komplekse, ikke-lineær, systemer. Det vil derfor være gunstig hvis gode estimater av designlasten kan bli oppnådd ved bruk av konturlinjemetoden. Begge framgangsmåtene krever en nøyaktig formulering av miljøparameterne i form av en kombinert sannsynlighetsfordeling. Dette har blitt løst ved å tilpasse en eksisterende miljømodell til målinger fra Hywind Demo området.

Totalt har 2580 tre-timers simuleringer blitt utført i langtidsanalysen. Fra hver tidssimulering blir den største verdien for strekk, i hver av ankerlinene, lagret. Basert på disse verdiene blir responsflater tilpasset ekstremverdiene. I tillegg blir Gumbel parameterne beregnet. Basert på responsflatene kan designverdiene beregnes på to måter, ved å løse langtidsintegralet og ved invertert førsteordens pålitelighetsmetode.

Den etablerte miljømodellen brukes til å konstruere konturoverflater som korresponderer til en gitt returperiode. Ved nærmere studie av ekstremverdiene på konturoverflaten, kan designpunktet defineres for alle ønskede tilfeller. I hvert designpunkt blir korttidsvariasjonen undersøkt i detalj og en designpunkt-fordeling blir funnet. Deretter kan det fraktilnivået som gir samsvar mellom konturlinjemetoden og langtidsanalysen finnes.

I studien blir det funnet at langtidsintegralet og den inverterte førsteordens pålitelighetsanalysen gir samsvarende resultater. I tillegg gir korttidsvariasjonen inntrykk av å være liten for ekstremresponsen i ankerlinene. Dette tyder på at designlasten kan bli tilstrekkelig estimert av medianverdien i designpunkt-fordelingen. Imidlertid, ved å undersøke ankerlinestrekkets avhengighet av vindparameteren blir det funnet at ankerlinestrekket ikke er monotont voksende. Dette bryter med grunnleggende prinsipper for konturlinjemetoden. Denne oppførselen skyldes det aktive kontrollsystemet på Hywind Demo og fører til konklusjonen at konturlinjemetoden er uegnet for bruk på Hywind Demo.

Preface

The work resulting in this Master's thesis has been carried out at the Department of Marine Technology at the Norwegian University of Science and Technology. The Master's thesis is the finale work of the five-year master program for the degree, Master of Science. The thesis is written during the spring term of 2013.

The assignment has been to investigate response processes at Hywind Demo, the first floating multi-megawatt wind turbine in the world. The topic of the thesis was proposed by Tor D. Hanson on behalf of Statoil ASA. I would like to thank Tor for the opportunity to write this inspiring thesis and for his excellent guidance.

Also I would like to present my sincere gratitude to my supervisor Bernt J. Leira and my co-supervisor Dag Myrhaug for their help and assistance.

Finally, I would like to thank my fellow students for five joyful years as a student in Trondheim.

Sjur Neuenkirchen Godø
Trondheim, June 10, 2013

Contents

Nomenclature

Abbreviations

ALS	Accidental limit state
API	American Petroleum Institute
BEM	Beam-Element Momentum
CDF	Cumulative Distribution Function
COB	Center of Buoyancy
COG	Center of Gravity
COV	Coefficient of Variation
CPR	Constant Power Regime
DNV	Det Norske Veritas
FLS	Fatigue limit state
IEC	International Electrotechnical Commission
IFORM	Inverse First Order Reliability Method
MPR	Maximum Power Regime
PDF	Probability Distribution Function
SLS	Serviceability limit state
TLP	Tension Leg Platform
ULS	Ultimate limit state
WTG	Wind Turbine Generator

Greek Symbols

α_h	Weibull shape parameter for the significant wave height-distribution in North Sea model
α_J	Spectral parameter in the Jonswap spectrum
α_S	Weibull location parameter suggested for the Hywind Demo location
α_w	Weibull shape parameter for wind-distribution in the North Sea model

β	Reliability index
β_h	Weibull scale parameter for the significant wave height-distribution in North Sea model
β_J	Form parameter in the Jonswap spectrum
β_S	Weibull scale parameter suggested for the Hywind Demo location
β_w	Weibull scale parameter for wind-distribution in the North Sea model
β_{3h}	Gumbel scale parameter for the extreme value distribution
γ_J	Peakdness parameter in the Jonswap spectrum
γ_S	Weibull shape parameter suggested for the Hywind Demo location
γ_{3h}	Gumbel location parameter for the extreme value distribution
γ_{dyn}	Partial safety factor for dynamic tension
γ_{mean}	Partial safety factor for mean tension
$\mu_{ln(T_p)}$	Expectation value for ln(Tp) in the peak period-distribution
Ω	Angular rotation speed
ρ_{air}	Density of air
σ_J	Spectral parameter in the Jonswap spectrum
$\sigma_{ln(T_p)}$	Standard deviation of ln(Tp) in the peak period-distribution

Roman symbols

$\overline{X}_{3h}$	Mean maximum response in a set of three-hour environmental states
F_D	Aerodynamic drag force
F_L	Aerodynamic lift force
F_{aero}	Force on a blade element
F_{ax}	Resulting actuator disk force
$f_{H_s\|W}(h \mid w)$	PDF for significant wave height given wind
$f_{T_p\|H_s,W}(t \mid h, w)$	Probability distribution function for peak period given significant wave height and wind

$f_{W,H_s,T_p}(w,h,t)$	Joint probability distribution function for wind
$f_W(w)$	Probability distribution function for wind
H_s	Significant wave height
$m_{3h,T}$	Number of three-hour environmental states in T-years
S_C	Characteristic capacity of the mooring line
S_{mbs}	Minimum breaking strength of mooring line component
T_p	Peak period
T_{C-dyn}	Characteristic dynamic line tension
T_{C-mean}	Characteristic mean line tension
T_{MPM}	Most probable maximum response value
W	Mean wind velocity at 10m elevation above sea level
X_T	Design response corresponding to a return period of T-years
X_{3h}	Maximum response during a three-hour environmental state
$\mathbf{g}$	Acceleration of gravity
$\mathbf{k}$	Wave number

List of Figures

List of Tables

1 Introduction

1.1 Motivation

The objective of this thesis is to investigate the application of the contour line method to predict design loads on Hywind Demo. Hywind Demo is with its 2.3MW turbine the first multi-megawatt floating wind turbine in the world. To obtain satisfactory result from the contour line method, it has to be calibrated with respect to a full long term analysis. In Norwegian rules and regulations the design load is given with respect to a certain probability of exceedance. In a long term response analysis the load corresponding to a specific return period is found based on a detailed analysis of all characteristic environmental states. The long term analysis can be particularly time consuming and it can therefore be beneficial to use the contour line method as an approximate approach to estimate the design loads.

The long term analysis and the contour line method both require a detailed environmental description in form of a joint probabilistic model. Therefore an important part of the work addressed in this thesis has been to establish an environmental model describing the conditions at the Hywind Demo location. Hywind Demo is located outside the areas typical for offshore activity and the environmental models developed by the offshore industry are not directly applicable for this location. These models can however be used as basis to develop an environmental model suited for the Hywind location.

In most cases regarding floating structures, the significant wave height and the peak period are the governing parameters that must be account for. The effect of wind is often neglected. For a floating wind turbine, proper design values cannot be obtained without also including wind as a parameter in the analysis.

1.2 Scope of Work

The scope of this work consist of three main parts which are to:

- develop a joint probabilistic model describing the probability of environmental combination to occur. The parameters included in the model are, significant wave height, peak period and wind.

- carry out a long term analysis of tension in the mooring lines. The long term analysis is based on numerous time-domain simulation in RIFLEX. The model used for simulations are developed by Statoil ASA. Development of this model is not included in the scope of work.

- evaluate the application of the contour line method by investigating if the same design loads can be obtained with this method.

1.3 Previous Work

Hywind Demo has produced electrical power for almost four years. Obviously there is a significant effort of work put into the design, building, installation and also maintenance of the wind turbine. This work is carried out by Statoil ASA, which has built and now operates Hywind Demo. During the years of operation data has been logged on Hywind Demo. Some of this data have resulted in publications by T. D. Hanson, B. Skaare, R. Yttervik and F. G. Nielsen on the behalf of Statoil ASA [4] [5]. Their work shows that there is good coherence between the measured data and computer results obtained from coupled SIMO/HAWK2 analyses [6].

Floating wind turbines has also been the topic of interest for other master students at the department of Marin Technology. T. Hordvik has discussed design and optimisation of mooring lines on floating wind turbines [7], and a parameter sensitivity study of fatigue has been carried out by I. Moy [8].

Rules and standards for design and operation of offshore wind turbines have been published by e.g. Det Norske Veritas (DNV) and International Electrotechnical Commission (IEC). A complete set of standards for offshore floating wind turbines are still to be published. This is currently under development by DNV.

Application of the contour line method and the long term analysis are well discussed subjects in the literature. For most cases the contour line method is evaluated with two slowly varying parameters, significant wave height and peak period [9] [10]. Some work including three parameters are performed, e.g. is a long term mooring analysis of Veslefrikk B carried out with three slowly varying parameters by T. Meling, K. Johannessen, S. Haver and K. Larsen [11].

Environmental modelling is an important part of a long term analysis. A joint probabilistic model for significant wave height, peak period and one-hour mean wind for the Northern North sea has been developed by Johannesen et al. [12].

1.4 Outline of Thesis

The thesis is organized as follows.

Chapter 2	gives a short historical overview and a presentation of the concept of offshore wind turbines.
Chapter 3	gives an introduction to design of wind turbines according to governing rules.
Chapter 4	is a structural description of Hywind Demo. The dimensions of the structure, the wind turbine blade control system and mooring line arrangement are explained in detail.
Chapter 5	contains the theoretical foundation which is the basis for the calculations and simulations carried out in the thesis.
Chapter 6	is an presentation of the computer model used in the reliability analyses.
Chapter 7	presents the the environmental model.
Chapter 8	presents the method, results and a discussion of these, for the reliability analyses.
Chapter 9	Conclusion and recommendations of further work.

2 Wind Turbines

2.1 History

It is believed that the concept of capturing wind energy into mechanical power was born somewhere in Asia between the 17^{th} and the 4^{th} century B.C. However the earliest documented design of wind turbines dates back to 200 B.C. where the Persians used wind turbines to grind grains.

The first modern wind turbine was invented in Denmark in 1890 and almost simultaneously in Ohio, USA. By the start of 1910, hundreds of wind turbines were producing electric power to villages in Denmark. In 1941 a huge development was made by Palmer C. Putman who constructed a 1250kW turbine. On this turbine it was possible to adjust the pitch on the blades to achieve constant rotation speed. The development of wind turbines continued trough out the late 1900 with Europe as a leading developer in wind energy [13].

In the search for renewable energy the developers of wind turbines were pushed towards previously untouched ground. The first offshore wind turbine was installed, also in Denmark in 1991 and nine years later the first offshore wind turbine in the UK was installed [14]. As of the first half of 2012 the total generation of electrical power from offshore wind parks reached 523.2MW in Europe [15]. Europe is a pioneer when it comes to offshore wind energy but other countries are starting to follow. Both China and Japan have operational offshore wind farms, and several offshore wind farms are under construction in the USA.

2.2 Offshore Wind Turbines

What categorizes offshore wind turbines is basically their support structure, i.e. the part of the wind turbine that is supporting the rotor and generator. Dependent on the foundation, offshore wind turbines can be categorized in two groups, floating wind turbines and non-floating wind turbines. In the literature, four types of non-floating wind turbines are described. They can be seen in Figure 2.1.

Gravity Based Structures

Wind turbines with a gravity based support structure are suited for operation in very shallow waters, i.e. less than 5m depth. The structure rests on the seabed and has a large flat base to withstand the overturning moment induced by the environmental loads.

Monopile

The monopile concept is the most common offshore wind turbine design and is also suited for shallow waters. The substructure consists of one pile which is driven in to the seabed. The diameter of the pile is normally between 4m and 5m and it is piled 15m to 30m into the seabed depending on the characteristics of the subsurface marine sediments. The end of the monopile is open allowing the sediments to be encased in the pile. This provides

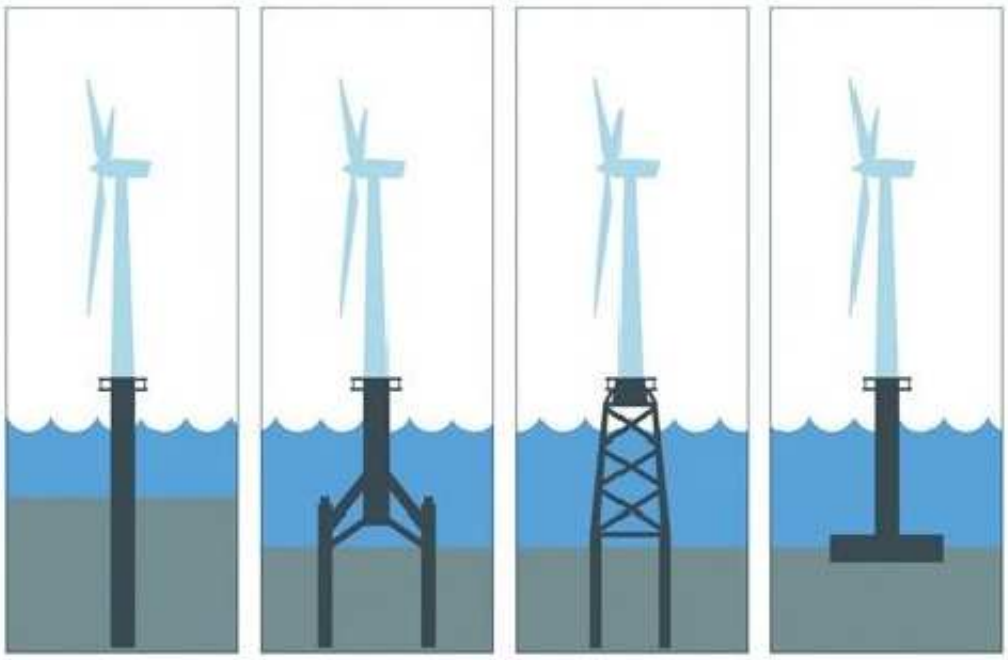

Figure 2.1: Concept drawing of bottom fixed wind turbines. Presented from the left: Monopile, three footed jacket, four footed jacket and gravity based structure [1].

additional structural support. As the water depth and height of the wind turbine increases the monopile concept will be to soft. Concepts with increased foundation stiffness must be used.

Jackets

There are several jacket types of substructures applied in the offshore wind turbine industry. It is common to divide between three- and four-legged jackets. Three legged jackets are applicable for depths up to 25m, but a four legged jacket it is possible to reach depths up to 100m. The wind turbine jackets are very similar to those used in the oil and gas industry. The jackets are piled to the seabed to ensure sufficient overturning moment capacity.

2.2.1 Floating Wind Turbines

In the literature one can find several concepts of offshore floating wind turbines. Some designs are depicted in Figure 2.2.

It can be divided between two types of mooring for floating wind turbines, i.e. catenary- and tensioned-mooring. The catenary moorings provide station-keeping true the weight of the cable and possibly additional weights. To achieve sufficient station-keeping three mooring lines are adequate, but by introducing several mooring lines redundancy are provided.

With tension mooring the wind turbine is moored with an unnatural high draught. The tension in the mooring lines, forces the wind turbine lower in the water than it would be when it is free floating. This results in an excess of buoyancy. In these cases the wind turbines will

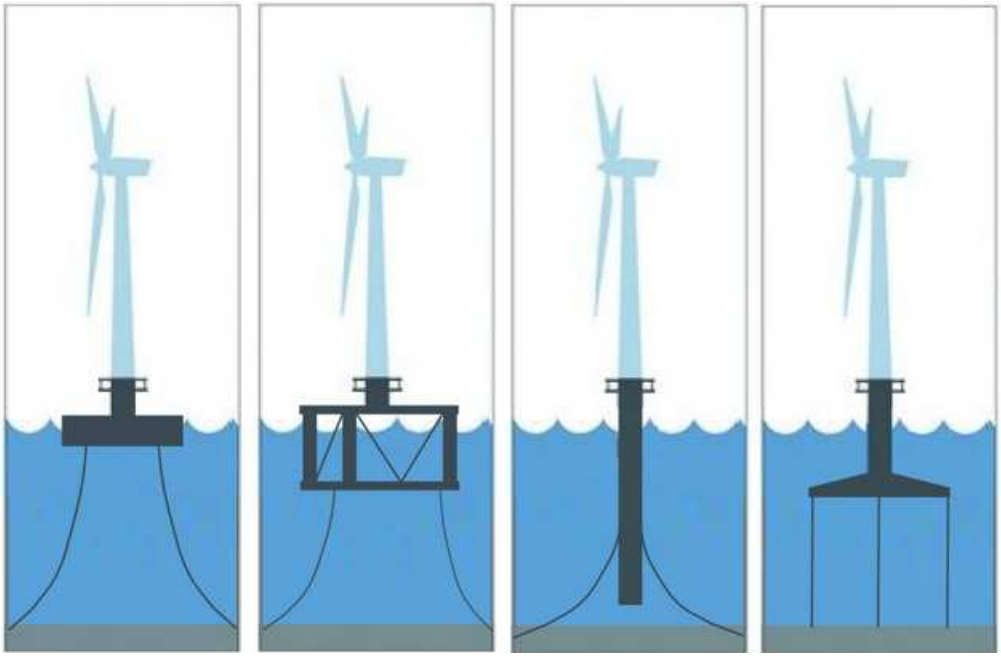

Figure 2.2: Design of some floating wind turbines [2].

have a very high stiffness in the vertical direction and the motions in heave, roll and pitch is minimized. A challenging problem with this type of wind turbines is the lack of stability in free floating condition, which in worst case might be non-existing. This introduces problems for the installation operation and makes the structure vulnerable to failure of the mooring lines.

Disc Buoy

This is possibly the simplest type of floating wind turbine. The wind turbine is mounted on a round disc which is floating on the surface. Initial stability will be ensured true the large water plane area and the structure is kept in place by catenary mooring. Advantages seams few compared to the disadvantages of this concept. To ensure adequate stability the diameter of the disc will have to be large, up to 40m [16]. Another disadvantage is the natural period of about 9s in heave and 13s in roll/pitch. This will be in the wave frequency domain and result in large wave induced motions.

Spar Buoy

The spar buoy has been used for several decades in the offshore oil and gas industry, though in bigger scales than what will be of interest for wind turbines. The spar buoy principle is based on a cylinder shaped structure which is submerged vertically. By adding ballast at the bottom, stability of the buoy is ensured. A relationship between the draught and the diameter is prevailing. As the draught of the buoy increases the diameter can be reduced. By tuning the geometry of the buoy, good results can be obtained with respect to natural periods. To suppress the heave motion, heave-suppression discs can be mounted at the

bottom of the buoy. This will increase the added-mass and damping of the structure, which can be used to tune the natural periods away from the wave frequency domain.

Tri-floater

To increase the stiffness of the roll and pitch motion an alternative to the spar buoy is a tri-floater. It consists of three spar buoy assembled together. This will increase the water plane inertia of the structure and therefore increase the stiffness. To decrease the heave motion, heave-suppression discs can be installed on each of the cylinders, similar to the spar buoy. Motion response will be a problem for this installation as the natural frequencies are expected to be around 15s [16].

Tensioned Spar

This option is similar to the spar buoy, but will have tensioned mooring instead of being catenary moored. This design will have insufficient stability during installation and lack of redundancy with respect to mooring line failure. On the upside will the natural periods of a tension moored buoy be ideal with respect to the wave environment.

Four Floater Tension Leg Platform

This concept consists of a fully submerged floater that is tensioned moored to the seabed. The floater is sufficiently submerged to avoid wave forces. Only the substructure of the wind turbine is piercing the surface and is centred between four floating compartments that each are moored to the seabed. This will give a stable structure since the attachment points of the mooring lines are moved away from the center of rotation.

3 Design of Wind Turbines

3.1 Introduction

In this chapter some of the rules and regulations which are governing for offshore wind turbines will be presented. It will be focused on environmental loading and design limit states with respect to the floating wind turbines and mooring of such structures.

3.2 Governing Regulations

The concept of floating wind turbines is relative new and therefore a complete standard governing design of such structures does not exist. Bottom supported wind turbines is however a fully commercialized concept with an established set of rules and regulations. Standards are provided by several instances, i.g. DNV, IEC and American Petroleum Institute (API). The standards from DNV will be discussed in more detail in the following sections.

DNV suggests using their standard DNV-OS-J101 - "Design of offshore wind turbine structures", in accordance with "DNV Guideline for Offshore Floating Wind Turbine Structures", for design of offshore structures. The Guideline suggests that until more suiting regulations are established the design of catenary moored floating wind turbine structures shall be in accordance with DNV-OS-E301 - Position Mooring. This standard contains criteria, technical requirements and guidelines on design and construction of position mooring system off offshore structures. Technical requirements regarding materials, manufacturing and testing of offshore mooring lines are covered by standards DNV-OS-E302, DNV-OS-E303 and DNV-OS-E304, for chain, fibre ropes and steel wire ropes, respectively.

3.3 Environmental Conditions

The environmental conditions to be used for mooring system analyses are described in DNV-OS-E301. The standard requires that the environmental loads, waves, wind and current shall be taken into account when designing offshore structures. It is also required to recognise loads from marine growth, tide and storm surge, earthquakes, temperature, snow and ice. However, in this work it will be focused on dynamic behaviour, where these effects are assumed to be less important.

It is recommended in the standard that the environmental conditions applied in response analyses of mooring lines shall include the most unfavourable combination of wind, waves and current, with a return period of at least 100-years. A deterministic approach is suggested where a combination of wind and waves with return period of 100-years and a current with return period of 10-years is assumed to meet this criterion. Some typical environmental parameters with return period 100-years are presented in Table 3.1, for two typical location in the North Sea.

Table 3.1: Environmental parameters with return period of 100-years for two sites in the north sea.

Variable	Haltenbanken	Ekofisk
H_s [m]	16.5	14.0
T_p [s]	17.0 - 19.0	15.0 - 17.0
W [m/s]	37	34
Current [m/s]	0.9	0.55

The standard suggests that reliability methods are used for, "novel designs for which limited or no experience exists". This is unquestionably the case for Hywind Demo. A reliability analysis can be carried out if sufficient environmental data are available to develop a joint probabilistic model for the environmental loads. This will give a more precise description of the response problem. If the joint environmental distribution can be obtained, it is proposed to investigate the set of combinations for significant wave height (Hs) and peak period (Tp) along the 100-year contour line defined by the FORM-method. Certain points on the upper part of the contour line are chosen for analysis together with constant values of wind and current. Recommended values for wind and current are the loads corresponding to a 100- and 10-year return period, respectively. A number of contour lines are suggested for different locations in the North Sea.

In DNV-OS-J101 rules for design of bottom supported offshore wind turbine structures are presented. Design is recommended based on the most unfavourable combination that returns with a period of 50-years. In current offshore regulations, which until further notice are governing for mooring lines on floating wind turbines, the return period is 100-years. It is reasonable that rules for design of manned floating structures require higher performance than unmanned wind turbines. But it is expected that when complete regulations are published for floating wind turbines, the rules for mooring will be in accordance with the existing rules for offshore wind turbines. This means that design of mooring lines for floating wind turbines most likely will be with respect to loads with return period of 50-years.

3.4 Design Limit States

According to DNV a limit state is a condition where the structure does not satisfy the design criteria any more. In their standards, DNV separate between four different limit states. This is in accordance with other standards concerning activity in the Norwegian waters, e.g. NORSOK. The four limit states are:

- Ultimate limit state (ULS)
- Fatigue limit state (FLS)
- Accidental limit state (ALS)

- Serviceability limit state (SLS)

A closer presentation of each limit state is presented in the next sections.

3.4.1 Ultimate Limit State

ULS corresponds to the maximum load-carrying resistance of the wind turbine. In ULS it is required that the structure is designed to withstand a load combination with a return period of 50-years, i.e. an annual probability of exceedance of 0.02. Examples of ultimate limits states are;

- -loss of resistance due to yielding or buckling.
- -brittle fracture
- -exceedance of ultimate resistance

In this thesis it will be focused on finding ULS design loads for some specific responses at Hywind Demo.

3.4.2 Fatigue Limit State

To evaluate the fatigue limit state the fatigue life of the structure must be predicted. The aim of fatigue design is to avoid failure due to cumulative damage as a result of cyclic loading. Based on the predicted fatigue life an efficient inspection program can be defined. DNV requires that FLS should be determined according to DNV-OS-C502. FLS will not be further discussed in this thesis.

3.4.3 Accidental Limit State

Two criteria are defined for ALS:

1. The structure is designed so that it will have sufficient maximum load-carrying capacity to resists accidental loads.
2. The structure is designed to maintain integrity and performance in spite of local damage or flooding, i.e. post-accidental integrity must be ensured.

ALS will not be subject to further investigation in this thesis.

3.4.4 Serviceability Limit State

In this limit state the structure fails due to motions, velocities or accelerations exceeding the limit where the structure is able to remain in normal operation. The SLS will not be discussed in further detail.

3.5 Line Tension

In the DNV-OS-E301 two components of characteristic line tension are considered. For time domain analyses the dynamic line tension is given in the flowing equation.

$$T_{C-dyn} = T_{MPM} - T_{C-mean}, \tag{3.1}$$

T_{C-mean}	The characteristic mean line tension, due to pretension and mean environmental loads.
T_{C-dyn}	The characteristic dynamic line tension, due to low-frequency and wave-frequency motion.
T_{MPM}	The most probable maximum from the extreme value distribution of the response, i.e. the 37% percentile for the Gumbel distribution.

The characteristic capacity of mooring lines shall be calculated on basis of the statistical parameters of the breaking strength. If these parameters are unknown the characteristic capacity, S_C, is given as:

$$S_C = 0.95 \cdot S_{mbs}, \tag{3.2}$$

where S_{mbs} is the minimum breaking strength of new components. The mooring line tension can now be compared to the characteristic capacity. In DNV-OS-E301 this is described by the ULS design equation:

$$S_C - T_{C-mean} \cdot \gamma_{mean} - T_{C-dyn} \cdot \gamma_{dyn} \geq 0. \tag{3.3}$$

The two γ-s in the equation are partial safety factors which are defined by the standard. The safety factors are given values based on the consequence a ULS failure will have. Two consequence classes are defined by DNV.

Class 1 -	Mooring system failure is unlikely to lead to unacceptable consequences such as loss of life, collision with an adjacent platform, uncontrolled outflow of oil or gas, capsize or sinking.
Class 2 -	Mooring system failure may well lead to unacceptable consequences of these types.

For ULS the partial safety factors are given in Table 3.2.

Table 3.2: ULS partial safety factor.

	Partial Safety factor of mean tension	Partial Safety factor of dynamic tension
Consequence Class	γ_{mean}	γ_{dyn}
1	1.1	1.5
2	1.4	2.1

4 Hywind Demo

4.1 Introduction

In this chapter an introduction to Hywind Demo will be given. Hywind Demo is one of the first full scale floating wind turbines in the world. It is designed and built by Statoil, and is located 11 kilometres of the west cost of Karmøy, Norway. It was officially opened in September, 2009, and has since then been producing electric power to the Norwegian power grid. Hywind is based on the deep spar buoy concept described previously in chapter 2.2.1. Following is a more detailed structural description and an introduction to the advanced blade pitch control system implemented on Hywind Demo. A short overview of the various data being logged on Hywind Demo is also presented.

4.2 Structural Description

Hywind Demo can roughly be divided in three parts, substructure, tower and Wind Turbine Generator (WTG). The substructure is the component on a wind turbine that connects the tower to the sea floor. For a floating wind turbine the substructure is the structure on which the tower is supported. The substructure will from now be mentioned as the hull. The hull on Hywind Demo is a 100m deep steel-cylinder and has a maximum diameter of 8.3m. The hull is heavily ballasted to lower the Center of Gravity (COG). On top of the hull the tower is mounted. The tower is about 50m tall and is the support structure for the WTG. The WTG consists of the nacelle, the generator and the three blades. The rotor diameter is 82.4m. By calculating the weight and COG for the three parts, the total weight and COG is found. Values for the masses and COGs of the different structural sections are presented in Table 4.1.

One of the key features of a spar buoy concept is its initial stable behaviour. This is due to the location of the COG and the Center of Buoyancy (COB). In ships and other conventional floating structures the COB is located below the COG and the uprightening moment is due to a relocation of the COB when the structure heel. For a spar buoy the COG is located below the COB which result in the exceptional good stability properties. To obtain this location of the COG the hull is heavily ballasted in the bottom with gravel and water. A detailed structural drawing of Hywind Demo is found in Figure 4.1.

Table 4.1: Partial and total mass and vertical placement of the COG for Hywind Demo.

Structure	**Mass [kg]**	**ZCOG [m]**
Hull	4820400	-74.77
WTG	136100	64.51
Tower	173300	31.56
Full structure	**5129800**	**-67.48**

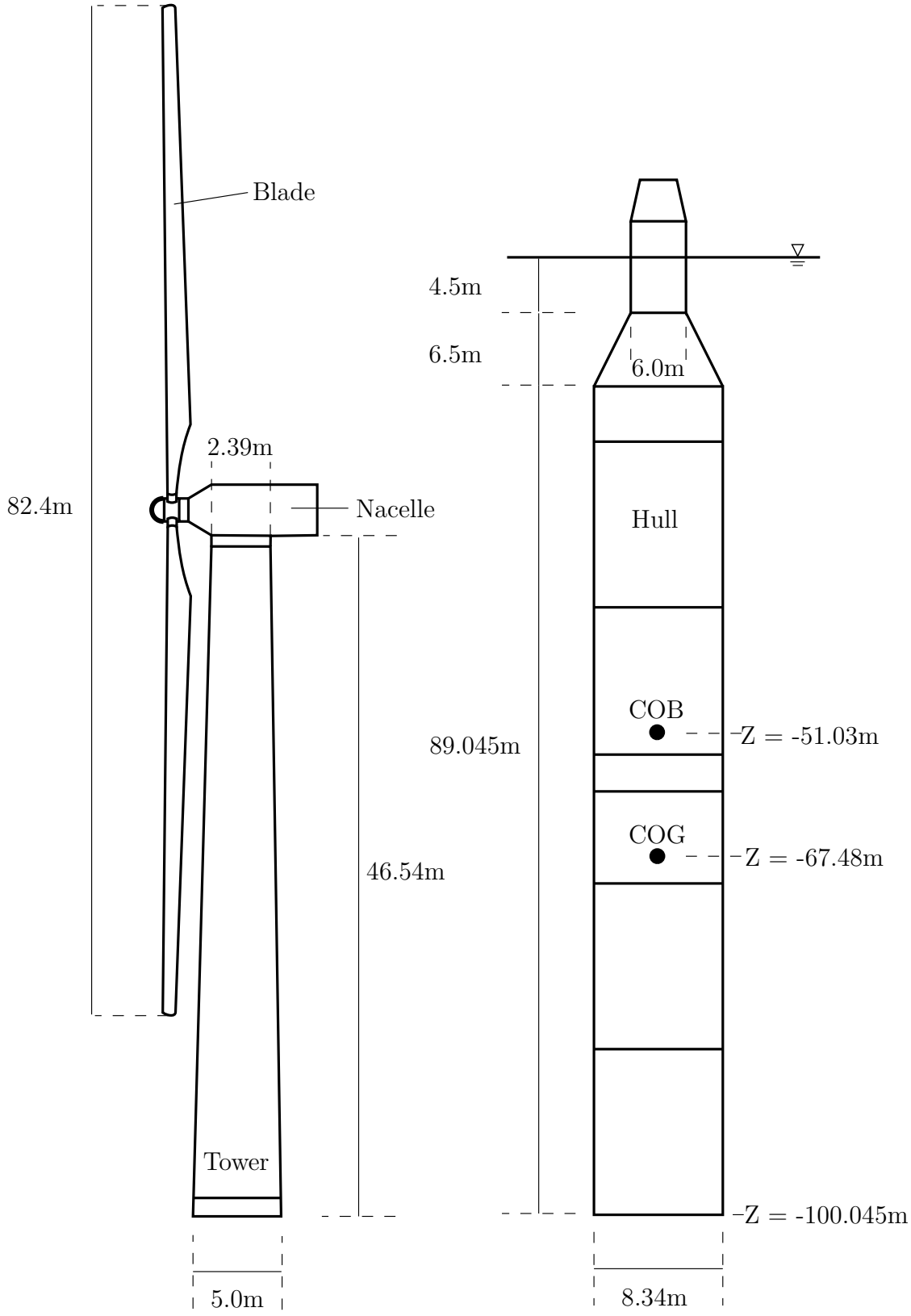

Figure 4.1: Structural drawing of Hywind Demo. The tower and the hull are not drawn in scale.

4.3 Natural Periods of Hywind Demo

In Table 4.2 the natural periods of Hywind Demo are displayed. Statoil ASA has estimated the natural periods as part of the design process. The natural periods are found in three different ways, an eigenvalue analysis in RIFLEX, by hand calculations and from measurements at Hywind Demo. A first comment is that all methods show good agreement. A small deviation is however seen in the hand calculations for the pitch natural period. Statoil also emphasises that the calculations of the yaw natural period has been difficult and that uncertainty is related to these values. It is seen that all the natural periods are larger than the typical wave periods of 8s - 12s. The surge natural period is just above two minutes and might be excited by slowly varying forces, such as mean wind or current.

A well-known dynamic phenomenon for spar buoys is the Mathieu instability. It is related to a time dependent restoring term in the equation of motion and can occur if the pitch natural period is close to the natural period [7].

Table 4.2: natural periods of Hywind Demo.

Mode	**DYNMOD eigenvalues**		**Hand calculations**	**Measured**
	Stiff mooring	As-built	As-built	
Surge [s]	95.80	126.30	-	125.00
Heave [s]	27.80	27.8	27.50	27.40
Pitch [s]	24.10	24.20	26.30	23.90
Yaw (with clump weights) [s]	21.10	23.40	22.30	23.80
Yaw (without clump weights)[s]	6.10	7.50	5.70	6.20

4.4 Mooring Lines

Hywind demo is catenary moored with three mooring lines. The mooring lines are approximately 800m long. Both chain and ropes are used in the mooring lines to achieve the optimal properties. A clump weight is attached to the mooring line about 150m from the hull, with a mass of 45 tons. The behaviour of the wind turbine is highly dependent on the configuration of the mooring lines. As seen in Table 4.2 the natural period in yaw is especially sensitive to the use of clump weights on the mooring lines.

About 50m from the hull the mooring line is split in two. From here it continues as two delta lines which connect to each side of the hull. This feature gives the wind turbine extra stiffness in the yaw direction. A schematic view of the mooring line configuration is seen in Figure 4.2.

In Figure 4.3 the mooring lines and the hull are seen from an overhead view. The name setting of the mooring lines are also shown, together with the wind and wave directions. The

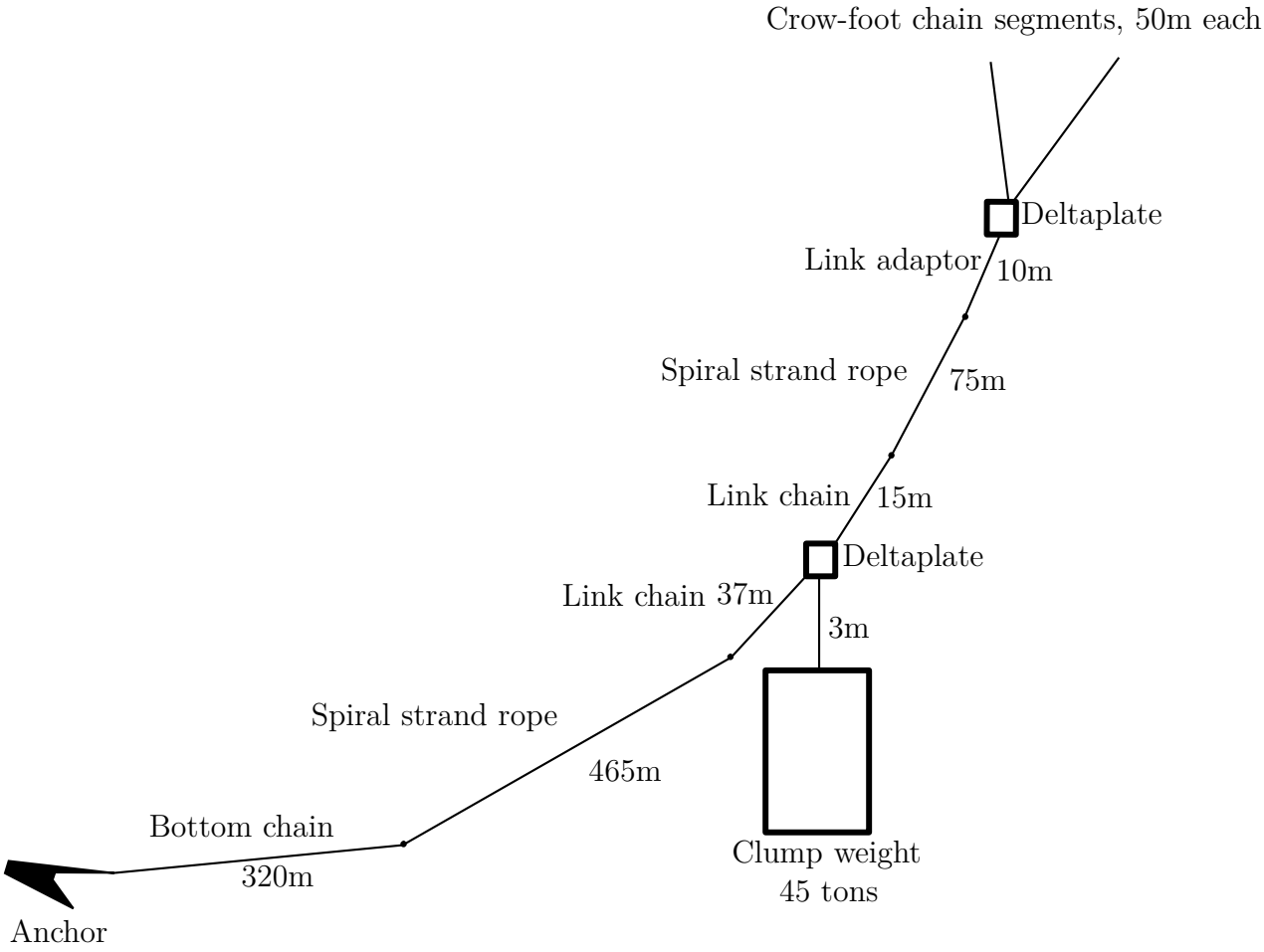

Figure 4.2: Schematic drawing of the mooring line configuration of Hywind Demo.

area marked red in Figure 4.3 are the delta-plate connecting the mooring line with the two delta lines.

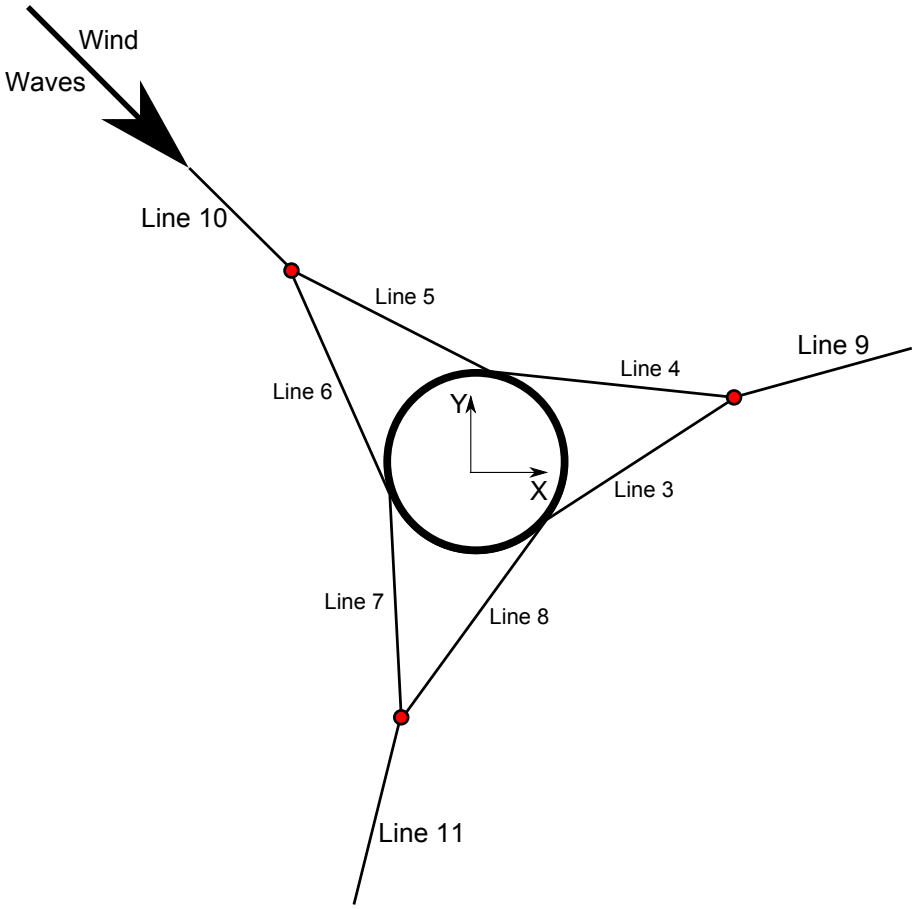

Figure 4.3: Schematic overview of the mooring line alignment, hull axis system and the wind and wave angel of attack.

4.5 Control System

The turbine on Hywind Demo is delivered by Siemens Wind Power and is a variable speed, collective blade pitch controlled 2.3MW wind turbine. The details related to the Hywind Demo control system are confidential, but a conventional, constant power control system can be considered to explain the basic concept and problems of a pitch controlled floating wind turbine. The standard conventional pitch controlled wind turbine has two main operating regimes:

Maximum Power Regime (MPR)	When the turbine is operating below the rated wind speed, 12m/s, the blade pitch angle is kept constant. The generator torque is controlled to obtained an optimal tip speed ratio to maximise the power coefficient.
Constant Power Regime (CPR)	When the turbine is operating above the rated wind speed the rotor speed is controlled. The goal is to obtain a constant desired rotor speed which ensures a constant power output. By adjusting the blade pitch angle the rotor speed is controlled.

Based on the conventional constant power control system described above, a characteristic curve for rotor trust force as function of relative wind speed can be obtained. From Figure 4.4 the two domains described previously are clearly seen. It is further seen that the maximum rotor thrust force is reached at a relative wind speed of about 12m/s, which is the rated wind speed.

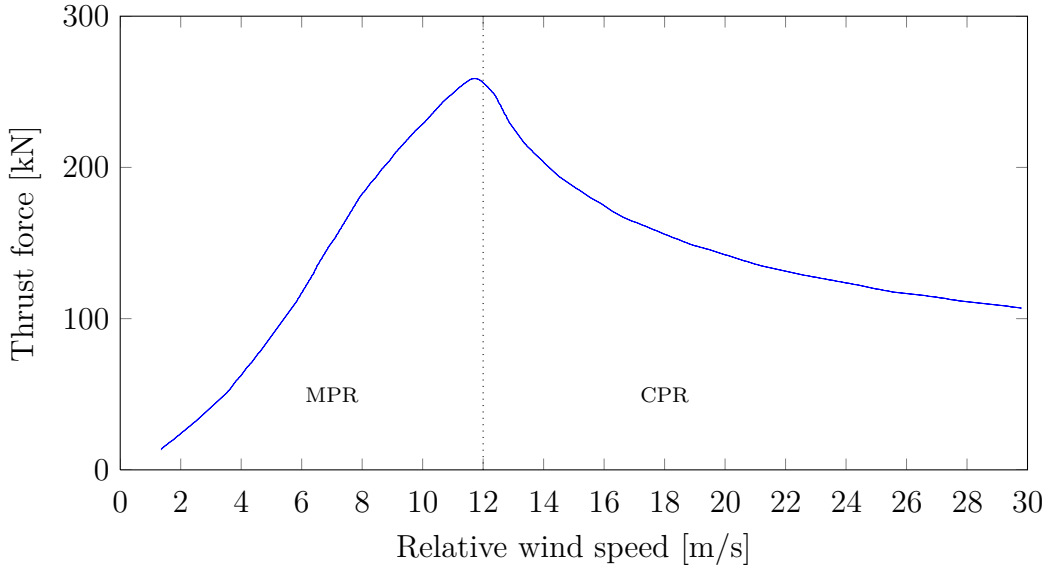

Figure 4.4: Rotor thrust force as a function of relative wind speed.

When a conventional constant power controller is used on a floating wind turbine, problems with negative damping can occur. This means that the control system is adding extra energy

to the system. The negative damping phenomenon can be explained with reference to Figure 4.4. For a turbine operating in the maximum power regime, below the rated wind speed, it is seen that the thrust force is increasing with increasing relative wind speed. This means that when the nacelle is moving towards the wind, the thrust force will increase and therefore damp the motion of the wind turbine. On the other hand when the wind turbine is operating in the constant power regime the thrust force is decreasing when the relative wind speed is increasing. This means that when the nacelle is moving towards the wind, i.e. the relative wind speed increases, the thrust force on the rotor is decreasing. This will make the thrust force act in phase with the motion of the wind turbine, and the system can have negative damping in the structure's surge or pitch modes.

In some cases the issue of negative damping can force the system to become unstable. Do to this phenomenon it is necessary with a specialized floater motion controller to minimize the pitch motion of the wind turbine. Such a controller has been developed by Statoil ASA, and controls the pitch motion in co-operation with the conventional constant power controller from Siemens.

4.6 Data Logging on Hywind

One of the key aspects of Hywind Demo is to collect measuring data to increase the knowledge of environmental and structural parameters of floating wind turbines. To measure metocean data a Seawatch buoy is installed close to the wind turbine. The buoy is equipped with the following sensors:

- Ultrasonic wind sensor
- Air pressure sensor
- Air temperature sensor
- Relative humidity sensor
- Directional wave sensor
- Sea surface temperature and salinity sensor
- Current profiling sensor
- Single point current meter

The data is stored locally and are collected during service trips to the buoy. Selected data are also transmitted to shore via satellite once each hour. In addition are the wind-speed and -directions, together with the buoy's displacement, transmitted to Hywind Demo via a radio link.
Hywind Demo is also equipped with a number of measuring instruments. The most important sensors are the Octans Gyro which logs the six degrees of freedom of the wind turbine, and

the Seatex MRU which logs the pitch and roll angle of the Nacelle. By comparison, the two sensors give agreeing data measurements [6]. The hull and the tower of Hywind Demo are instrumented with strain gages at key locations. With good knowledge of the strains in the structure, valuable information regarding ultimate stresses and fatigue are obtained. A number of sensors are also installed to log important parameters regarding the wind turbine system. Some of the parameters being stored are the generator speed, blade pitch angle, and the generator power. Also the flap- and edge-wise bending moments are measured on each rotor blade.

The mooring line tension is measured with sensors placed between the delta lines and the hull. There are in total six sensors logging the mooring line tension, one for each delta line. The tension is measured in horizontal x-direction and vertical y-direction. Each sensor has two data channels for each direction to ensure redundancy in the logging system.

5 Theory

5.1 Environmental Modelling

Two environmental models are discussed in this thesis. The first model is developed by Johannessen et al. based on measurements in the Northern North Sea [12]. In this classical article, wind and waves are combined in a joint distribution model. The second model is developed by Statoil based on measurements at the Hywind location. In Statoil's environmental model the distributions for wind and waves are not joined. The two models are presented in the following sections.

5.1.1 Environmental Model - Northern North Sea

Based on the articles by Meling et al. [11] and Johannessen [12] the following joint Probability Distribution Function (PDF) has been proposed as an model for the environmental parameters, wind, Hs and Tp:

$$f_{W,H_s,T_p}(w,h,t) = f_W(w) \cdot f_{H_s|W}(h|w) \cdot f_{T_p|H_sW}(t|h,w), \tag{5.1}$$

where:

$f_{W,H_s,T_p}(w,h,t)$	Joint PDF for wind, Hs and Tp	[-]
$f_W(w)$	PDF for wind	[-]
$f_{H_s\|W}(h\|w)$	PDF for Hs, given wind	[-]
$f_{T_p\|H_sW}(t\|h,w)$	PDF for Tp, given Hs and wind	[-]

According to Meling the wind is assumed to dominate the environmental loads and is therefore chosen as the primary parameter. The Cumulative Distribution Function (CDF) of the mean wind is given by a 2-parameter Weibull distribution:

$$F_W(w) = 1 - exp\left[-\left(\frac{w}{\beta_w}\right)^{\alpha_w}\right], \tag{5.2}$$

with:

α_w	Weibull shape parameter for the wind distribution	[-]
β_w	Weibull scale parameter for the wind distribution	[-]

Where, based on measurements from the Northern North Sea in the period 1973 - 1997, the following values are found for the two parameters [12]:

$$\alpha_w = 1.708, \qquad \beta_w = 8.426. \tag{5.3}$$

Further on, the conditional distribution of Hs is also given by a Weibull-distribution. The Weibull-parameters are now given as functions of the mean wind velocity. The constants are found by a regression analysis and the following parametrizations of the shape and the scale parameters are proposed:

$$\alpha_h(w) = 2.0 + 0.135w, \qquad \beta_h(w) = 1.8 + 0.1w^{1.322}, \tag{5.4}$$

where:

α_h	Weibull shape parameter for the significant wave height distribution	[-]
β_h	Weibull scale parameter for the significant wave height distribution	[-]

For the spectral peak period a log-normal distribution is proposed for given wind and significant wave height:

$$f_{T_p|H_s,W}(t|h,w) = \frac{1}{\sqrt{2\pi}\sigma_{ln(T_p)t}} exp\left[-\left(\frac{ln(t) - \mu_{ln(T_p)}}{\sqrt{2}\sigma_{ln(T_p)}}\right)\right], \tag{5.5}$$

where:

$\mu_{ln(T_p)}$	Expectation value of $ln(T_p)$	[-]
$\sigma_{ln(T_p)}$	Standard deviation of $ln(T_p)$	[-]

The expectation value and standard deviation of $ln(T_p)$ are defined as follows:

$$\mu_{ln(T_p)} = ln\left[\frac{\mu_{T_p}}{\sqrt{1+\nu_{T_p}^2}}\right], \qquad \sigma_{ln(T_p)}^2 = ln\left[1+\nu_{T_p}^2\right], \tag{5.6}$$

where:

$$\nu_{T_p} = \frac{\sigma_{T_p}}{\mu_{T_p}}, \mu_{T_p} = \bar{T}(h)\left[1 - 0.19\frac{w - \bar{w}(h)}{\bar{w}(h)}\right], \sigma_{T_p} = 0.1\mu_{T_p}, \tag{5.7}$$

and:

$$\bar{T}(h) = 4.883 + 2.68h^{0.529}, \qquad \bar{w}(h) = 1.764 + 3.426h^{0.78}. \tag{5.8}$$

5.1.2 Environmental Model - Statoil

Statoil's model is based on measurements at the Hywind location. For wind, data from the Hirlam hindcast model, Grid Point 1412, has been used to establish a long term distribution. The measurements are taken over a period from 1957 - 2002, with a sampling interval of three hours. The measurements have then been adjusted to 65m above MSL by the NORSOK

wind profile [17]. A Weibull distribution has been found adequate to model the long term distribution of wind at the Hywind location:

$$F(u) = 1 - exp\left[-\left(\frac{u - \alpha_S}{\beta_S}\right)^{\gamma_S}\right], \tag{5.9}$$

where:

u	1-hour mean wind speed	[m/s]
α_S	Location parameter	[m/s]
β_S	Scale parameter	[m/s]
γ_S	Shape parameter	[-]

Based on the Hirlam hindcast model and measurements from Utsira the in Table 5.1 are the following values suggested for the Weibull wind parameters:

Table 5.1: Omni-directional Weibull parameters for wind speed at 65m above mean sea level.

Weibull parameters		
Shape	Scale	Location
1.77	10.541	0

This parameters are for wind 65m above the sea surface. For input to RIFLEX the parameters must describe the wind 10m above the sea surface. This will be discussed in the succeeding chapter.

The waves are described by a joint distribution of Hs and Tp:

$$f_{H_s,T_p} = f_{H_s}(h_s) \cdot f_{T_p|H_s}(t_p|h_s), \tag{5.10}$$

where:

$$\begin{aligned} f_{H_s}(h_s) &= \frac{1}{\sqrt{2 \cdot \pi} \cdot \alpha_S \cdot h_s} \cdot exp\left(-\frac{(ln(h_s) - \theta)^2}{2\alpha_S^2}\right), \quad for \qquad h_s \leq \eta \\ f_{H_s}(h_s) &= \frac{\beta_S}{\rho}\left(\frac{h_s}{\rho}\right)^{\beta_S - 1} exp\left[-\left(\frac{h_s}{\rho}\right)^{\beta_S}\right], \qquad for \qquad h_s > \eta. \end{aligned} \tag{5.11}$$

Hs is here described by two distributions, where smaller sea states are described by a log-normal distribution. This approach is chosen to obtain a better fit to the smaller values in the data region. For higher values of Hs a Weibull distribution is used. Further on the distribution of Tp is also log-normal and is dependent on the value of Hs:

$$f_{T_p|H_s}(t_p|h_s) = \frac{1}{\sqrt{2\pi} \cdot \sigma \cdot h_s} exp\left(-\frac{(ln(t_p) - \mu)^2}{2\sigma^2}\right), \tag{5.12}$$

where:

$$\mu = a_1 + a_2 \cdot h_s^{a_3},$$
$$\sigma^2 = b_1 + b_2 exp(-b_3 \cdot h_s). \tag{5.13}$$

Values for the parameters in Equations 5.11, 5.12 and 5.13 are found in the Hywind Metocean Design basis and are obtained from measurements in the Hywind area.

Table 5.2: Values for the parameters in the Hywind environmental model.

β_S	ρ	η	α_S	θ	a_1	a_2	a_3	b_1	b_2	b_3
1.192	1.612	3.133	0.65	0.345	1.780	0.290	0.480	0.005	0.15	0.370

5.2 BEM - Airfoil Theory

The forces acting on the wind turbine blades can be calculated by Beam-Element Momentum (BEM) theory. In BEM theory a stream tube is assumed to enclose the turbine blades. The blades will act as an actuator disc. When passing the disk the air will be slowed down, creating a wake behind the wind turbine. The loss in airflow velocity will according to Bernoulli's equation result in a pressure difference and so also a resulting force, F_{ax}, from the turbine on the airflow. This resulting force can now be calculated from momentum theory, assuming incompressible, homogeneous and horizontal flow. From Bernoulli's equation the following is obtained [18]:

$$F_{ax} = \frac{1}{2} A_{disk} \rho_{air} V_0^2 \cdot 4a(1-a), \tag{5.14}$$

where a is an induction factor given by:

$$a = \frac{V_0 - V_{disk}}{V_0}, \tag{5.15}$$

with:

F_{ax}	Resulting force on the actuator disk	[N]
V_0	Undisturbed wind velocity	[m/s]
V_{disk}	Wind velocity at the actuator disk	[m/s]
A_{disk}	Area of the rotor disk	$[m^2]$

To solve Equation 5.14, blade element theory is used. Each of the blades is considered to consist of blade elements, which each have its own aerodynamic features, e.g. drag and lift coefficients. The coefficients are calculated by specialized aero-elastic design programs. The

wind load on each blade element can be calculated from the following equation:

$$F_{aero} = \frac{1}{2} C_{aero} \rho_{air} A V_{section}^2, \tag{5.16}$$

where:

F_{aero}	Wind load	[N]
C_{aero}	Aerodynamic coefficient	[-]
ρ_{air}	Density of air	$[kg/m^3]$
A	Exposed area of the section	$[m^2]$
$V_{section}$	Wind velocity at the centre of the section	[m/s]

Each element is considered to be infinite long, so boundary effects and interaction between different elements are neglected. Tip and root effects can be incorporated by computer programs when the total blade force is calculated. The section velocity, or the relative wind speed, is given by the wind speed at the disk and the rotation speed. This is described as:

$$V_{rel} = \sqrt{V_{disk}^2 + V_{rot}^2}, \tag{5.17}$$

$$V_{disk} = V_0(1 - a), \qquad V_{rot} = \Omega \cdot r, \tag{5.18}$$

where:

V_{rel}	Relative wind speed at a blade section	[m/s]
V_{disk}	Wind velocity at airfoil	[m/s]
V_{rot}	Linear rotation speed at a blade section	[m/s]
Ω	Angular rotation speed	[rad/s]
r	Distance of blade element to axis of rotation	[m]
a	Induction factor, see Equation 5.15	[-]

The lift and drag loads can now be calculated:

$$\begin{aligned} F_L &= \frac{1}{2} C_L(\alpha) \rho_{air} V_{rel}^2 c_a \Delta r, \\ F_D &= \frac{1}{2} C_D(\alpha) \rho_{air} V_{rel}^2 c_a \Delta r, \end{aligned} \tag{5.19}$$

where:

F_L	Aerodynamic lift	[N]
F_D	Aerodynamic drag	[N]
$C_L(\alpha)$	Aerodynamic lift coefficient	[-]
$C_D(\alpha)$	Aerodynamic drag coefficient	[-]
ρ_{air}	Mass density of air	$[kg/m^3]$
c_a	Airfoil chord length	[m]
Δr	Radial length of blade element	[m]
α	Angle of attack	[deg]
θ	Pitch angle	[deg]
ϕ	Angle of inflow	[deg]

By decomposing the drag and the lift force in x-direction, the horizontal force exerted on one element can be found:

$$F_x = F_L cos(\phi) + F_D sin(\phi), \tag{5.20}$$

and by summing the force on all elements the total axial load is obtained:

$$F_{ax} = N_b \sum_{r=root}^{r=tip} F_{x,r}. \tag{5.21}$$

The angle of attack for the relative wind velocity is not necessarily parallel with the blade axis. The orientation of the velocities and the lift- and drag-forces are shown in Figures 5.1 and 5.2, respectively.

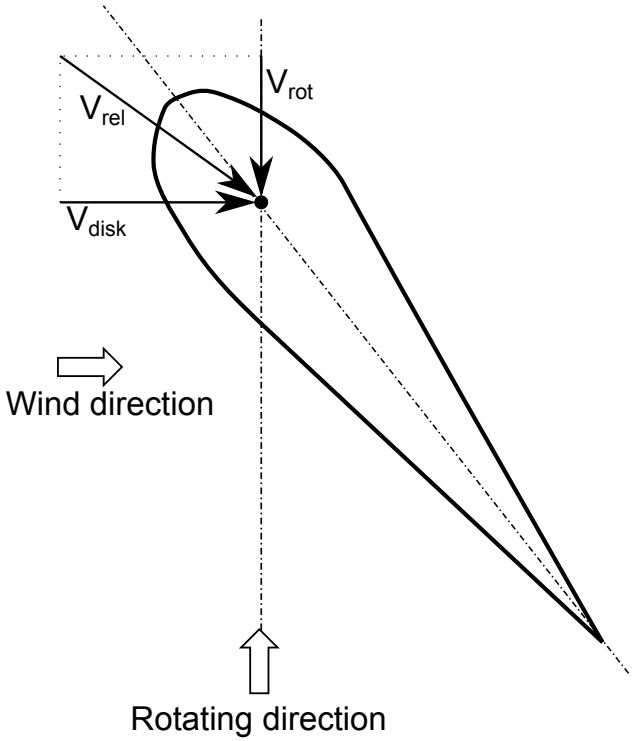

Figure 5.1: Combination of rotating- and wind-velocity results in a relative velocity with an angel of attack, α, to the blade axis.

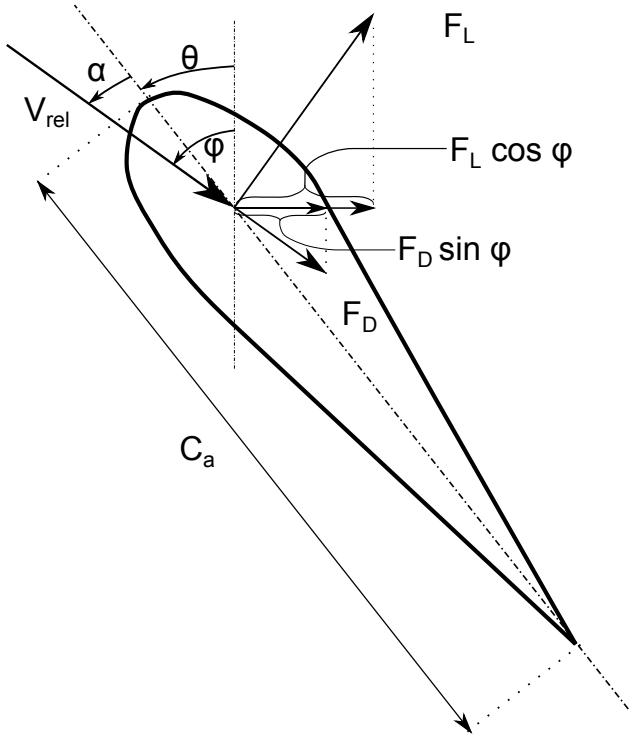

Figure 5.2: Drag- and lift-force acting on a blade element. Horizontal components are also shown in the figure. The drag-force arrow is not in scale with the lift-force arrow.

5.3 Rosenblatt Transformation

The Rosenblatt transformation is used in the contour line method to transform the joint distribution function into the independent standard Gaussian space. Mathematical the Rosenblatt transformation is described as:

$$\begin{array}{lcl} \Phi(u_1) = F_W(w) & & u_1 = \Phi^{-1}[F_W(w)] \\ \Phi(u_2) = F_{Hs|W}(hs|w) & \Rightarrow & u_2 = \Phi^{-1}[F_{Hs|W}(hs|w)] \\ \Phi(u_3) = F_{Tp|Hs,w}(tp|hs,w) & & u_3 = \Phi^{-1}[F_{Tp|Hs,W}(tp|hs,w)] \end{array} \tag{5.22}$$

In the standard Gaussian space all environmental combinations with constant probability of occurrence are located at the same distance from the origin. For a problem with three variables this will define a sphere. The radius in the sphere, β, will be a function of the return period. The relation between β and the return period is described as:

$$\beta = -\Phi^{-1}(p(T_R)), \tag{5.23}$$

where, $p(T_r)$, is the probability for the return period value to be exceeded. Now the values for u_i can be found by inverting the following equaiton:

$$\beta = \sqrt{\sum_{i=1}^{3} \hat{u}_i^2}. \tag{5.24}$$

For each value of u_i the corresponding values for W, Hs and Tp are found by the inverse Rosenblatt transformation. The sphere in the standard Gaussian space is transformed back to the original space. In this space the surface shape is still closed but will most likely not be spherical. The Rosenblatt transformation scheme is illustrated in Figure 5.3 for a 2-dimensional problem. As seen in the figure, the contour surface is reduced to a contour line for the 2-dimensional problem.

5.4 Long Term Analysis

At least two different ways of linear long term analysis is described in the literature. They are according to Haver [19]:

- Long term distribution of global maxima
- Long term distribution of d-hour extremes

They will both be presented in the following and application of these methods to non-linear systems will be discussed.

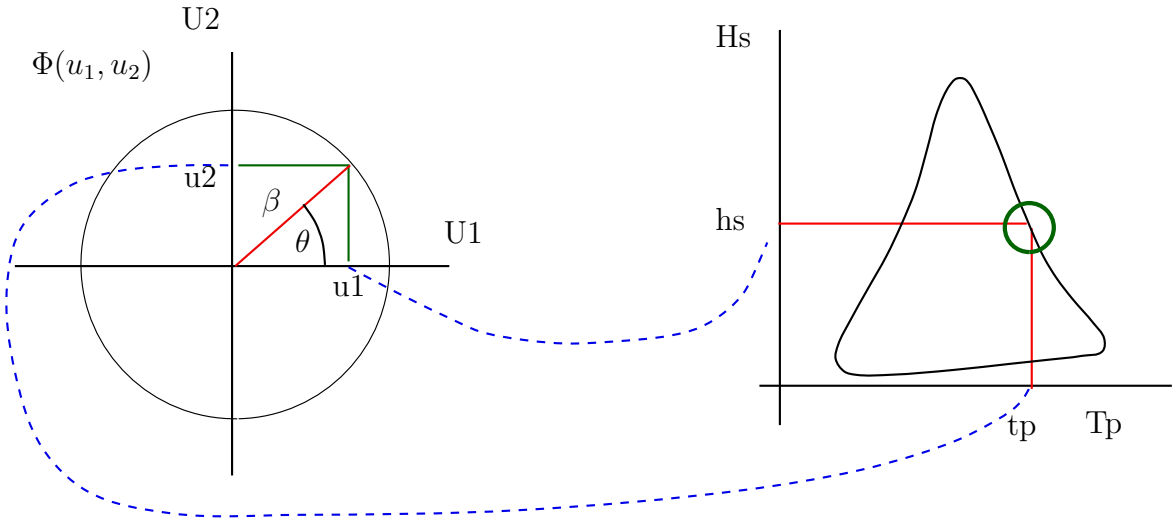

Figure 5.3: Rosenblatt transformation of a 2-dimensional problem [3].

5.4.1 Long Term Distribution of Global Maxima

In this method all global maxima in each sea state are found. Global maxima are defined as the largest maximum between adjacent zero wave up-crossings. If the process is narrow banded there will be one maximum for each zero wave up-crossing. In cases where the process is broad banded, one or several local maxima will occur for each zero wave up-crossing.
A critical maximum response value is x, and the probability of not exceeding this value by an arbitrary maximum in a given sea state is for a Gaussian process given by the Rayleigh distribution:

$$F_{X_d|H_sT_pW}(x|h,t,w) = 1 - exp\left\{-\frac{1}{2}\left[\frac{x}{\sigma_d(h,t,w)}\right]^2\right\}. \tag{5.25}$$

$F_{X_d\|H_sT_pW}(x\|h,t,w)$	Rayleigh conditional distribution for maxima	[-]
$\sigma_d(h,t,w)$	Standard deviation of the maximum response	[-]
x	Response	[-]

It is seen that the standard deviation is a function of the sea state parameters, so the maxima distribution will also be a function of these parameters. The long term distribution of maxima is given as:

$$F_{X_d}(x) = \frac{1}{\overline{v^+_{d,0}}(h,t,w)} \int_h \int_t \int_w v^+_{d,0}(h,t,w) F_{X_d|H_sT_pW}(x|h,t,w) f_{H_sT_pW}(h,t,w) dt dh dw. \tag{5.26}$$

The cumulative distribution of the response maxima, $F_{X_d|H_sT_pW}(x|h,t,w)$, is often modelled by a Rician distribution. The Rician distribution is a general distribution which will tend to the Normal or the Rayleigh distribution for limiting cases. For a narrow banded process the limiting case will be Rayleigh distributed, while it will tend to a Normal

$F_{X_d}(x)$	Cumulative distribution of the response maxima	[-]
$F_{X_d\|H_sT_pW}(x\|h,t,w)$	Cumulative distribution of the maximum response for given sea state	[-]
$f_{H_sT_pW}(h,t,w)$	Joint probability density function of the sea state parameters	[-]
$v^+_{d,0}(h,t,w)$	Zero wave up-crossing frequency for each sea state	[-]
$\overline{v^+_{d,0}}(h,t,w)$	Long term mean zero wave up-crossing frequency	[-]

distribution for a broad banded process. Over a period of T-years the expected number of global response maxima is given by:

$$n_T = T \cdot 365 \cdot 24 \cdot 3600 \cdot \overline{v^+_{d,0}}(h,t,w), \tag{5.27}$$

where:

$$\overline{v^+_{d,0}}(h,t,w) = \int_h \int_t \int_w v^+_{d,0}(h,t,w) f_{H_sT_pW}(h,t,w) dt dh dw, \tag{5.28}$$

and $v^+_{d,0}(h,t,w)/\overline{v^+_{d,0}}(h,t,w)$ is a weight factor which adjust the estimated number of global maxima in each sea state. The background of this weight factor can be found in the literature, see Haver [19]. The response value corresponding to a return period of T-years, i.e. the value which is expected to only be exceeded once in T-years, can be found by solving the following equation:

$$1 - F_{X_d}(x_{d,T}) = \frac{1}{n_T}. \tag{5.29}$$

5.4.2 Long Term Distribution of d-hour Extremes

This approach is similar to the former one. Instead of estimating all global maxima in each sea state, we now find the largest global maxima within each sea state. The sea state length is arbitrary to some degree, but should be chosen so that the sea state can be described as a stationary process. Haver proposes lengths from 20 minutes to 6 hours [19]. Shorter sea states lengths, e.g. 30 minutes, are often used for the Gulf of Mexico where shorter hurricane conditions are more common. In the North Sea it is customary to use a sea state length of 3 hours, which will be the choice for this thesis. The long term probability of exceeding the critical response value x is now given by Equation 5.30, this will later be called the long term formulation or the long term integral:

$$F_{X_d}(x) = \int_h \int_t \int_w F_{X_d|H_sT_pW}(x|h,t,w) f_{H_sT_pW}(h,t,w) dt dh dw, \tag{5.30}$$

where, $F_{X_d|H_s,T_p,W}(x|h,t,w)$, often is modelled by a Gumbel distribution:

$$F_{X_d|H_s,T_p,W}(x|h,t,w) = exp\left\{-exp\left\{-\left[\frac{x-\gamma_G}{\beta_G}\right]\right\}\right\}. \tag{5.31}$$

The parameters in the Gumbel distribution are dependent of distribution of the global maxima. If the global maxima are Rayleigh distributed the parameters are given as:

$$\gamma_G = \sigma_d(h,t,w)\sqrt{2ln\left(n_t(h,t,w)\right)}, \tag{5.32}$$

$$\beta_G = \frac{\sigma_d(h,t,w)}{\sqrt{2\left(ln\left(n_t(h,t,w)\right)\right)}}. \tag{5.33}$$

This assumption is valid as long as the initial response process can be said to be Gaussian, which often is the case for linear system.

In Equation 5.30 the weight function is left out. This is due to the simple fact that the frequency of extreme values in each sea state is equal to one. The value corresponding to a return period of T years is now given by:

$$1 - F_{X_{3h,T}}(x_{3h,T}) = \frac{1}{m_{3h,T}}, \tag{5.34}$$

where, $m_{3h,T} = T \cdot 365 \cdot 8$, is the number of three-hour sea states in T-years when all sea states are included in the sample.

5.4.3 Long Term Analysis of Non-linear Problems

When the structure in question is subjected to non-linearities the previous assumption of Rayleigh distributed maxima is no longer valid. Examples of non-linear problems can be slamming forces, second order loading, non-linear roll damping, non-linear stiffness, non-linear mooring stiffness and more. The integrals in Equation 5.26 and 5.30 are not directly affected by introducing non-linearities, and can still be used. However a new distribution for the response maxima has to be established when Equation 5.26 is going to be used. The response maxima for the non-linear problems can often be well modelled by a Weibull distribution [19]. The Gumbel distribution is well suited if the initial distributions has an exponential tail, but the parameters calculated from Equation 5.33 and 5.32 must be updated. More suited parameters can be established from the moment estimators and are valid for all situations:

$$\beta_G = \frac{\pi}{\sqrt{6}}s, \tag{5.35}$$

$$\gamma_G = \overline{x} - 0.577\beta. \tag{5.36}$$

In cases where numerical simulations can be performed a long term analysis can be carried out by running k, three-hour simulations for a large number of sea states. For each sea state that has been analysed k maxima are found. The mean, $\bar{x}$, and standard deviation, s, are calculated from these k maxima, and the Gumbel parameters are found from Equation 5.35 and 5.36. If sufficient number of sea states are analysed a grid of Gumbel point estimates is obtained and a response surface can be interpolated to fit the results. The Gumbel

parameters are then given as functions of the environmental variables:

$$\gamma_G = \gamma_G(h, t, w), \qquad \beta_G = \beta_G(h, t, w). \tag{5.37}$$

The long term distribution of the given response is found from the long term formulation using the parameters from Equation 5.37.

5.5 Equation of Motion

The motion x, of an floating structure can be found be solving the Equation of Motion:

$$m\ddot{x}(t) + c(x, \dot{x})\dot{x}(t) + k(x, \dot{x})x(t) = F(t) \tag{5.38}$$

m	Mass of the system (including added mass)	[kg]
$c(x, \dot{x})$	Non-linear damping coefficient	[Ns/m]
$k(x, \dot{x})$	Non-linear stiffness coefficient	[N/m]
F(t)	External load acting on the mass in the direction of the selected degree of freedom	[N]

The x in this equation is a generalized motion and can be consider as translation or rotation, and is often given on vector notation. The mechanical properties of the problem are characterized by the left hand side of Equation 5.38. In the right hand side the external loading is defined.

When solving the equation of motion it is normal to distinguish between linear and non-linear problems. The motion will by nature be non-linear, but in many cases the following linearisation approximation can be made, $c(x, \dot{x}) \rightarrow c(\dot{x})$ and $k(x, \dot{x}) \rightarrow k(x)$. If in addition the loading is a linear function of the surface elevation, the problem is said to be linear. This equation is solved numerically by Newmark's method in RIFLEX.

5.6 Hydrodynamics

The wave-induced excitation forces, i.e. Froude-Kriloff and diffraction forces, are assuming a long wave approximation and added mass and potential damping for the actual cross section together with the wave kinematics are computed. The viscous loads are computed using the drag term in Morison's equation.

5.6.1 Morison's Equation

Long and slender structures will be dominated by drag forces. For this kind of structures the load on a unit length is given by Morison's equation:

$$dF = \rho\pi\frac{D^2}{4}C_m\dot{u} - \rho\pi\frac{D^2}{4}(C_m - 1)\ddot{x} + \frac{\rho}{2}C_D D|u - \dot{x}|(u - \dot{x}), \tag{5.39}$$

where:

ρ	Density of water	$[kg/m^3]$
D	Diameter of structure	[m]
C_M	Mass coefficient	[-]
C_D	Drag coefficient	[-]
$\dot{x}$	Velocity of structure in x-direction	[m/s]
$\ddot{x}$	Acceleration of structure in x-direction	$[m/s^2]$
$\dot{u}$	Acceleration of water particle in x-direction	$[m/s^2]$
u	Velocity of water particle in x-direction	[m/s]

The mass- and drag-coefficients will be dependent on the Reynolds number, the Keulegan-Carpenter number, the surface roughness ratio and others. Faltinsen suggest to use the value two, for the mass coefficient [20]. Then half the contribution will be due to Froude-Kriloff forces and the other from diffraction force. Values between 0.4 and 1.2 are suggested for the drag coefficient.

5.6.2 Linear Wave Potential Theory

Regular waves can be modelled by Airy theory. The wave potential is expressed as:

$$\phi_0 = \frac{\zeta_a g}{\omega}C_1 cos\left(-\omega t + kXcosbeta_\zeta + kYsinbeta_\zeta + \psi_\zeta\right), \tag{5.40}$$

where:

ζ_a	Wave amplitude	[m]
g	Acceleration of gravity	$[m/s^2]$
k	Wave number	[1/m]
β_ζ	Direction of propagating wave	[rad]
ψ_ζ	Phase angle	[rad]

C_1 is for finite- and deep-waters, respectively, given as:

$$C_{1,finite} = \frac{coshk(Z + d)}{cosh(kd)}, \qquad C_{1,deep} = e^{kZ}, \tag{5.41}$$

and d is the water depth. Based on the wave potential the particle velocity and acceleration can be found. The velocity and acceleration are given as:

$$\begin{aligned} v_x &= -\zeta_a \omega cos\beta C_1 sin\Psi, \\ v_y &= -\zeta_a \omega sin\beta C_2 sin\Psi, \\ v_z &= \zeta_a \omega C_3 cos\Psi, \\ a_x &= \zeta_a \omega^2 cos\beta C_1 cos\Psi, \\ a_y &= \zeta_a \omega^2 sin\beta C_2 cos\Psi, \\ a_z &= -\zeta_a \omega^2 C_3 sin\Psi, \end{aligned} \tag{5.42}$$

where:

$$\Psi = -\omega t + kXcos\beta + kYsin\beta. \tag{5.43}$$

For deep water, $C_1 = C_2 = C_3 = e^{kZ}$, and for finite water C_1 is given in Equation 5.41 while C_2 and C_3 is:

$$C_2 = \frac{coshk(Z+d)}{sinh(kd)}, \qquad C_3 = \frac{sinhk(Z+d)}{sinh(kd)}. \tag{5.44}$$

5.6.3 Irregular Wave Theory

In the ocean it is rare to observe single regular waves as described with Airy theory. Normally the situation is more chaotic and irregular. To describe this situation we need to apply irregular wave theory. The idea is to simulate irregular sea by super imposing a large number of linear waves. Mathematically this is written as a sum of wave components:

$$\zeta = \sum_{j=1}^{N} A_j sin\left(\omega_j t - k_j x + \epsilon_j\right), \tag{5.45}$$

where:

ζ	Wave elevation	[m]
A_j	Wave amplitude	[m]
ω	Wave frequency	[rad/s]
k	Wave number	[1/m]
ϵ_{jk}	Random phase to recover statistic behaviour	[-]

By now introducing the wave spectrum, $S(\omega)$, the wave amplitude can be written as:

$$\frac{1}{2}A_j^2 = S(\omega_j)\Delta\omega. \tag{5.46}$$

The wave elevation is then, by combining Equation 5.46 and 5.45:

$$\zeta = \sum_{j=1}^{N} \sqrt{2S(\omega_j)\Delta\omega} sin\left(\omega_j t - k_j x + \epsilon_j\right). \tag{5.47}$$

Several wave spectra exist to describe different sea states at different location. In the North Sea there are two standardized spectra which are common to use if the details of the site in question is unknown. They are the Pierson-Moskowitz spectrum, which is based on measurements from the North Atlantic Ocean. The second wave spectrum is the Jonswap spectrum, which is based on measurements from the south-eastern part of the North Sea. In this thesis the Jonswap spectrum will be used. The Jonswap spectrum is built in to SIMO and can be chosen as basis for the irregular wave model. From the SIMO user manual [21] the Jonswap spectrum is given as:

$$S_\zeta^+(\omega) = \frac{\alpha_J g^2}{\omega^5} exp\left(-\beta_J \left(\frac{\omega_p}{\omega}\right)^4\right) \gamma_J^{exp\left(-\frac{(\omega/\omega_p-1)^2}{2\sigma_J^2}\right)}, \tag{5.48}$$

with:

α	Spectral parameter	[-]
ω_p	Peak frequency	[rad/s]
γ_J	Peakedness parameter	[-]
β_J	Form parameter, default value $\beta = 1.25$	[-]
σ_J	Spectral parameter, default value $\sigma_a = 0.07$ for $\omega \leq \omega_p$ $\sigma_b = 0.09$ for $\omega > \omega_p$	[-]

This is a 5-parameter Jonswap spectrum, where β and σ are used with their default values, and the other parameters are functions of Hs and Tp. The spectral parameter is:

$$\alpha_J = \left(\frac{H_s \omega_p^2}{4g}\right)^2 \frac{1}{0.065\gamma_J^{0.803} + 0.135}, \tag{5.49}$$

and the peakedness parameter is given as:

$$\gamma_J = exp\left[3.484(1 - 0.1975\delta \frac{T_p^4}{H_s^2}\right], \tag{5.50}$$

with:

$$\delta = 0.036 - 0.0056 \frac{T_p}{\sqrt{H_s}}. \tag{5.51}$$

5.7 Wind

In SIMO the wind field is 2-dimensional propagating in the horizontal direction. The wind model is superimposed by two parts, one constant mean wind velocity and one fluctuating part called gust. The constant mean wind is often described by the one hour mean velocity at a reference elevation. The gust is assumed to be a Gaussian stochastic process and can be

described by a number of gust spectra. The following wind spectra are available in SIMO, Harris, Davenport, Wills, Sletringen, ISO 19901-1 (NPD) and API [21].

The variation of wind in vertical direction is described by a wind profile valid for all wind spectra. In SIMO this wind profile is given by

$$u(z) = u_r(\frac{z}{z_r})^{\alpha_W}, \tag{5.52}$$

where:

z	Elevation above mean water level	[m]
z_r	Reference height	[m]
$u(z)$	Velocity at height z	[m/s]
u_r	Average velocity at reference height	[m/s]
α_W	Height coefficient (0.11 - 0.14)	[-]

Statoil has in their Hywind Metocean Design Basis proposed to use the ISO 19901-1 spectrum to model the wind. The design wind speed, $u(z,t,)$ at height z above sea level corresponding to an averaging period of $t \leq t_0 = 3600s$ is:

$$u(z,t) = U(z)\left[1 - 0.41 \cdot I_u(z) \cdot ln\left(\frac{t}{t_0}\right)\right]. \tag{5.53}$$

The one hour mean wind speed, U_z is:

$$\begin{aligned} U(z) &= W\left[1 + C \cdot ln\left(\frac{z}{10}\right)\right], \\ C &= 5.73 \cdot 10^{-2}(1 + 0.15 \cdot W)^{\frac{1}{2}}, \end{aligned} \tag{5.54}$$

and the turbulence intensity factor is

$$I_u(z) = 0.06\left[1 + 0.043 \cdot W\right] \cdot \left(\frac{z}{10}\right)^{-0.22}, \tag{5.55}$$

where W is the one hour mean wind speed at $z = 10m$. The dynamic wind behaviour can be modelled by adding longitudinal wind speed fluctuations to the mean wind speed. The spectrum is given as:

$$S(f) = \frac{320\left(\frac{W}{10}\right)^2 \cdot \left(\frac{z}{10}\right)^{0.45}}{\left(1 + \bar{f}^n\right)^{\frac{5}{3n}}}, \tag{5.56}$$

where, $n = 0.468$, and:

$$\bar{f} = 172f\left(\frac{z}{10}\right)^{\frac{2}{3}} \cdot \left(\frac{W}{10},\right)^{-0.75} \tag{5.57}$$

with:

$S(f)$	Spectral density at frequency $f(Hz)$	$[m^2s^{-2}/Hz]$
z	Height above sea level	[m]
W	1-hour mean wind speed at 10m above sea level	[m/s]

The behaviour of the fluctuating wind can be seen by plotting the gust spectra. This is shown in Figure 5.4. It is seen that the behaviour of the wind fluctuation is influenced by the mean wind velocity.

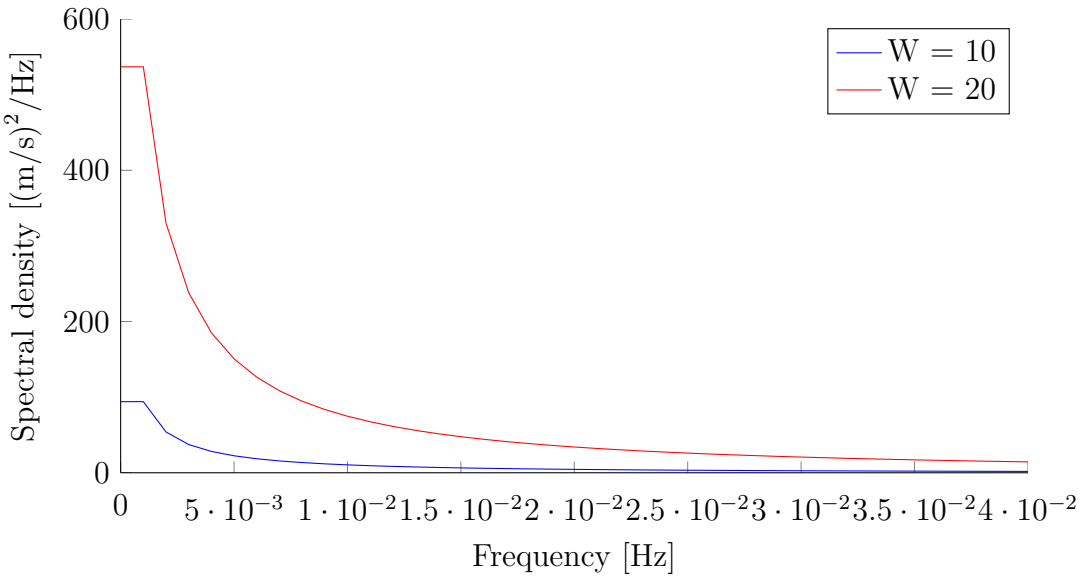

Figure 5.4: Wind gust spectrum

The wind is also fluctuating in the direction normal to the mean wind direction. This is described by normal spectrum given by the following equation:

$$S_v^+(z,\omega) = \frac{ku(z)^{-2}Kx'}{\omega(1+9.5x')^{\frac{5}{3}}}, \tag{5.58}$$

where:

S_v^+	Spectral density normal to mean wind direction	$[(m/s)^2/(rad/s)]$
k	von Karmans constant = 0.4	[-]
K	scale factor = 17	[-]
x'	$\omega z/2\pi u(z)$	[-]

6 Computer Analyses

6.1 Introduction

In this chapter the procedure of the computer analyses will be explained. An introduction to the applied computer programs will also be given. The tool applied in this work is the RIFLEX/SIMO software which is used to run time-domain simulations of a wind turbine model made by Statoil. The wind turbine model will later be referred to as just the model.

The computer analyses have been carried out in two stages. First the full long term analysis is performed, and based on the results from the long term analysis a detailed analysis of the response at the design point is carried out for selected responses. Each of the two stages will be described in detail later.

6.2 RIFLEX

RIFLEX is a computer program for structural analyses based on a finite element approach. It was first developed as a tool for static and dynamic analysis of slender marine structures, such as mooring line systems, umbilicals and conventional steel risers. One great advantage of RIFLEX is its robust non-linear time domain formulation which also is applicable for irregular wave analysis. This feature makes RIFLEX well suited for analyses of complex structural systems. Another advantage is its capabilities to couple with external programs, which expands the range of problems possible to solve.

In general, a RIFLEX-model is built by supernodes and lines. The supernodes define connection points in the model, and can be classified as free, fixed, or prescribed depending on their boundary conditions. The supernodes are connected by lines which are linear structural elements. They are identified by a line number and a line type. The properties of the line are defined in the line type, which can be referred several times in a system. This is very convenient for systems with multiple identical lines. A line can be sequenced into several segments with homogeneous cross sectional properties. For each segment the cross-section component, length and number of finite elements is specified. The element mesh will be computed automatically based on the topology, line and component description [22]. The arrangement of nodes, line and segments are shown in Figure 6.1

In RIFLEX the cross-sectional parameters is given as input. In the model there are defined two different types of cross-sections. The first one is used for the turbine blades, and the second for all other parts. All lines are modelled as beam elements except for the mooring lines which are bar elements. For each cross-section the axial, bending and torsional stiffness are given for beam elements. For bar elements only the axial stiffness is given. Hydrodynamic force coefficients are also assigned as part of the cross-section properties. Linear- and quadratic-drag is assigned together with added mass. For the foil-cross section the airfoil coefficients are defined instead of the hydrodynamic coefficients. The drag-, lift- and mass-coefficients are defined as functions of the angle of attack.

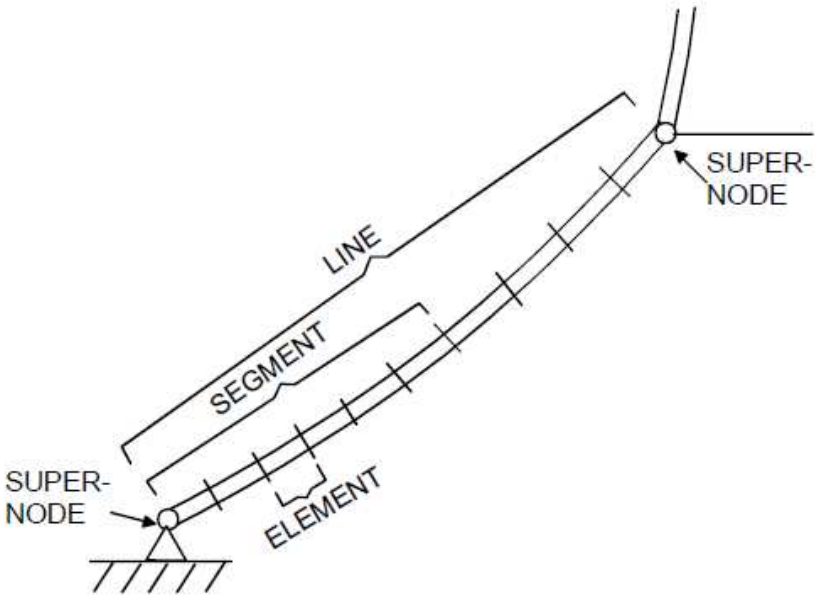

Figure 6.1: System definitions terms in RIFLEX-model.

6.3 SIMO

SIMO is, according to the user manual, a computer program for simulation of motions and station-keeping behaviour of a complex system of floating vessels and suspended loads. SIMO carries out a time domain simulation and presents the results as time traces, statistic and spectral analysis for all forces and motions for all bodies in the analysed system. This means that while RIFLEX calculates the structural displacements and rotations, etc. SIMO generates the environment which is applied as load to the structure.

6.4 SIMA

SIMA is currently under development at MARINTEK and provides a graphical interface to RIFLEX and SIMO. SIMA has in this work been used to run the computer analyses. SIMA offers to run sets or spaces of simulations. With this option it is possible to run several cases or parameter variations as one analysis in SIMA. This is very useful. It is also possible to implement scripts so that parameters can be computed as functions of other variables during the analysis. This is used to change the wave- and wind-seed number for each simulation. SIMA also offers to run multiple analyses simultaneously on multiple CPUs. This can be extremely time-saving when a large number of simulations are analysed.

6.5 Modelling of Mooring Lines

The modelling of the mooring lines will be presented in the following section. Structural descriptions of the mooring lines are seen in Figures 4.2 and 4.3. Each of the mooring lines

can be divided into three parts, the main mooring line, and the two delta lines. In the model, the main- and delta-mooring lines are modelled as nine lines. The three main mooring lines are identical and are modelled with the same line type. The same is true for the delta lines, which also are modelled with an identical line type. It can be seen from Figure 4.2, that the main mooring lines consist of different components of chains and ropes. When this is to be modelled in RIFLEX it is convenient to have a segment representing each of the different components. The cross-sectional parameters for the main mooring lines are seen in Table 6.1. The same line type is used for all three main mooring lines.

Table 6.1: Cross-sectional parameters for the line describing the main mooring lines.

	Mass coefficient [kg/m]	External Area [m^2]	Axial Stiffness [N]	Quadratic Drag [-] (Normal)	Diameter [m]	Added Mass [-] (Normal)
Bottom chain	126	0.02	5.45E+08	1.273	0.152	1
Spiral Strand Rope	32	0.01	6.10E+08	1.000	0.078	1
Link Chain	127	0.02	5.45E+08	1.273	0.152	1
Clump Weight	66640	19.83	5.45E+08	1.000	5.000	1
Link Chain	126	0.02	5.45E+08	1.273	0.152	1
Spiral Strand Rope	32	0.01	6.10E+08	1.000	0.078	1

For the mooring lines it is possible to define linear and quadratic drag in normal and tangential direction. In Table 6.1 only the quadratic drag in normal direction is presented. All of the other drag contributions are zero. In the same manner is the added mass coefficient also given in normal and tangential direction. The tangential added mass is zero for all mooring lines and is therefore not included.

The delta lines consist of 50 meter long chain segments and are modelled by one segment with cross-sectional specifications seen in Table 6.2. The same line type is used for all of the delta lines.

Table 6.2: Cross-sectional parameters for the line describing the delta lines.

	Mass coefficient [kg/m]	External Area [m^2]	Axial Stiffness [N]	Quadratic Drag [-]	Diameter [m]	Added Mass [-]
Delta line	139	0.02	5.44E+08	1.273	0.152	1

The mooring line system on Hywind Demo is modelled with bar elements. This is a good model for chains, which in fact have zero bending stiffness. Ropes however can have some bending stiffness, and the obtained configuration can depend on the choice of element. The behaviour of bar- and beam-elements have been compared in [23], for modelling of risers in uniform current. It is found that the beam curvature is very close to the cable curvature, and the configuration of the mooring line must thus be the same for bar and beam elements. It will therefore be adequate to model the full length of the mooring lines as bar elements.

6.6 Modelling of Hull and Tower

Since the Hull and Tower of Hywind Demo is so long and slender it is possible to model also these parts in RIFLEX. The hull and tower is modelled with two lines, line 1 and line 2. Line 1 defines the hull from the keel to the attachment point of the mooring lines, i.e. from z = -100 to z = -53. Line 2, models the remaining hull and tower, i.e. from z = -53 to z = 65. The cross-sectional properties of Line 1 and Line 2 are defined by Line Type 1 and Line Type 2. The cross-sectional specifications of the two line types are given in Table 6.3. For values that vary over the length of the hull, the minimum and maximum values are given in the tables. The varying parameters are also plotted as functions of the height in Figures 6.2 and 6.3. In Figure 6.2 the structural parameters mass per meter, external area and hydrodynamical radius are plotted. The parameters are constant over the length of a segment and a discrete function is thus obtained. The same can be said for the stiffness parameters in Figure 6.3. By considering the plot of the mass per meter it is clearly seen how heavily ballasted the structure is towards the bottom of the hull. Two inconsistencies are seen in the plot of the stiffness. At approximately height, z = 17, and, z = 27, two spikes occur. This is due to the flanges connecting the different parts of the tower, which are particularly stiff.

Table 6.3: Structural input parameters for the hull and the tower.

	Number of Segments	Mass coefficient [ton/m]	External Area [m^2]	Gyration Radius [m]
Line 1	16	9.75 - 162	54.6	1.62 - 5.08
Line 2	52	0.9 - 43.3	4.49 - 54.6	1.20 - 6.00
	Stiffness			
	Axial [N]	Bending [Nm^2]	Shear [m]	Torsional [Nm^2/m]
Line 1	2.08e+11	1.79e+12	0.00e+00	8.97e+11
	2.73e+11	2.35e+12		1.17e+12
Line 2	2.49e+07	1.98e+07	0.00e+00	9.89E+06
	5.86e+08	2.35e+09		1.17E+09

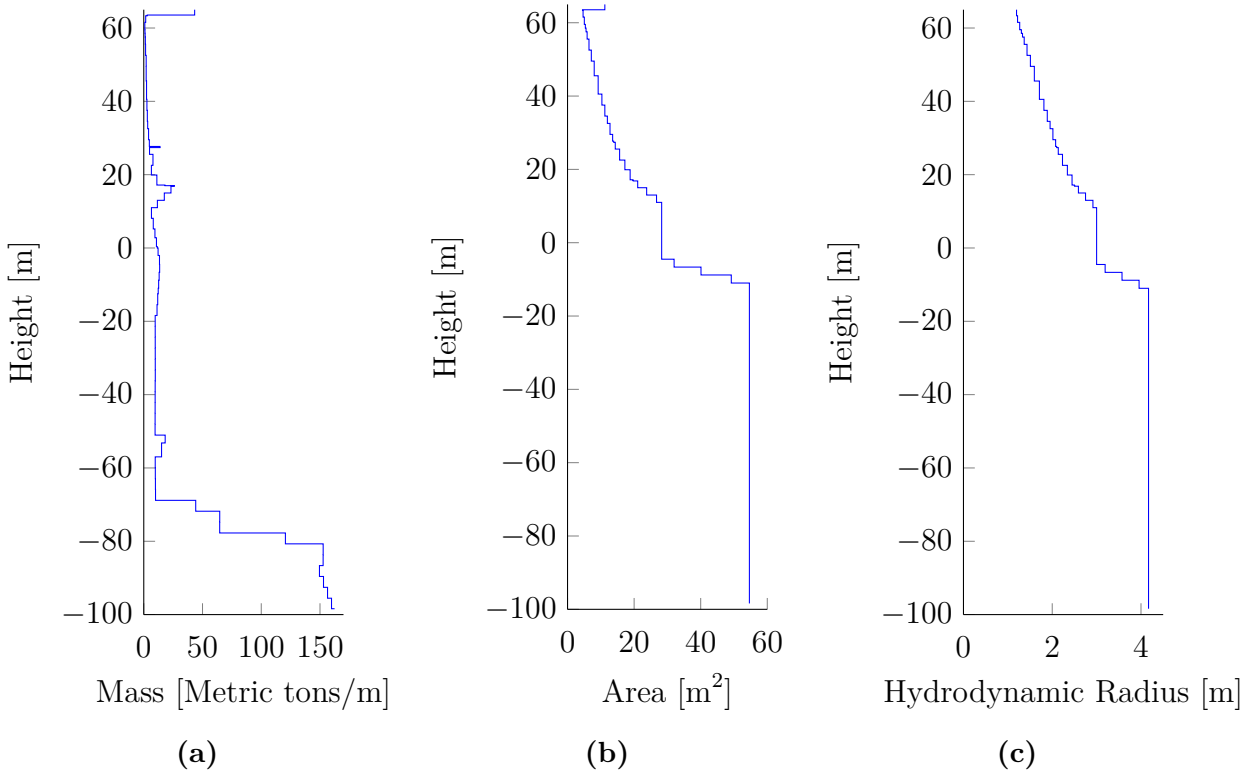

Figure 6.2: Cross sectional parameters for the hull and the tower.

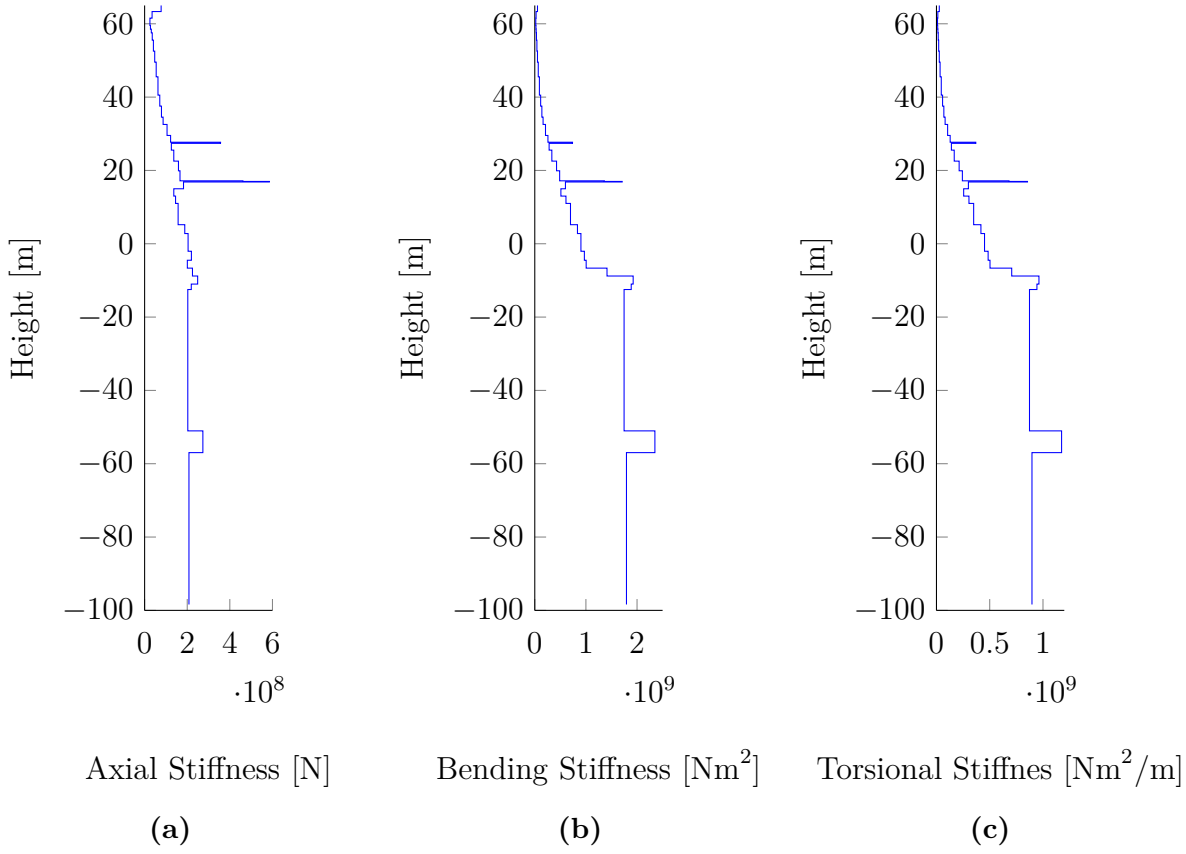

Figure 6.3: Structural cross sectional parameters for the hull and tower.

6.7 Modelling of Wind Turbine Blades

A wind turbine module is implemented in RIFLEX. This module makes it possible to consider loads on the wind turbine blades. It is also possible to apply a pitch-angle control system and simulate extraction of electrical power.

The wind turbine blades are modelled in the same manner as the rest of the RIFLEX-structure. There are three blades with line number bl1, bl2 and bl3 in the model. They are all described by the same line type. The blade line type consists of 41 different segments with its own cross-section. A special foil cross-section type is defined for the wind turbine blades. For these foil cross-sections, aerodynamic coefficient are stored in an air-foil library. These values are obtained from wind tunnel test of the turbine blades. For each segment the mass-, drag- and lift-coefficients are defined as functions of the angle of attack, α, which is defined in Figure 5.2. The aerodynamic coefficients are unique for each segment. The mass per meter, the coord-length of the foil, the projected area and the stiffness parameters must also be given for the foil cross-sections. For one air-foil segment the aerodynamic coefficients are shown in Figure 6.4. The structural coefficients are presented in Figures 6.5 and 6.6. They are here plotted as discrete functions of the blade length.

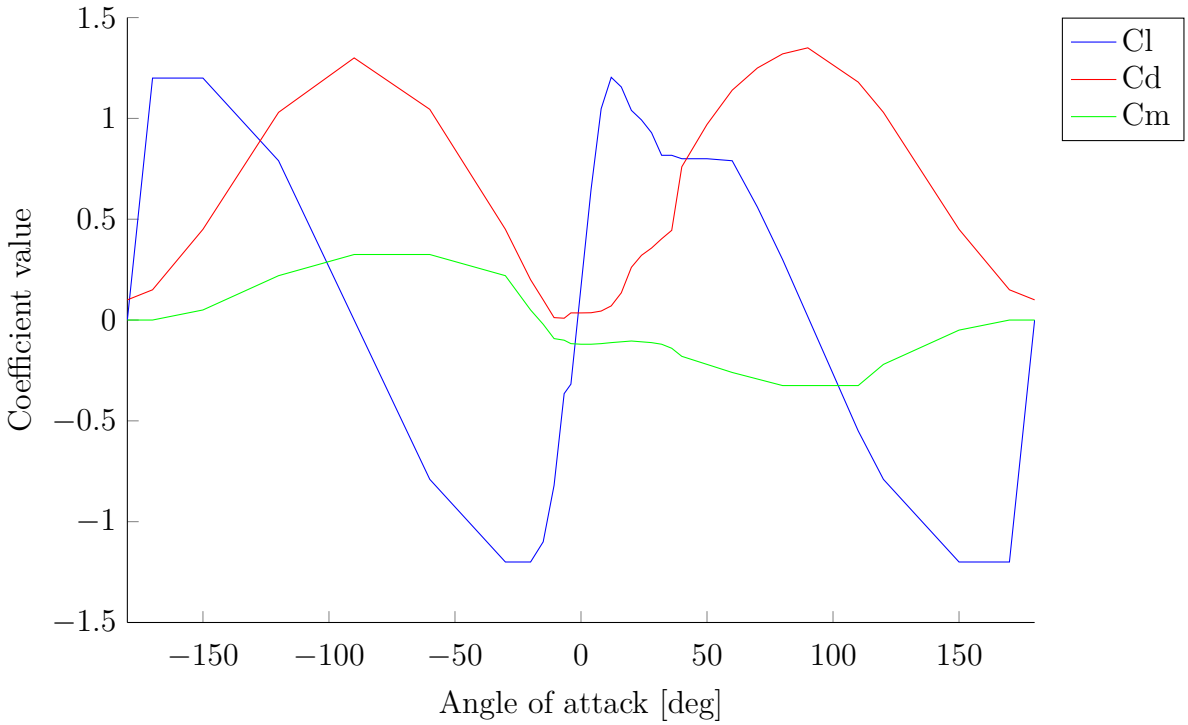

Figure 6.4: Plot of the aerodynamic coefficients as function the inflow angle for air-foil segment 10.

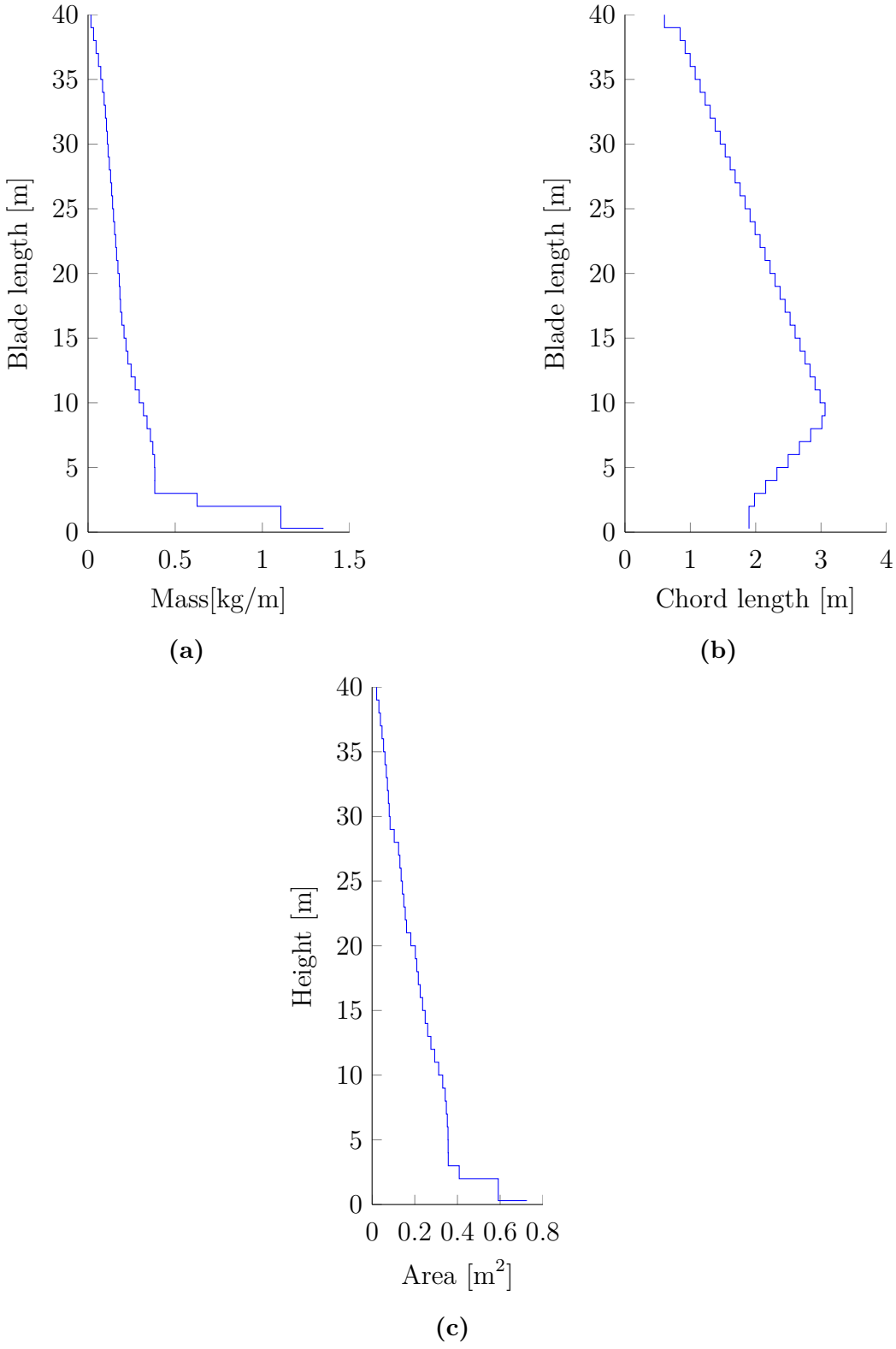

Figure 6.5: Foil cross sectional parameters.

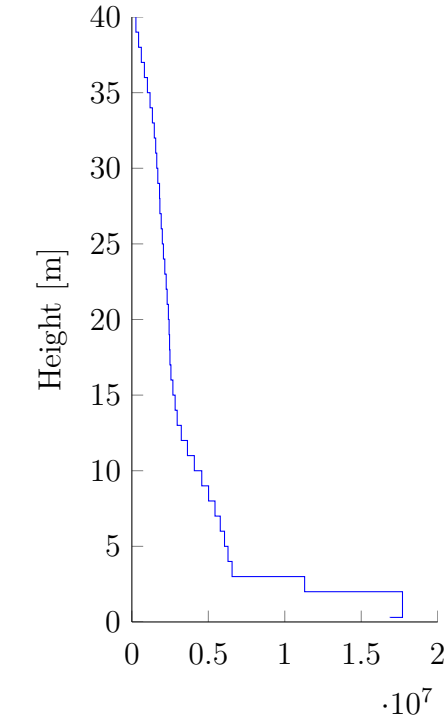

Blade Axial Stiffness [N]

(a)

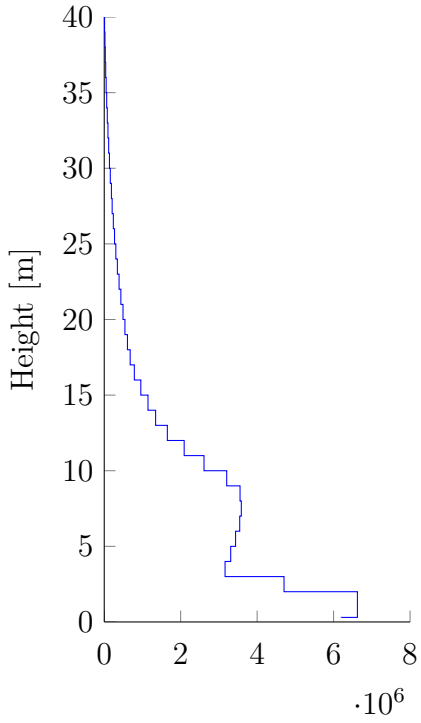

Blade Bending Stiffness [Nm^2]

(b)

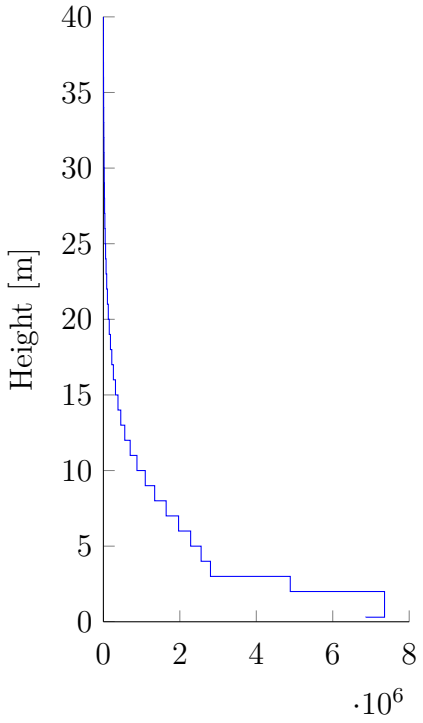

Blade Bending Stiffness, y [Nm^2]

(c)

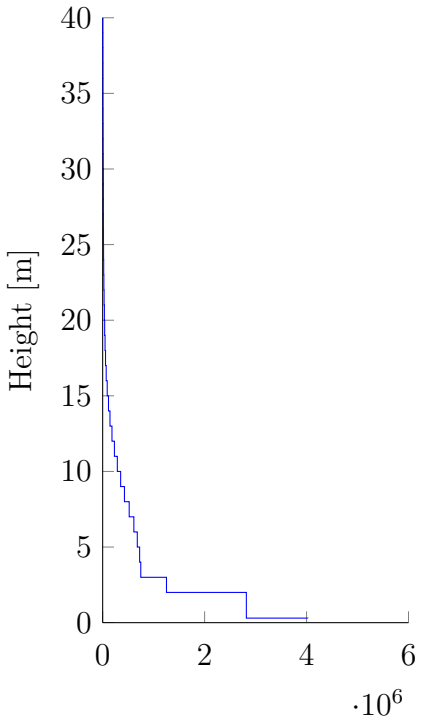

Blade Torsional Stiffnes [Nm^2/m]

(d)

Figure 6.6: Foil cross sectional structural parameters.

6.8 Modelling of Waves

The waves are generated in SIMO where a Fast-Fourier transformation algorithm computes the wave train from the given wave spectra. The seed number is changed for each analysis so that the same phase angles are not used again for different realisations of the same sea state. This is accomplished by the helpful script option in SIMA where the wave seed number is a function of other variables in the computation:

$$Waveseednumber = seedwave + (H_s \cdot T_p \cdot W) + 1000, \tag{6.1}$$

where seedwave is ranging from 1 to 15 for the 15 realisations of one environmental state.

There is an option in SIMO to generate Stokes 5^{th}-order waves. This is the normal approach to simulate waves and it describes deterministic waves well. However, for modelling of irregular waves it is only possible to use Airy-theory in SIMO. The most significant difference between the two approaches is that the pressure boundary condition at the surface, p = 0, is only valid at the mean water level for Airy theory, while it is approximately correct at the wave surface for Stoke's theory. The Gaussian assumption, adopted for the Airy theory, will under predict the most extreme crest heights in real ocean sea states with 10-20% [19]. This must be accounted for when the problem is sensitive to the details in the surface process. It is assumed that this is not the case for Hywind Demo.

6.9 Modelling of Wind

Turbulent wind can be understood as an evolving 3-dimensional vortex field that is swept by the structure. There are numerous ways to model wind fields. Say that the direction of the mean wind is called, x, the horizontal direction across the wind, y, and the vertical direction, z. If the wind field is uniform it has no variations in the horizontal plane, i.e. the xy-plane. This is opposite to the uncorrelated wind which will vary as a function of all the spatial parameters. Moreover stationary wind will be independent of time which is opposite of fluctuating wind. To catch the full behaviour of the entire wind turbine the wind has to be modelled as an uncorrelated 3-dimensional fluctuating wind field.

A real wind field vary in the spatial direction. It also varies with respect to time, i.e. a totally different picture would be seen at time t_2 than for t_1. To generate such wind external software must be used, e.g. TDHMill. Such software has not been available for this thesis, so the wind is modelled as a uniform wind field. This means that there is no variation of the wind in the horizontal directions.

The wind field will vary with time due to the super imposed fluctuation spectrum. No interaction between the wind field and the structure is accounted for. There are plans to include this in later versions of RIFLEX/SIMO. The relative velocity between the wind and the wind turbine are however accounted for. The forces on the wind turbine blades are calculated according to the BEM theory described in Chapter 5.2.

As for the waves it is wanted to have different wind seed numbers for each realisation of the time-domain simulation. A wind seed number can also here be defined as a function of the other parameters in the simulation. The following equation is implemented in the SIMA set-up:

$$Waveseednumber = seedwind + (H_s \cdot T_p \cdot W) + 2000. \tag{6.2}$$

where seedwind is ranging from 1 to 15 for the 15 realisations of one environmental state.

6.10 Modelling of Current

A stationary current is applied in all simulations. The current is applied in the same direction as the wind and the waves, i.e. along with mooring line 10. Current values are obtained from measurements at the Troll field and adopted for used at the Hywind Demo location. Current corresponding to the 1-year return period is applied in all of the simulations. The current is modelled as a partially linear profile with the following values:

Table 6.4: Current profile values.

Depth [m]	Current speed [cm/s]
3	142
25	101
50	95
100	64
200	61
220	0

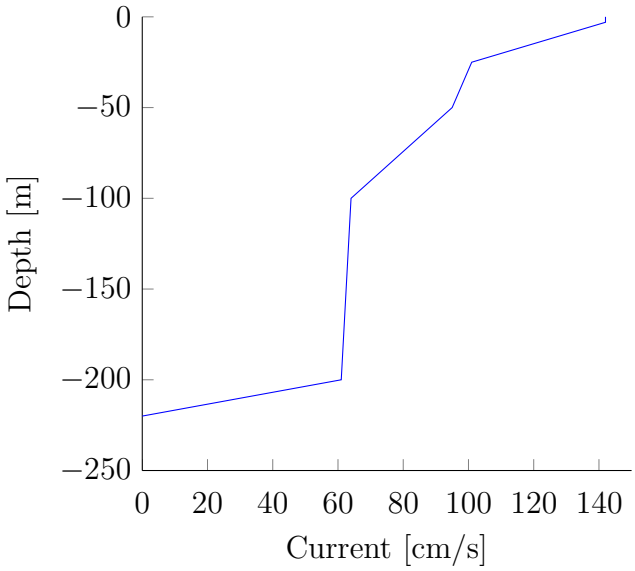

Figure 6.7: Plot of the current profile.

6.11 Post-processing

With the total number of analyses in SIMA exceeding 2000, a lot of effort has been put into data handling and post processing. Matlab is well suited for handling large amounts of data and is therefore a natural choice for the post processing. The float in the post processing is inspired by RIFLEX, where each part of the analysis writes a result file which can be used by the following programs. The same approach has been adopted for the post processing part of this thesis. The results from each matlab routine are stored in mat-files.

The float of the post processing and the reliability analysis are presented in Figure 6.8. In the post processing part, the binary files from the RIFLEX analyses are treated. The extreme values are extracted from the time-series and the Gumbel parameters are computed. The results of the post processing are stored in the mat-file, for_reg.mat. This file can then be reopened by the reliability analysis.

The reliability analysis is run from the Matlab routine, Main.m. The method of reliability analysis is presented in more details in Chapter 8 and the Matlab routines are included as a digital appendix which can be read more about in Appendix D.

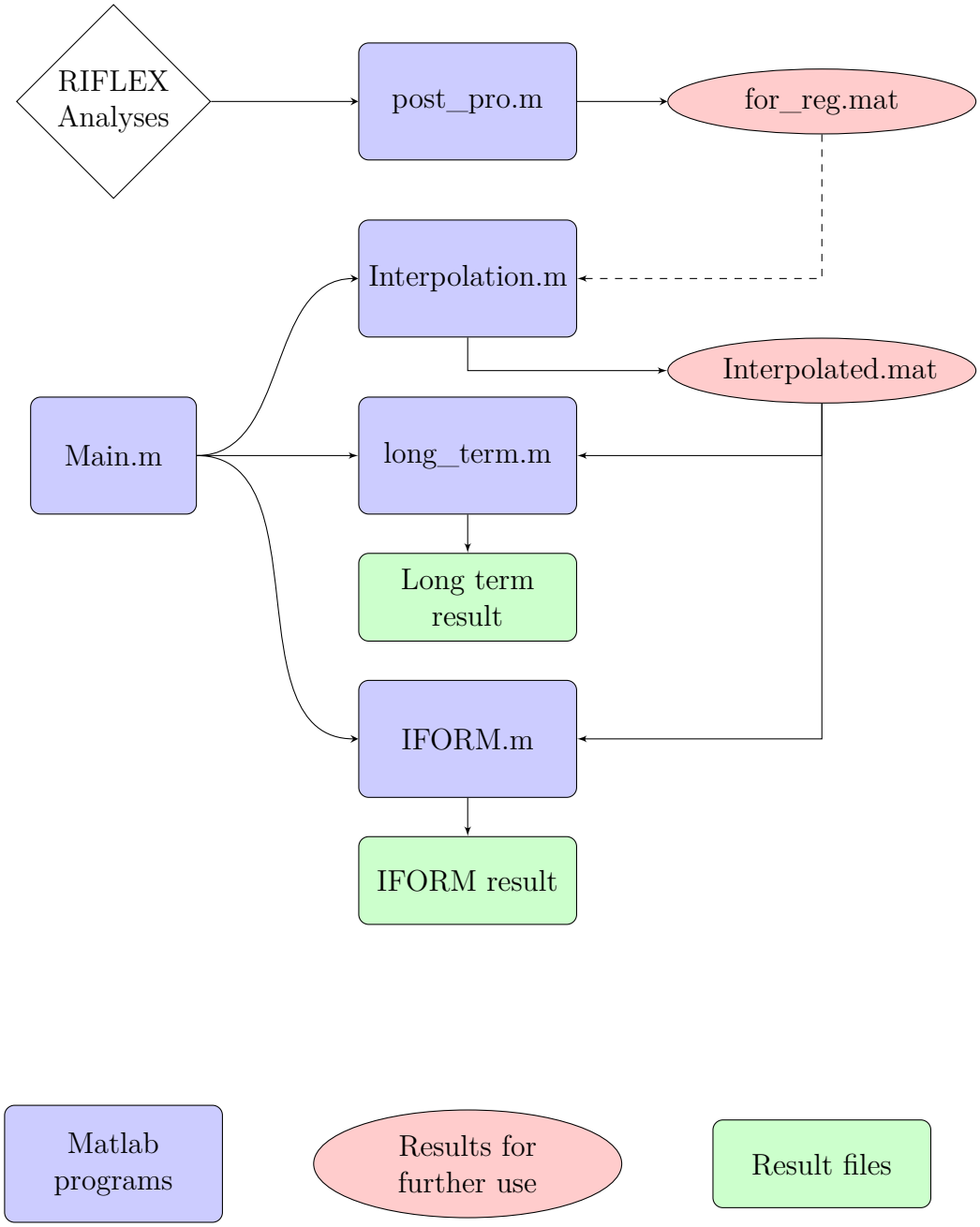

Figure 6.8: Flowchart

6.12 Discussion of The Computer Analysis

6.12.1 Start-up Transients

A computer analysis in RIFLEX/SIMO is carried out in two parts, static and dynamic analysis. The static analysis is always performed before the dynamic analysis. In the static analysis the structure is taken from a stress free configuration, to a static equilibrium by applying static forces and initial displacements. In the dynamic analysis the dynamic loads, such as wind and wave loads, are applied. When the dynamic forces are acting on the structure the mean position from the static analysis will change to a new mean position for the dynamic analysis. For severe environmental loading this new mean position can deviate significantly from the old static position and it will therefore be meaningful to exclude this transition range from the domain of the statistical parameters.

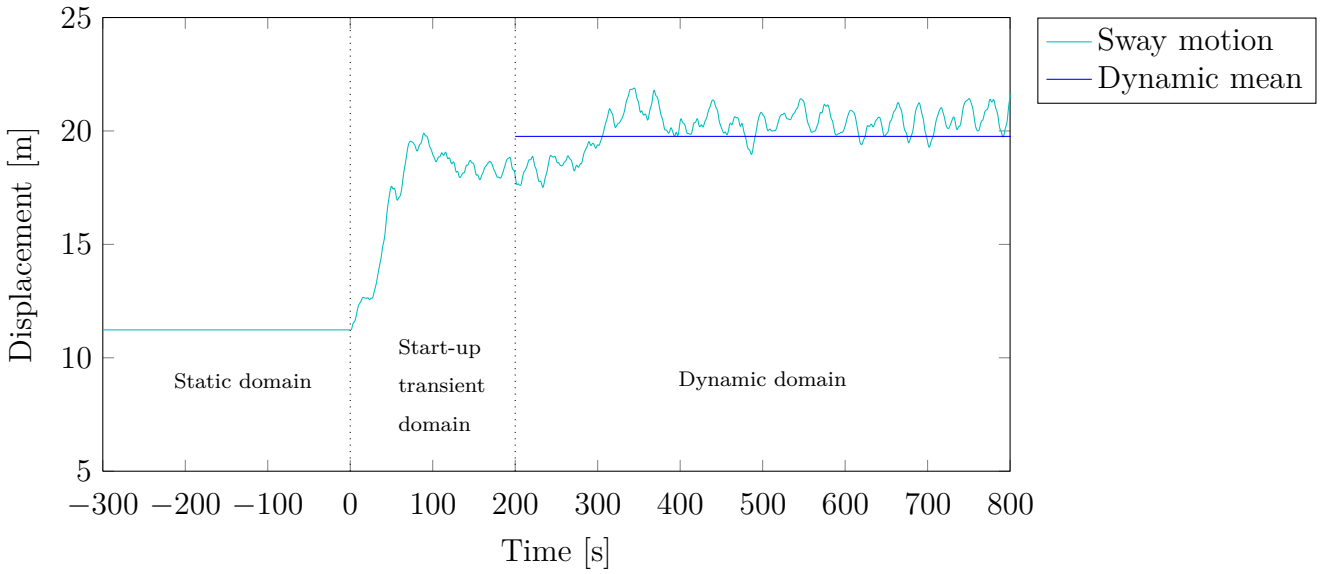

Figure 6.9: Time-series plot with start-up transients. Statistical parameters are calculated based on the region

For the time-domain simulations a start-up period of 200s is selected. The value of 200s is found to be sufficient for the structure obtain its new mean position. An illustration of this problem can be seen in Figure 6.9. The importance of the transition range on the statistical parameters is quite significant according to Moy [8]. His results shows a deviation of up to 16% for the mean value of axial stress with and without start-up transients.

According to DNV the design load in the mooring lines is split in one static- and one dynamic-part. This is useful to give different safety factors to the two parts. In this analysis this has not been done, since it is of interest to calculate the the design loads without including safety factor.

6.12.2 Convergence

A convergence study is carried out to determine the time increment optimal for the time-domain simulations. Four time increments are compared, with ΔT as 0.05, 0.02, 0.01 and 0.005. The simulation length is 1000s. The numeric time integration which is performed by RIFLEX to solve the time-domain problem has shown to be sensitive to the time increment used in the calculation. If the time step is too large the numerical integration will become unstable and the calculation will diverge. If this is the case SIMA will in most cases exit the simulation with a warning. In Figure 6.10 the roll response of four time-domain simulations are plotted. The set-up of these four analyses is identical except for the time increment which is varied. In Figure 6.10 a part of the time series plot from the convergence study is presented.

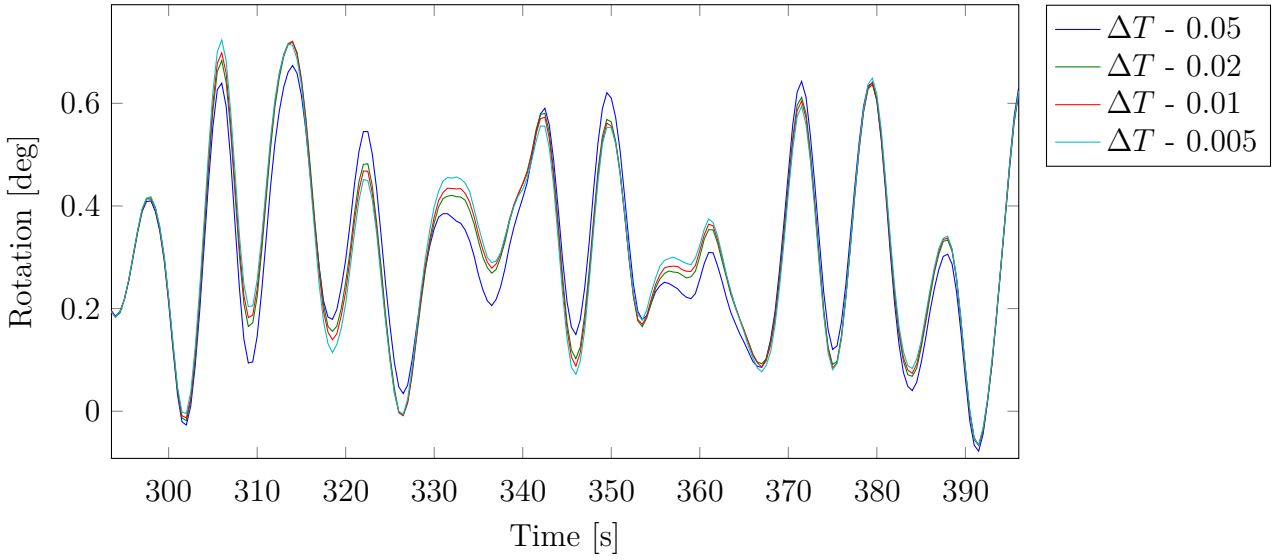

Figure 6.10: Time series plot of roll with different time increments.

Some remarks can be made from Figure 6.10. First it is seen that the local maxima and minima have the same location in time for varying time steps. This means that the period of the response is the same for all the time increments. Secondly, it is seen that the deviations are located near the local turning points, but there is no consistency in which case give the highest value.

In Figure 6.11 are the most important results from the convergence test presented. The smallest time increment, $\Delta T = 0.005$, is taken as the exact solution. It is off interest to evaluate the residual between the exact case and the three others. The mean and standard deviation of the maxima- and residual-values can be calculated and are presented in Table B.1. Variations of the time increment are seen to influence the mean and standard deviation of the maxima to a rather small extent. The mean residual is found to be almost zero for all cases. However a decreasing tendency is seen for the standard deviation of the residual as the time increment is reduced. Last a normalized value of the residual standard deviation is presented. These values are obtained by dividing the standard deviation of the residual

Table 6.5: Results of the convergence study. The three motions roll, pitch and heave are evaluated.

	Time increment	0.05	0.02	0.01	0.005
Roll	Mean Maxima	2.116	2.119	2.1189	2.1216
	Standard deviation of maxima	0.519	0.5112	0.5104	0.5087
	Mean residual	-0.006	-0.003	-0.003	-
	Standard deviation of residual	0.073	0.026	0.016	-
	Normalized standard deviation	3.462 %	1.221 %	0.762 %	-
Pitch	Mean Maxima	0.448	0.453	0.454	0.455
	Standard deviation of maxima	0.131	0.131	0.130	0.131
	Mean residual	-0.007	-0.002	-0.001	-
	Stadndard deviation of residual	0.031	0.012	0.007	-
	Normalized standard deviation	6.847 %	2.597 %	1.498 %	-
Heave	Mean Maxima	0.368	0.369	0.369	0.369
	Standard deviation of maxima	0.109	0.110	0.110	0.110
	Mean residual	-0.001	0.000	0.000	-
	Stadndard deviation of residual	0.006	0.002	0.001	-
	Normalized standard deviation	1.561 %	0.527 %	0.290 %	-
	Computational time	239	355	731	1092

with the mean value of the maxima. The normalized standard deviation is seen to be small for all time increments, there are however significant differences between each of the cases.

In Figure 6.11, values for the pitch motion are plotted. The standard deviation of the residual is normalised with respect to the mean of the maxima, and plotted together with the computational time of that case. This gives an impression of how much the time invested in the computations is really worth. By going from a time increment of 0.05s to 0.02s the computation time increases with about 50%, while the normalized standard deviation of the residual is decreased to one third. Further on, by decreasing the time increment additionally to 0.01s, the computational time increases with over 100%. This only pays off with a decrease of 40% in the normalized standard deviation. A 40% decrease in the standard deviation is always of interest, but since the values already are small the time cost is too high. Based on this it is chosen to use a time increment of $\Delta T = 0.02s$ for the time-domain simulations in the reliability analysis.

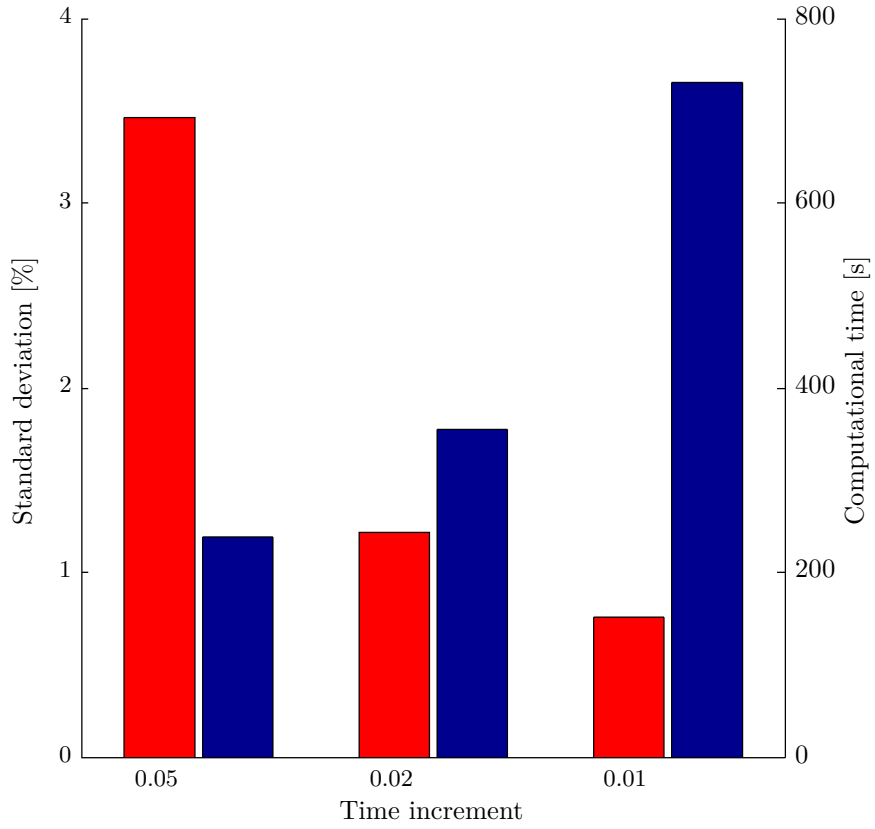

Figure 6.11: The standard deviations of the errors are shown with red bars. In blue bars are the computational time.

6.12.3 Verification of Model

A thorough comparison of the measurements at Hywind Demo and simulations in RIFLEX/SIMO has been executed by Tor D. Hanson, Bjørn Skaare, Rune Yttervik, Finn Gunnar Nielsen and Ole Havemøller in Statoil. This work resulted in the paper "Comparison of measured and simulated responses at the first full sale floating wind turbine Hywind" [6]. They have studied the measurements from three different sea states and compared them to time-domain simulations of Hywind Demo. By comparing power spectra it is possible to compare time-series from the measurements and the simulations. They conclude with finding good agreement between measurements and simulations.

7 Environmental Modelling

7.1 Environmental Models

In the theory chapter two environmental models are described. The first one is proposed by Johannessen and has a joint distribution for all three environmental parameter, Hs, Tp and mean wind velocity at 10m elevation above sea level (W). The second model is proposed by Statoil in their Hywind Metocean [24] and has a joint distribution for Hs and Tp and an independent distribution for W. The format of the first model is the form wanted for the environmental model used in the long term analysis. Thus it is proposed to use the same dependence between wind- and wave-parameters as suggested by Johannessen. Since the wave behaviour at the Hywind location is somewhat known true measurements it is possible to determine how well the dependent wave model from Johanessen actually fits the Hywind location. This can be accomplished by integrating over the wind variable in the following manner:

$$F_{Hs} = \int_w F_{Johannessen} \cdot f_{wind}, \tag{7.1}$$

where:

F_{Hs}	CDF of Hs for all wind conditions.
$F_{Johannessen}$	CDF of Hs with parameters calculated as proposed by Johannessen in equation 5.4.
f_{wind}	PDF of the wind at the Hywind Demo location

The result of this integral is a CDF describing the significant wave height for all wind conditions. The function can be compared to measurements from the location of Hywind Demo. It is seen from Figure 7.1a that it is not a good fit and a better model must be developed. This is done by a semi-automatic iterative scheme in Matlab, where the constants in equation 5.4 are adjusted one by one to minimize the residual of the two CDFs. The Matlab scheme is found in Appendix E.1. The new values found by the iteration scheme are presented in the next equation:

$$\alpha_h(w) = 1.2132 + 0.0647w, \qquad \beta_h(w) = 0.3912 + 0.0927w^{1.3113}. \tag{7.2}$$

The CDF for the calibrated model is seen in Figure 7.1b. These values are important to establish a suitable environmental contour surface for the Hywind Demo location.

The wind parameters are adopted from the Statoil model described in chapter 5.1.2. Before these values can be used they most be scaled down so that they describe the wind field at 10m elevation. This can be accomplished with the wind-shear formulation described by equation 5.52. A Monte-Carlo scheme is used to find the new parameters. Which are presented in Table 7.1. The Monte-Carlo procedure can be studied in Appendix E.4.

The Statoil environmental model describes the Hs-parameter by a bisected distribution

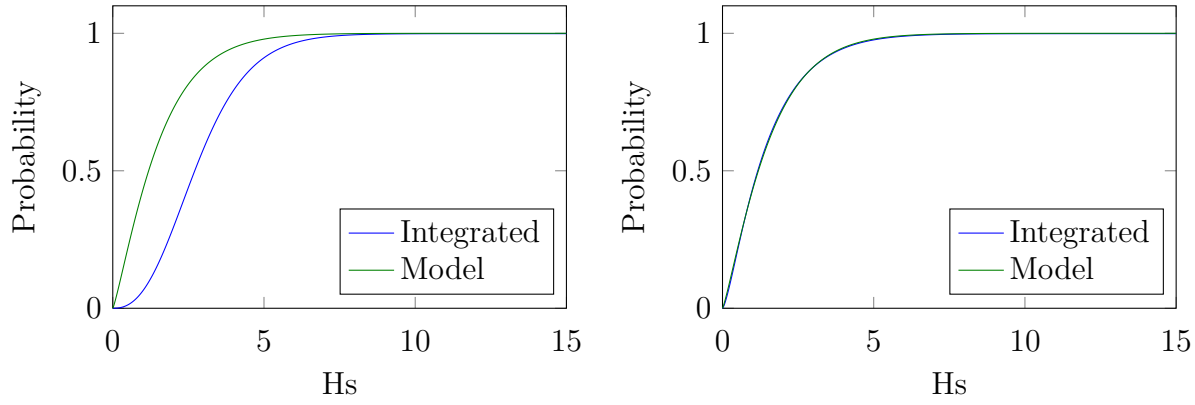

(a) Fit of Haver's environmental model at the Hywind loacation.

(b) Fit of calibrated environmental model.

Figure 7.1: Comparison of significant wave height computed by the two models.

Table 7.1: Omni-directional Weibull parameters for wind speed at 10m above mean sea level.

Weibull parameters		
Shape	Scale	Location
1.770	8.078	0

to get a better fit for the lower wave heights. When calibrating the distribution only the Weibull distribution for the larger values is included.

7.2 Environmental Contour Surfaces

Based on the calibrated environmental model the environmental contour surface are found. They are computed by a Matlab script based on the Rosenblatt transformation described in chapter 5.3. On the environmental contour surface all combinations of environmental parameters corresponding to a certain return period, say T-years, are located. Combinations located inside the closed curve will occur more often then the specified return period, and combinations outside will occur more seldom. In the following Figures 7.2 and 7.3, the 50-year environmental contour surfaces for the two environmental models are presented. The Matlab script computing the contour surfaces can be studied in Appendix E.2.

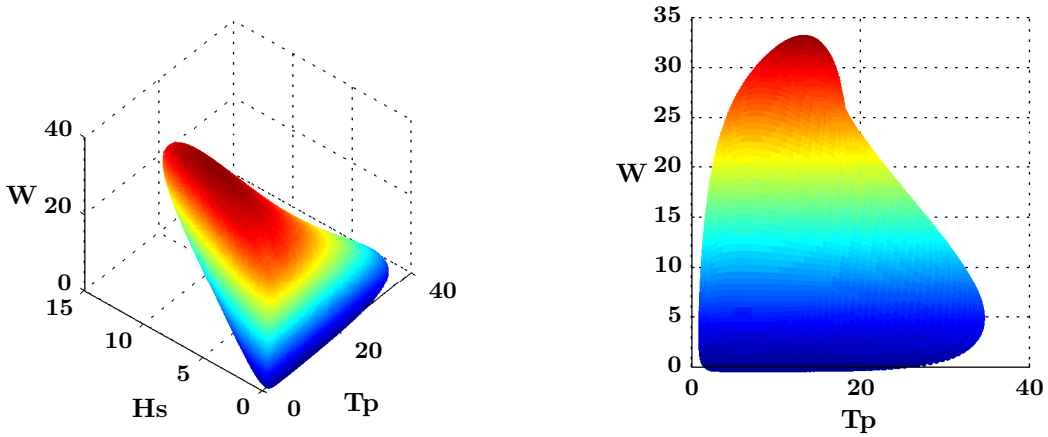

(a) Rendered view of calibrated environmental contour surface. For reference, north is in positive direction of Hs.

(b) Environmental contour surface for the calibrated model seen from the south.

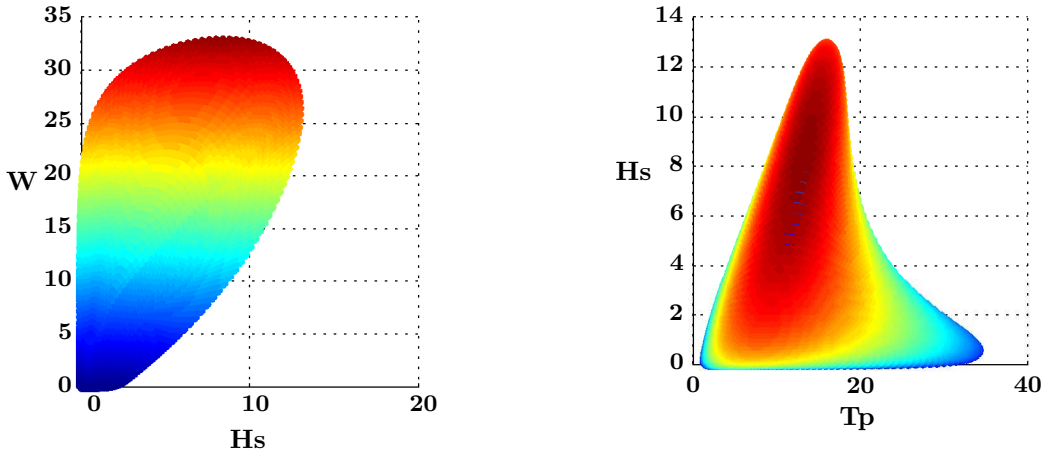

(c) Environmental contour surface for the calibrated model seen from the east.

(d) Environmental contour surface for the calibrated model seen from above.

Figure 7.2: 50-year environmental contour surface for the calibrated environmental model.

It is seen from Figures 7.2 and 7.3 that the original model describes slightly worse environmental conditions than the calibrated. In the original model the largest 50-year return wind and 50-year return significant wave height are respectively seen to be about 37m/s and

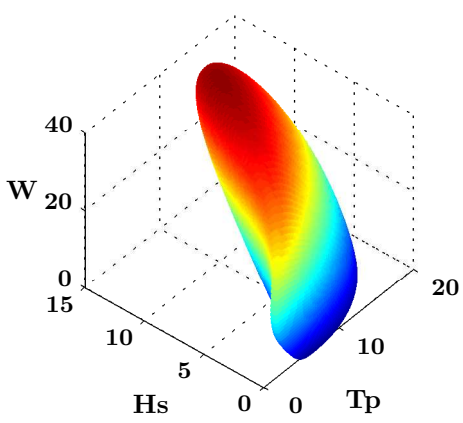

(a) Rendered view of Johannessen's environmental contour surface. For reference north is in positive direction of Hs.

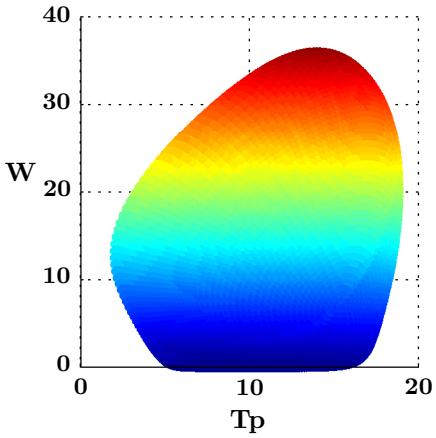

(b) Environmental contour surface for Johannessen's model seen from the south.

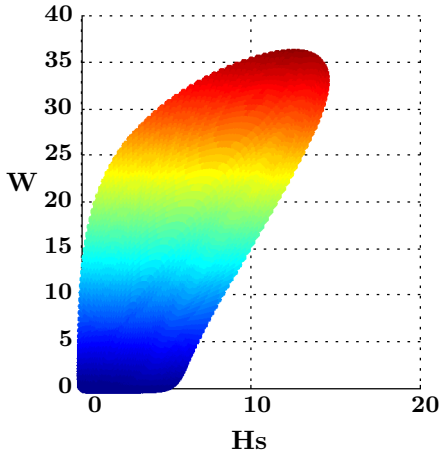

(c) Environmental contour surface for Johannessen's model seen from the east.

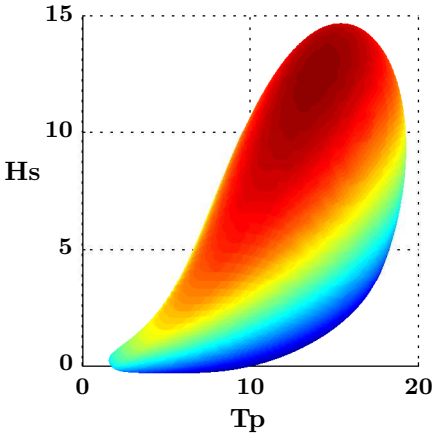

(d) Environmental contour surface for Johannessen's model seen from above.

Figure 7.3: 50-year environmental contour surface for Johannessen's environmental model.

14m. For comparison the 50-year return values for the calibrated model are 33m/s wind and 13m significant wave height. These are reasonable tendencies as it is expected that the environmental conditions at the Hywind Demo location will be less sever than for the locations where the environmental model first was developed.

It is also seen that the a significant deviation is found when comparing the largest values of Tp on the two environmental contour surfaces. The values are approximately 35s for the calibrated model and 19s for the original. This is not a reasonable tendency as there is no obvious reason for the peak period to be large at the Hywind location. However this detail is not expected to affect the results of the long term analysis as it only applies to combinations of small values of W and Hs.

7.3 Environmental model

Previously a suitable environmental model for the Hywind Demo location was established. This is a statistic model and contains information about the probability for each environmental state to occur. To get an impression of which sea states are important, the environmental joint probability function is plotted in Figure 7.4. Hs and Tp are here varying while the wind is kept constant.

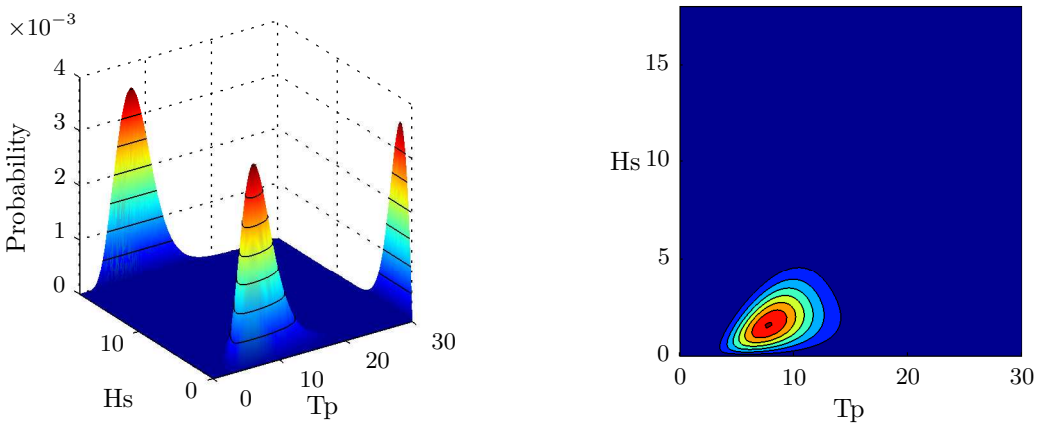

(a) Rendered view of the environmental PDF with constant wind equal to 11m/s. The PDF-surface is projected on to the walls of the figure.

(b) Contour view of the environmental PDF with constant wind equal to 11m/s.

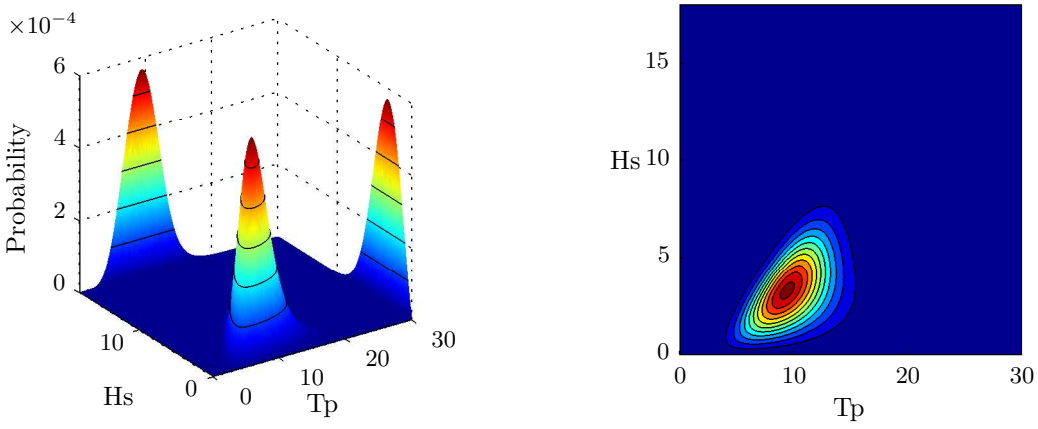

(c) Rendered view of the environmental PDF with constant wind equal to 17m/s. The PDF-surface is projected on to the walls of the figure.

(d) Contour view of the environmental PDF with constant wind equal to 17m/s.

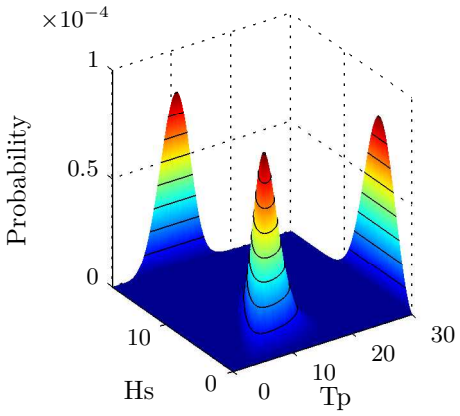

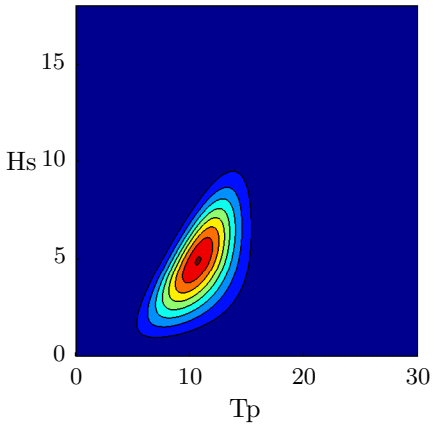

(e) Rendered view of the environmental PDF with constant wind equal to 22m/s. The PDF-surface is projected on to the walls of the figure.

(f) Contour view of the environmental PDF with constant wind equal to 22m/s.

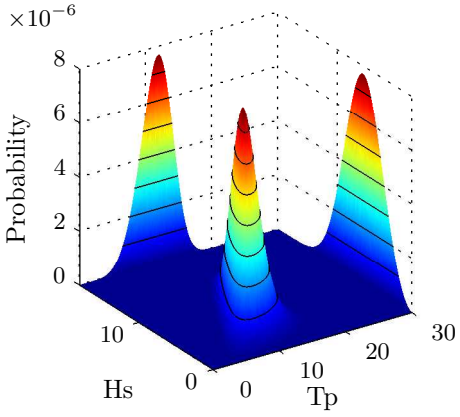

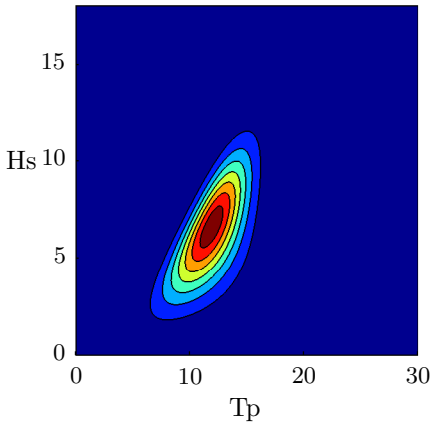

(g) Rendered view of the environmental PDF with constant wind equal to 27m/s. The PDF-surface is projected on to the walls of the figure.

(h) Contour view of the environmental PDF with constant wind equal to 27m/s.

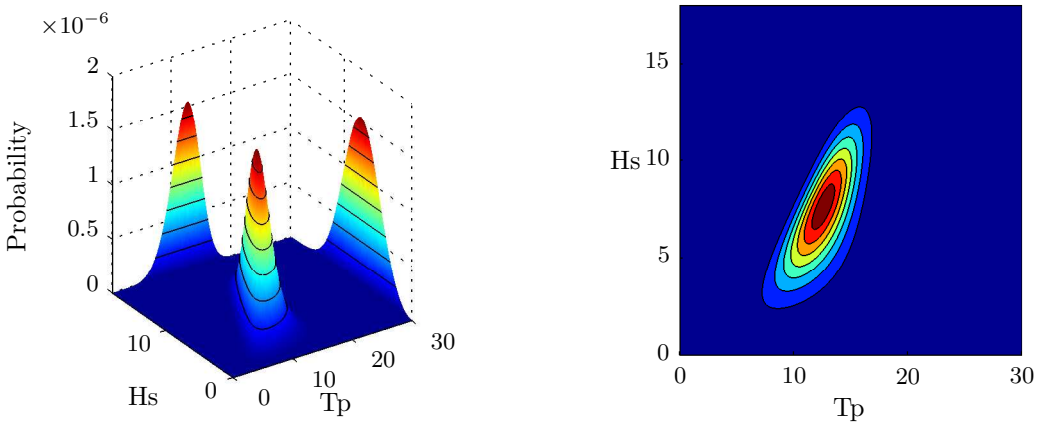

(i) Rendered view of the environmental PDF with constant wind equal to 30m/s. The PDF- surface is projected on to the walls of the figure.

(j) Contour view of the environmental PDF with constant wind equal to 30m/s.

Figure 7.4: The joint environmental probability function for the calibrated model.

8 Reliability Analysis

8.1 Introduction

A goal for design load calculations is to establish loads or responses corresponding to predetermined return periods of T-years, e.g. 50 years for wind turbines. This can be accomplished either by a deterministic- or a reliability-approach. An example of deterministic approach is to combine the 50-year wind with the 50-year wave and use the calculated response as an estimate of the 50-year return period. This approach is in general conservative and more precise results can be obtained with a reliability analysis [25]. A reliability approach will be adopted in this work, where two methods will be applied to obtain design values. The two methods are:

1. A Full Long Term Analysis - the obtained design response is actually the T-year return response, i.e. the response corresponding to a 50-year return period is found.

2. An Environmental Contour Line Method - the combined loads corresponding to the given T-year return period are used to calculate the design response, i.e. the combination of 50-year return loads are used to estimate the design response.

To better understand these two methods and their differences the subject of short term variation must be elaborated. For a realisation of a sea state a given extreme value of the response will appear. In another realisation of the same sea state a different extreme value appears. Evidently there is an underlying variation of the extreme response process. This variation is called the short term variation.

In the full long term analysis the short term variation is investigated by obtaining several realisations of each sea state. Hence, the short term variation is account for when determining the design loads. In the contour line method the short term variation is only investigate for the worst combination of environmental parameters. The sources of variations will be further discussed in the next section. A description of the long term analysis is also presented along with the obtained results.

8.2 Long Term Analysis

8.2.1 Introduction

In this section the long term analysis will be presented. The long term analysis will consider extremes of the response. An extreme is defined as the largest response during a stationary sea state of duration d-hours. The extreme response will be named, X_d. The duration of the sea state is location specific and is often taken as three hours in Norwegian waters, and 30 minutes in the Gulf of Mexico. For time-domain simulations of Hywind Demo, d = 3, is assumed suiting.

A joint probabilistic model is required for both the long term analysis and the contour line method. According to the Norwegian rules, a number of environmental effects shall be

taken into account when the design load is estimated. Proposed by DNV as governing effects are wind, waves, current, marine growth, tide and storm surge, earthquake, temperature, snow and ice [25]. It will be impossible establish a joint probabilistic model for all of these parameters. Simply do to the detailed simultaneous measurements required. Further on the number of simulations required in the long term analysis will increase exponentially with the number of environmental parameters. Therefore it will be necessary to limit the number of environmental parameters included in the analysis.

Norwegian rules states that the response quantities used for design shall correspond to a certain annual exceedance probability, or a return period. The exceedance probability is the effect of two types of randomness which essentially are due to completely different sources. The two sources are:

1. The inherent randomness of the slowly varying parameters that define the short term event, often called long term variability.

2. The inherent randomness of the largest response maximum during a given short term event, often called short term variability.

The first source of randomness is often referred to as the long term variability and is due to the inherent randomness of the environmental processes. This is the most important reason for randomness. It is accounted for by establishing a joint probabilistic model for the environmental parameters, e.g. $f_{W,H_s,T_p}(w, h_s, t_p)$. The second source of randomness is less important but cannot be neglected in general. This is the part that account for the physics, or the degree of non-linearity, in the system. By neglecting the short term variability one must assume to under predict the response extremes with 10-15% for linear systems. For non-linear system the under-prediction can exceed 30% [19]. In the long term analysis both types of randomness are accounted for.

In the next section the set-up of the long term analysis will be described. The computation of response surfaces will also be discussed. Then the extreme response corresponding to a return period of T-years, from now called the T-year response, will be found by solving the long term integral and by the Inverse First Order Reliability Method (IFORM). In the end a discussion of the long term analysis and a presentation of the results are found.

8.2.2 Time-domain Simulations

In the full long term analysis, time-domain simulations are carried out for 172 different environmental states. At each environmental state 15 three-hour realisations are computed. By varying the wave- and wind-seed number it is ensured that each of the realisations is unique. In total 2580 time-domain simulations are carried out to complete the long term analysis.

Which environmental states to simulate are chosen based on the 100-year environmental contour surface. The results from the simulations will be used to fit response surfaces. This affect the choice of environmental states selected for simulation. To obtain a good response

surface the analysed states should be based on results spread over the entire domain enclosed by the contour surface. To avoid extrapolation of the response surface it is made sure that also combinations outside the environmental contour surface are evaluated.

Eight wind conditions are selected for analysis. The wind speeds are in meters per second; 5.5, 11, 17, 22, 27, 30, 33 and 35. For each wind speed the contour line is found. Then Hs and Tp is selected so that they cover the area enclosed by the contour line. It is assumed that the response will be larger for higher Hs, so more sea states are selected for higher Hs. An illustration of the contour line and selected sea states are shown for mean wind speed 22m/s in Figure 8.1.

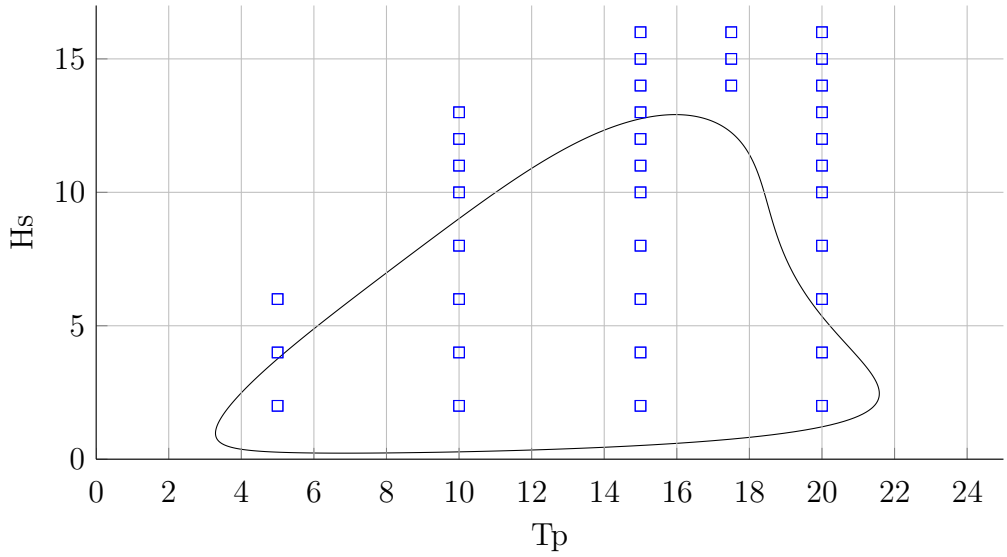

Figure 8.1: Contour line for given mean wind speed 22m/s and sea states selected for analysis.

From Figure 8.1 it is seen that the analysed sea states cover the area enclosed by the contour line. Plot of the analysed sea states in the other wind conditions are found in Appendix A.

From the figure it is seen that the contour line takes values below the smallest values of Hs and Tp. Since there are some physical problems running analyses for the cases with Hs or Tp equal to zero an alternative approach must be adopted to obtain values at these locations. In this work a simple and slightly conservative approach has been adopted. By projecting the smallest values of Hs and Tp down to the respective axes this problem is solved.

8.2.3 Response Surface

For each three-hour time-domain simulation the extreme response, X_{3h}, can be found. For each analysed environmental state 15 values of X_{3h} are obtained, i.e. $X_{3h,1}$, $X_{3h,2}$, $X_{3h,3}$,...,$X_{3h,15}$. This will be referred to as a set of extreme response values. By taking the mean of a set the mean extreme response, $\overline{X}_{3h}$, with standard deviation, s_{3h}, is found. This can be done for all the analysed environmental states. Then point estimates for $\overline{X}_{3h}$ and

s_d are obtained as discrete functions of Tp, Hs and W, i.e. $\overline{X}_{3h}(t_p, h_s, w)$ and $s_{3h}(t_p, h_s, w)$. Gumbel distribution can be fitted to each set of extreme values. The Gumbel parameters are obtained by Equations 5.36 and 5.35. In the same way as for $\overline{X}_{3h}$ and s_{3h}, point estimates for the Gumbel parameters are obtained as discrete functions of the environmental parameters, so that $\beta_{3h}(h_s, t_p, w)$ and $\gamma_{3h}(h_s, t_p, w)$. These discrete functions are not sufficient to solve the long term integral with adequate accuracy, thus continuous functions of the four statistical parameters are need. This is accomplished by interpolating the discrete functions. The results of the interpolations are continuous surfaces called response surfaces.

The discrete functions are interpolated in three dimensions with a linear method. Preferably a more sophisticated interpolation method, e.g. cubic or spline-interpolation should be used, but unfortunately these options are not available for 3-dimensional interpolation in Matlab.

The response surfaces will be function of three variables, this means that it can only by visualized if one of the parameters are kept constant. In Figure 8.2 the response surface for $\overline{X}_{3h}$ is presented for the axial tension in mooring line 10. The wind parameter is her kept constant at a value of 17m/s.

A contour plot is seen below the response surface. The response surface is smoothly increasing with increasing values of Hs. The mean extreme response seams to vary little with respect to Tp.

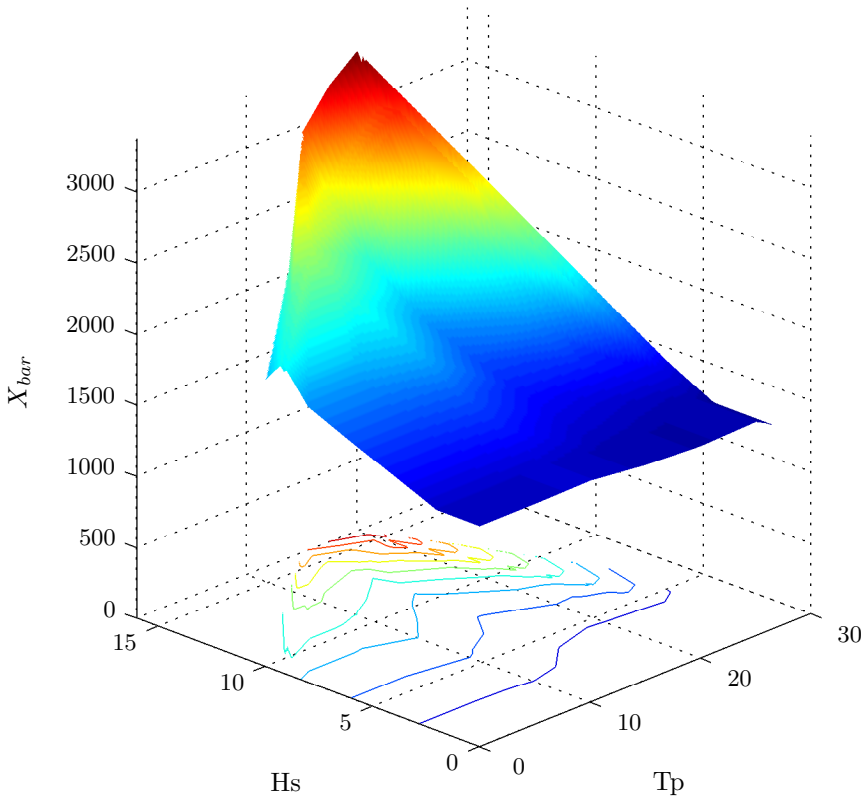

Figure 8.2: Response surface of mean maximum mooring line tension for wind speed 17m/s

8.2.4 Choice of Extreme Value Distribution

The Gumbel distribution will in general be a good representation of extreme maxima if the initial distribution has an exponential tail. By plotting the extreme values from a set in Gumbel-paper, the fit of the distribution can be evaluated. In Figure 8.3, 15 extreme response values are plotted on Gumbel paper. They are obtained from the analysed sea state with wind 11m/s, Hs = 8m and Tp = 12.5s. From Figure 8.3 it seems like the Gumbel distribution describes the process well. In general are 15 measurement values are too few to establish a proper distribution fit with sufficient certainty. To investigate the variability in the process a bootstrapping procedure can be performed.

First the Gumbel-parameters for the set are found. By using these parameters in a Monte-Carlo procedure, new sets of 15 realisations can be drawn. This is repeated a number of times, say 50. The 50 sets can now be plotted together in the Gumbel-paper. The result of the bootstrap is seen in Figure 8.4. With 50 sets in the plot, the black dots are approximately representing the 96% confidence-interval.

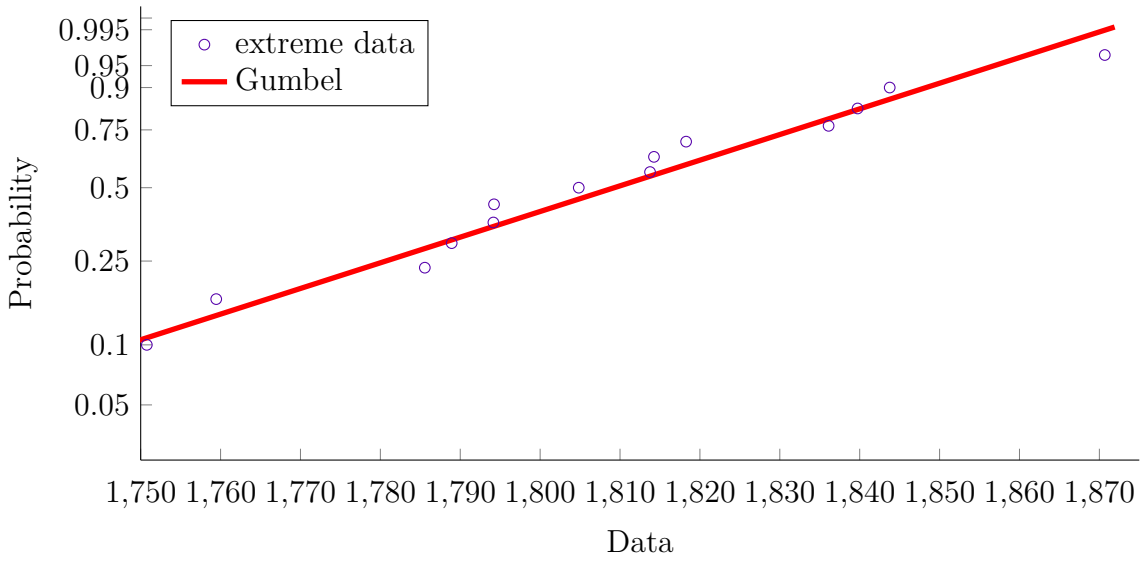

Figure 8.3: The 15 extreme maxima from the specific sea state plotted in Gumbel probability paper.

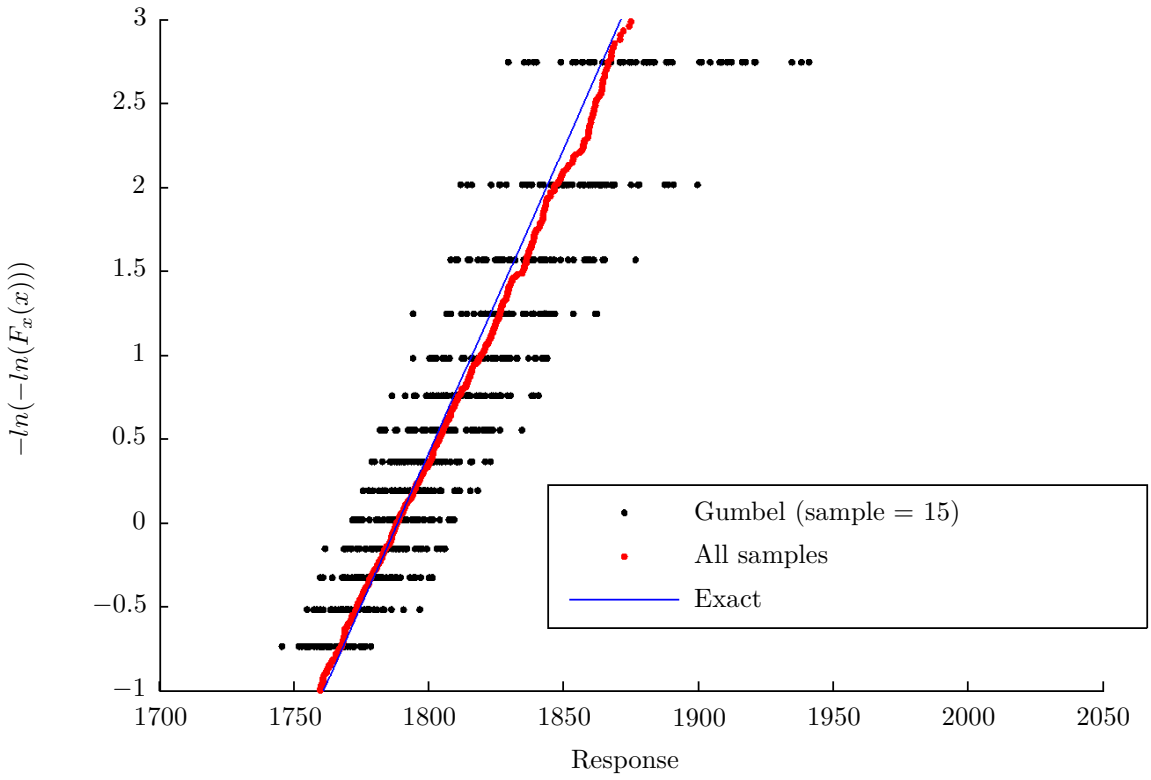

Figure 8.4: Bootstrapping for environmental combination wind 11m/s, Hs = 8m and Tp = 12.5s. The black dots are approximately referring to a 96% confidence-interval.

8.2.5 Results of The Long Term Integral

When response surfaces for $\overline{X}_{3h}$, s_{3h}, β_{3h} and γ_{3h} are found the long term response with return period T-years can be computed. This is done by solving the long term integral, see Equation 5.30. The result of this integral is a CDF which describes the long term response distribution. The long term CDF for extreme axial tension in mooring line 10 is depicted in Figure 8.6. The integral is solved with a numerical approache and the CDF is found to depend more on the increment of Hs than the two other environmental parameters. The result of the long term integral is here presented with three different values for ΔHs. The increments of the other values are constant equal to 1. For increment values of Hs smaller than 1, the computation becomes exceedingly time-consuming. It is seen that the CDF converges to zero for the lower values of exceedance probability. However, it is interesting to see that the values for larger probability of exceedance is rather unaffected by the decreasing increment value of Hs. This means that the extreme response values to a small extent will depend on the increments of the numerical integration.

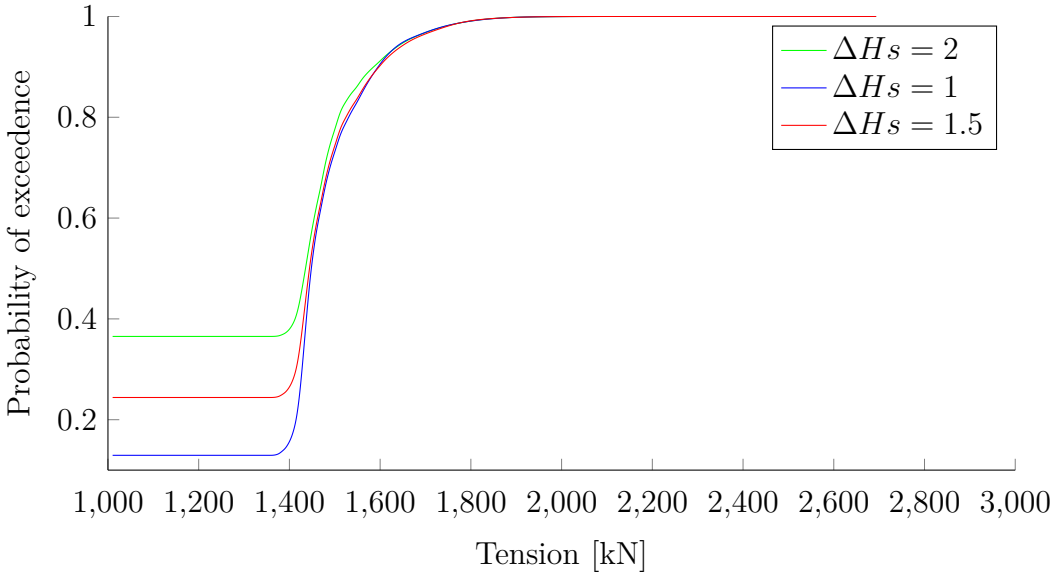

Figure 8.5: Resulting CDF of the long term integration.

The extreme response corresponding to an annual exceedance probability of q, or a return period of T-years, X_T, can be found by combining the CDF in Figure 8.5 with Equation 5.34. Some typical response values are shown in Figure 8.6 for return periods of 1-, 10-, 50- and 100-years.

All environmental loading, i.e. wind, wave and current, is aligned parallel to mooring line 10. It is therefore no surprise that the largest extreme response is found in this line. The effective tension in line 10 is approximately two times the tension in the other mooring lines, which are located down-stream. The deviations between extreme axial tension in mooring line-9 and -11 are 11.7, 6.8, 6.0 and 5.8 percent for the 1-, 10-, 50- and 100-year return periods, respectively. The causes of these deviations are unknown. It was expected that the

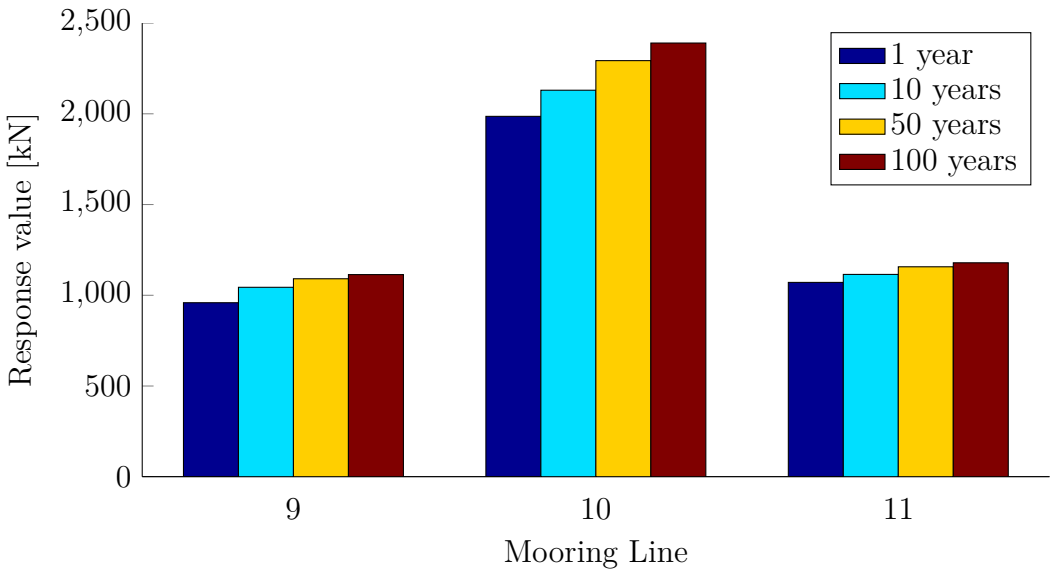

Figure 8.6: Design response in the main mooring lines, corresponding to return periods 1-, 10-, 50- and 100-years. The values are obtained from the long term integral.

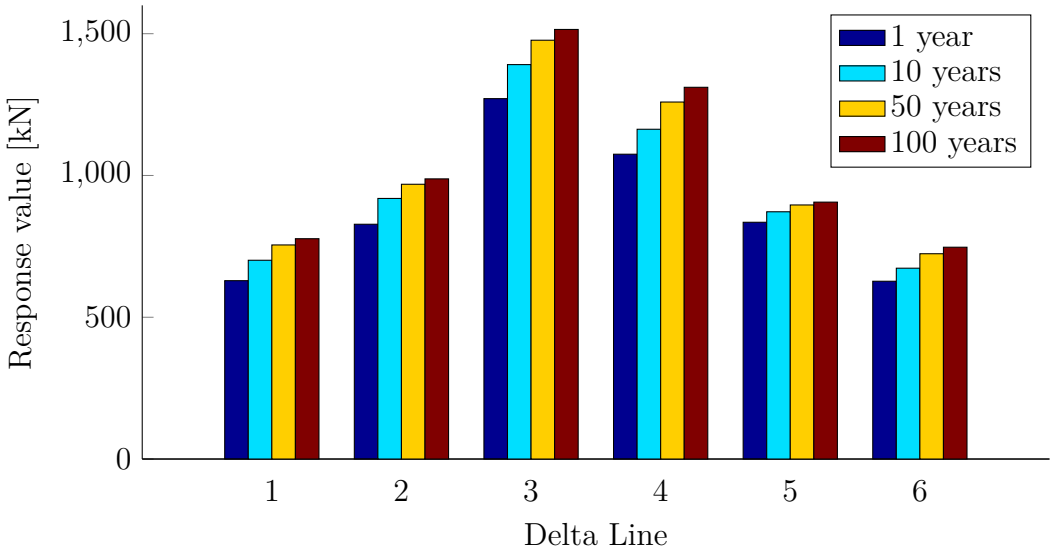

Figure 8.7: Design response in the delta lines, corresponding to return periods 1-, 10-, 50- and 100-years. The values are obtained from the long term integral.

response values in these two lines would be identical due to the symmetry. One possibility is that the loading is not perfectly aligned with the mooring line which results in an eccentricity in the load history. Another possibility is that the eccentricity is due to some Coriolis forces occurring from the rotating blades. It is not expected that the eccentricity is caused by statistical uncertainty since the number of simulations are so many.

In the delta lines the largest extreme responses are found in line-5 and -6. These are the two lines which are connected to mooring line 10. For the other delta lines it is seen that the extreme response is larger in the delta line closer to mooring line 10. There are some deviations between line-9 and -11 also here.

8.2.6 Inverse First Order Reliability Method

As described previously the T-year design response, X_T, can be found by solving the integral in Equation 5.30. The design response can also be found by the Inverse First Order Reliability Method. The IFORM is based on the Rosenblatt transformation described in chapter 5.3. All stochastic variables in the system, i.e. Hs, Tp, W and the extreme response variable, X_{3h}, are combined in the standard Gaussian space, from now called the U-space. In the U-space all combinations of the four parameters corresponding to the same annual probability of exceedance, will be located at the same distance from the origin. For a two-parameter problem this will be equivalent to a circle, and for a three-parameter problem it will be a sphere. This case is a four-parameter problem and the shape of the surface will be a four dimensional sphere. The radius is often referred to as the reliability index, β_R. Values for β_R corresponding to certain return periods can be found in Table 8.1.

Table 8.1: Values of annual exceedance probability and corresponding reliability index.

Return period	Probability of exceedance in arbitrary 3-hour period	β_R
1 year	3.42e-04	3.40
10 years	3.42e-05	3.98
50 years	6.85e-06	4.35
100 years	3.42e-06	4.5

The 4-D sphere can, by utilizing the Rosenblatt transformation, be transformed into the physical space. The shape of the surface will now have changed, but it is still four dimensional and is still closed. The IFORM algorithm locates the point on the surface corresponding to the largest response value. This will be the largest value of the response occurring during the T-year period, and the combined environmental parameters causing this response defines the design point.

The environmental parameters corresponding to the T-year response are located inside the corresponding T-year environmental contour surface. This can be seen as a reduction in the reliability index. This reduction in β_R is connected to the short term variability of the T-year response. If the design point of the T-year response is located at the T-year environmental contour surface, it would be no short term variability of the response. As the variability of the T-year response increases the design point will move away from the T-year environmental contour surface and towards the origin. This means that the environmental conditions corresponding to a design load will possibly occur several times over the T-year period, without actually obtaining the design load.

The IFORM analysis is carried out in Matlab. From different starting points around the sphere, a step in arbitrary direction is taken and the new position is transformed to the physical space. If the location after the step is on a higher response-contour than the previous, a new step is taken in the same direction. This continues until the new step is on a lower response-contour. Then the step direction is changed and the same process is repeated.

The algorithm can be compared to climbing a mountain where the location of the peak is unknown. As long as you keep climbing the summit will be reached. Since it is possible to have multiple local maxima on the surface the starting point is changed to ensure that the largest maxima are reached. The Matlab routine with the IFORM procedure is included in Appendix E.3.

8.2.7 IFORM Results

The IFROM algorithm is run for return periods 1-, 10-, 50- and 100-years. A bi-product of the IFORM analysis is the importance factor, which is a measure of the variability of the parameters with respect to each other at the design point. The response is calculated at the top of the mooring line, i.e. the location where the mooring line and the delta lines connect. The results for the main mooring lines computed by the IFORM are presented in Figure 8.8. The results for the delta lines are presented in Figure 8.9.

The importance factors for the main mooring lines are presented in figures 8.10, 8.11 and 8.12. These figures show that the largest relative variability is found for the wind velocity and the significant wave height. The significant wave height seems to be more important for mooring line 10 which is up-stream. The variation of the response is small in cases with high return periods. For the 1- and 10-year return periods the variability of the response is larger, up to 25%. For all three of the mooring lines it is hard to see a general tendency. This indicates that the numbers of realisations in the sets are too small.

At first glans the results obtained from the IFORM seems to be in accordance with the results from the long term integral. This will be discussed more in the next section. The numerical values of the IFORM are found in Appendix E.3.

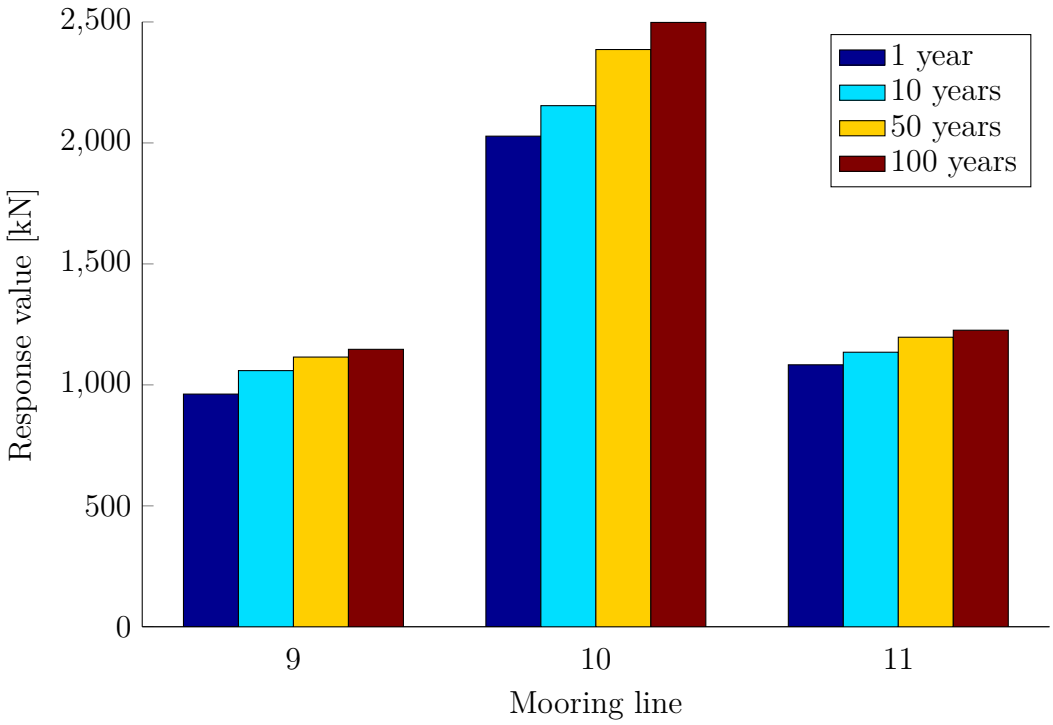

Figure 8.8: Design response in the main mooring lines, corresponding to return periods 1-, 10-, 50- and 100-years. The values are obtained from the IFORM.

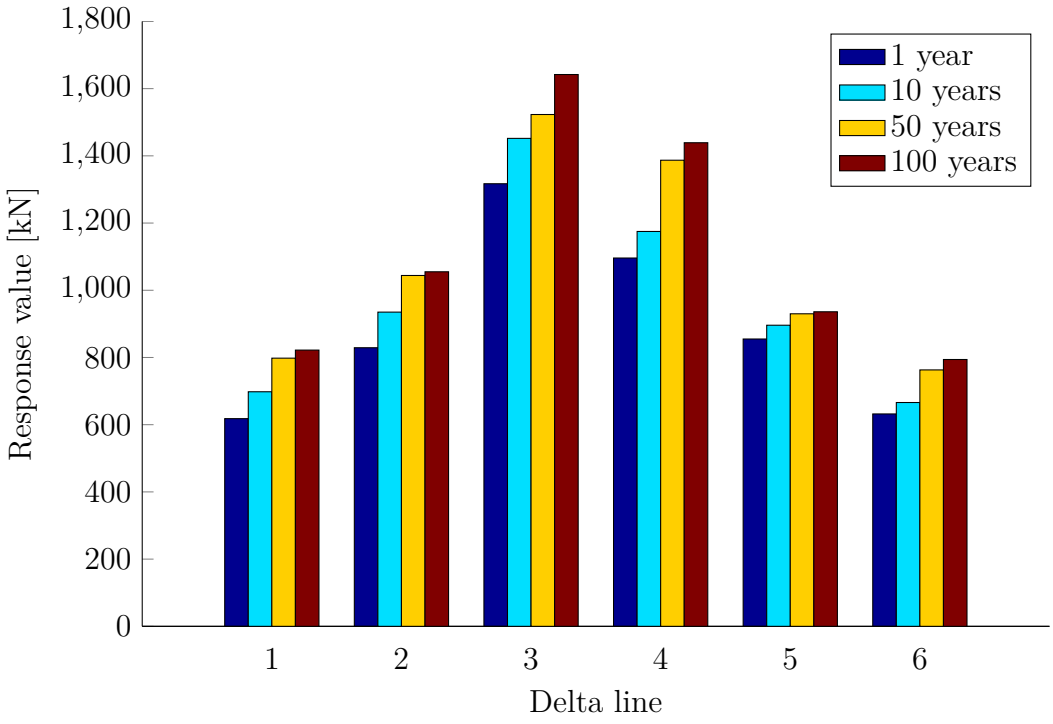

Figure 8.9: Design response in the main mooring lines, corresponding to return periods 1-, 10-, 50- and 100-years. The values are obtained from the IFORM.

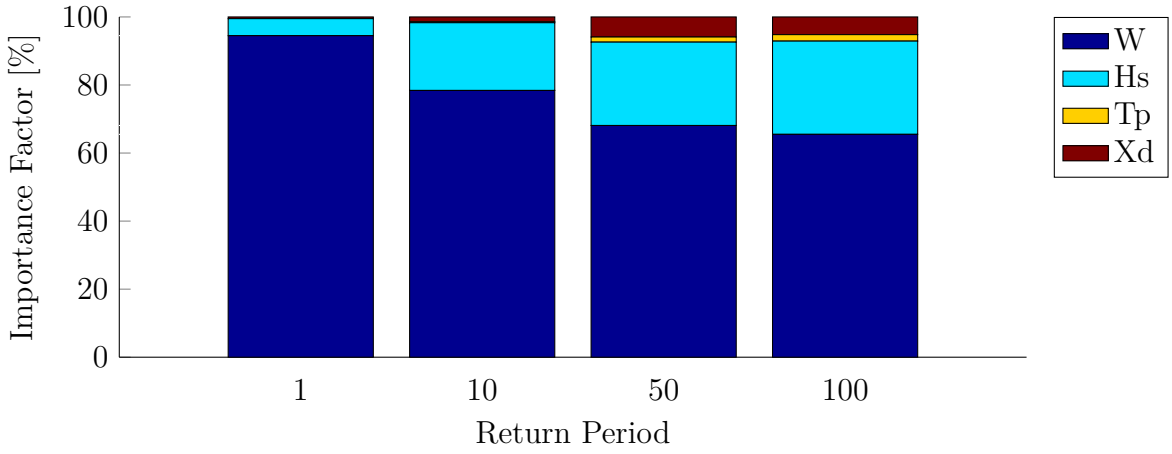

Figure 8.10: Importance factors for mooring line 9.

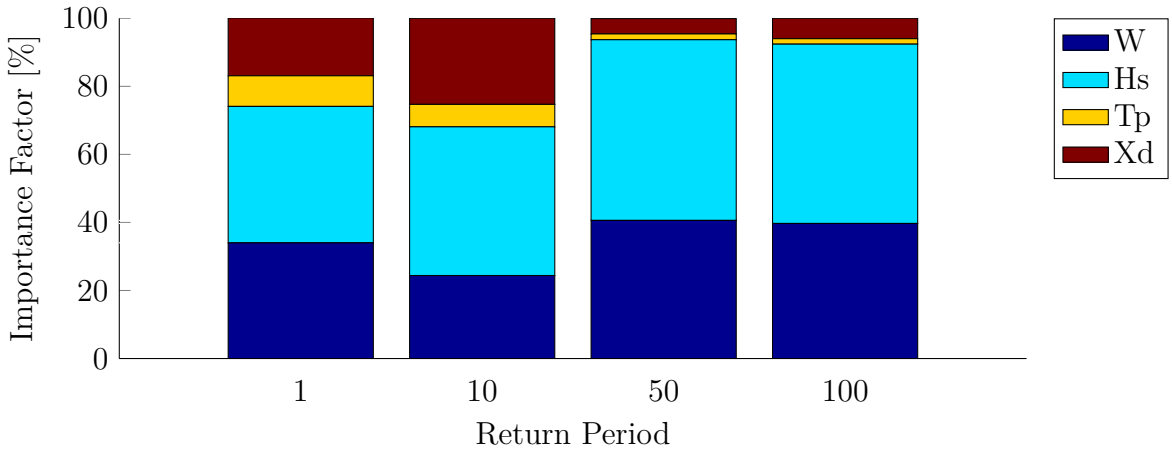

Figure 8.11: Importance factors for mooring line 10.

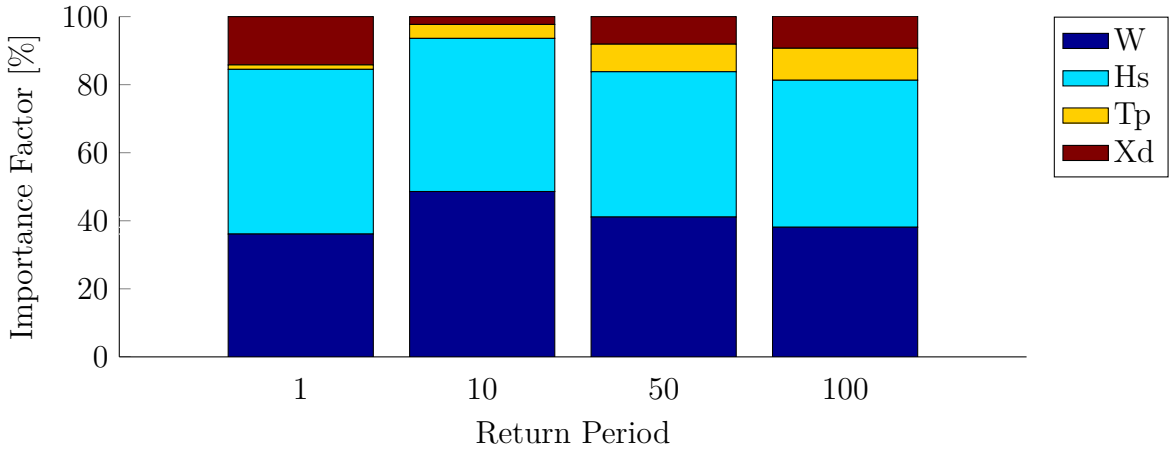

Figure 8.12: Importance factors for mooring line 11.

8.2.8 Discussion of The Long Term Analysis

The advantage with a long term analysis approach in the design process is that the obtained results are particularly precise. This is especially of interest for the design of new and novel concepts where the experience is limited. For a linear problem the long term analysis is also fast with respect to computational time, as it can be solved with a frequency-domain approach.

There is however some very obvious down sides with the long term analysis. First of all it sets high requirements for the environmental modelling, as a joint-environmental distribution for all parameters involved must be established. This requires that a detailed set of simultaneous measurements are available. Another down side is that for non-linear problems the long term analysis is particularly time consuming, as it requires a large number of time-domain simulations. For some cases, especially related to floating structures, reliable time-domain simulation cannot give the sufficient accuracy. In such cases model tests can provide data to calibrate the time-domain simulations. Then a combination of model tests and simulations can be used to create the response surfaces [19]. To perform a long term analysis solely on the results of model tests will in practice not be possible do to the high economical costs and the amount of time spent.

When solving the long term integral it is assumed that adjacent sea states are statistical uncorrelated. This is a slightly conservative assumption. According to Haver the result can be expected to be 3-5% on the conservative side [19]. Except for this the results of the long term analysis will mostly depend on the possibility to sufficiently model the environmental conditions.

The results from the long term integral and the IFORM analysis can be compared. The deviations between the two are shown in Figure 8.13. It is seen that the deviations are small, below 5% for all of the main mooring lines. A certain deviation between the two approaches is expected. This is due to the linearization performed by the IFORM routine.

The IFORM is consequently giving a larger value than the long term integral, hence, the IFORM is in this case conservative. This means that the failure surface is curved towards the origin, and will be overestimated by the linearization in the IFORM. The deviations in the delta lines are presented in Figure 8.14.

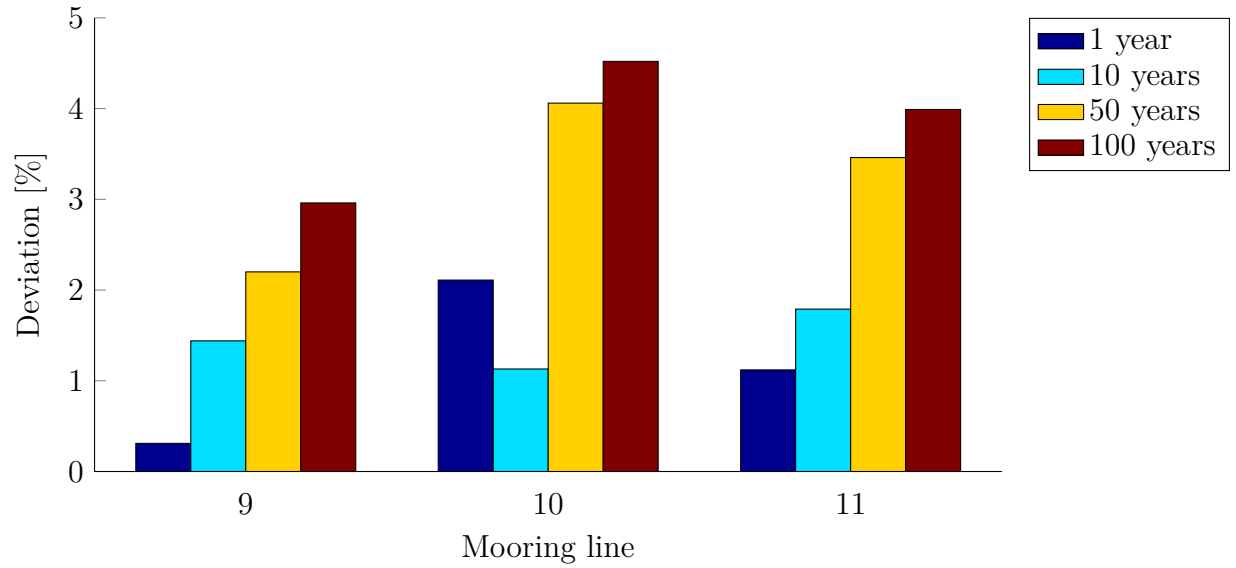

Figure 8.13: Deviation of design response between the long term integral and the IFORM in the main mooring lines.

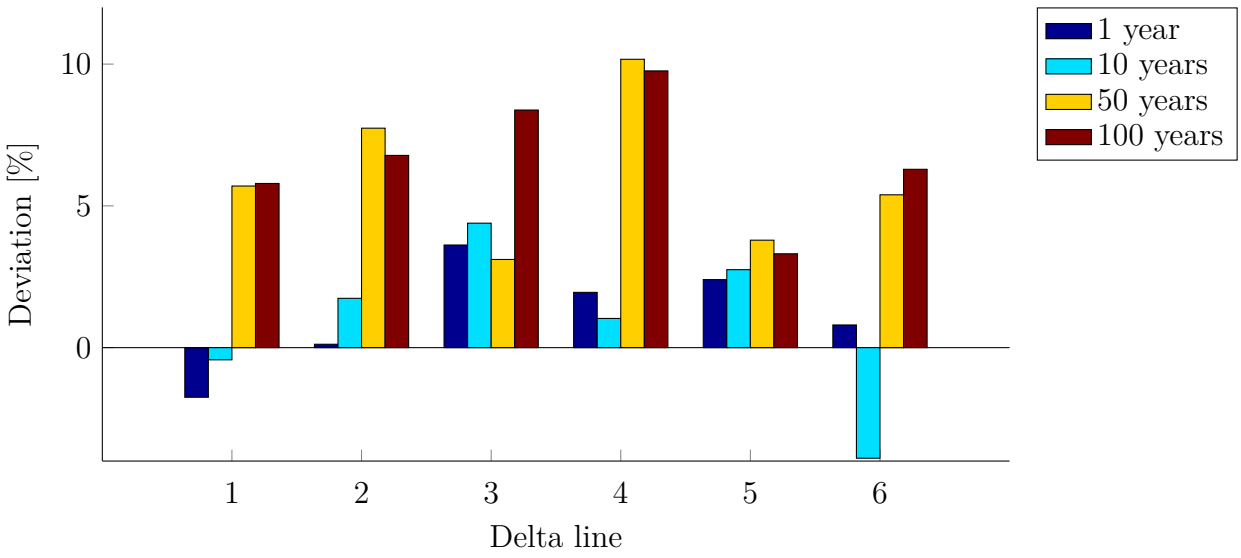

Figure 8.14: Deviation of design response between the long term integral and the IFORM in the delta lines.

8.3 The Contour Line Method

8.3.1 Introduction

In this section a more thorough presentation of the contour line method and its application on Hywind Demo will be given. It will here be focused on the three main mooring lines, i.e. line-9, -10 and -11.

As seen in the previous section the long term analysis requires that the short term distribution of the extreme response must be found for a large number of sea states. This can be problematic or in best case time consuming for non-linear problems where numerous comprehensive time-domain simulations must be carried out to establish the proper short term distributions of the response. In such cases the contour line method can be a good alternative. Before a more thorough description of the contour line method is given, it is meaning full to define some terminology. The design point is the combination of environmental parameters resulting in the highest extreme response. This response value will be called the design value. By investigating the response process at the design point a suiting distribution can be adapted. This will be called the design point distribution.

8.3.2 Application of The Contour Line Method

In Chapter 8.2.1 two reasons for randomness, the long term- and short term-variability, were discussed. The idea of the contour line method is to decouple this two by first neglecting the short term variability and compensate for this in some way, a posterior. If there is no short term variation in the extreme response, X_{3h}, the PDF of the extreme response will approach a Dirac delta function. If this is the case the T-year response, X_T, can be replaced by the median value, $x_{50\%}$, of the design point distribution. This means that the T-year response value will occur during the environmental conditions corresponding to a return period of T-years. Obviously this is a huge advantage since the environmental states that must be evaluated now are limited to those located on the contour surface. It is for most problems rather straight forward to locate a region on the contour surface where the most unfavourable environmental condition must be located. By closer investigation of this region the environmental conditions leading to the largest response is found. This point is called the environmental design point.

Since it for physical problems is not possible to neglect the short term variability it is wanted to account for the short term randomness without including the extreme response as a random variable. This is possible by three alternatives [19].

1. The contour surface may be artificially inflated. This way the environmental parameters are worsened to compensate for the short term randomness. The level of inflation will depend on the physical problem, i.e. the level of non-linearity.

2. The median value, $x_{50\%}$, is scaled with a correction factor such that the design value becomes $X_T = \gamma_{cf} \cdot x_{50\%}$. Typical value for γ_{cf} will be between 1.1 and 1.3.

3. Instead of choosing the median value, $x_{50\%}$, as the design response value, a higher percentile of the design point distribution can be selected. Which percentile level to select will depend on the response problem. The 90% percentile is suggested for problems with two slowly varying parameters [17]. For problems with three or more slowly varying parameters the percentile level is expected to be lower [11] [19]. If the annual probability of exceedance is decreased, or the return period is increased, the percentile value is also expected to increase. This method seems to be the most used and is thoroughly proven in the literature [11] [9].

For the remaining part of the thesis the third alternative will be treated in detail. The other two approaches will not be further discussed.

8.3.3 Environmental Design Points

In a case with no short term variability the T-year design point is located on the T-year environmental contour surface. For the rest of this section the design point refers to the T-year design point with neglected short term variability. The exact location of the design point on the environmental contour surface will vary for differing response signals.

The results from the long term analyses can be used to locate the design point. Normally this would be done by a screening analysis along the contour surface. In this case these values are already computed and stored in the response surfaces. Estimated values for the mean extreme response, $\overline{X}_{3h}$, can be obtained by projecting the values from the response surface onto the environmental contour surface. The design point is found as the point on the environmental contour surface with the largest value of $\overline{X}_{3h}$. The projection process is shown in Figure 8.15 for wind speed 22m/s. The idea is that the value of the response at each of the red marks are stored together with the corresponding environmental coordinates from the contour surface, here represented by the blue line. If this process is repeated for every wind condition the complete environmental contour surface is obtained with projected values of $\overline{X}_{3h}$. The largest value on the surface is located together with the coordinates of Tp, Hs and W. In Figure 8.16 the 100-year environmental contour surface is shown with projected values of mean extreme response. The values of $\overline{X}_{3h}$ are represented by the color on the surface. As expected are the values of $\overline{X}_{3h}$ most dependent on Hs.

To see the location of the design point a cut through Figure 8.16 can be made at the wind value corresponding to the design point. This is shown in Figure 8.17. It is here seen that the design point is located very close to the highest level of Hs. The case of 50-year return period is also included. The 50-year and 100-year contour surfaces are relatively close to each other. The coordinates for all of the design points are presented in the next section.

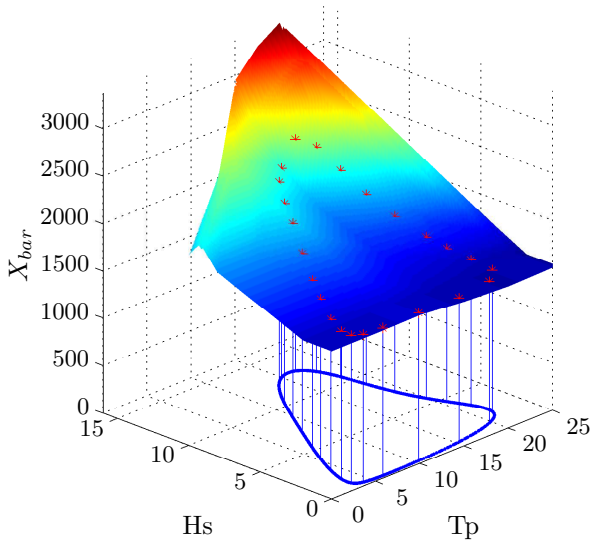

Figure 8.15: Representation of how the response surface is projected onto the environmental contour surface.

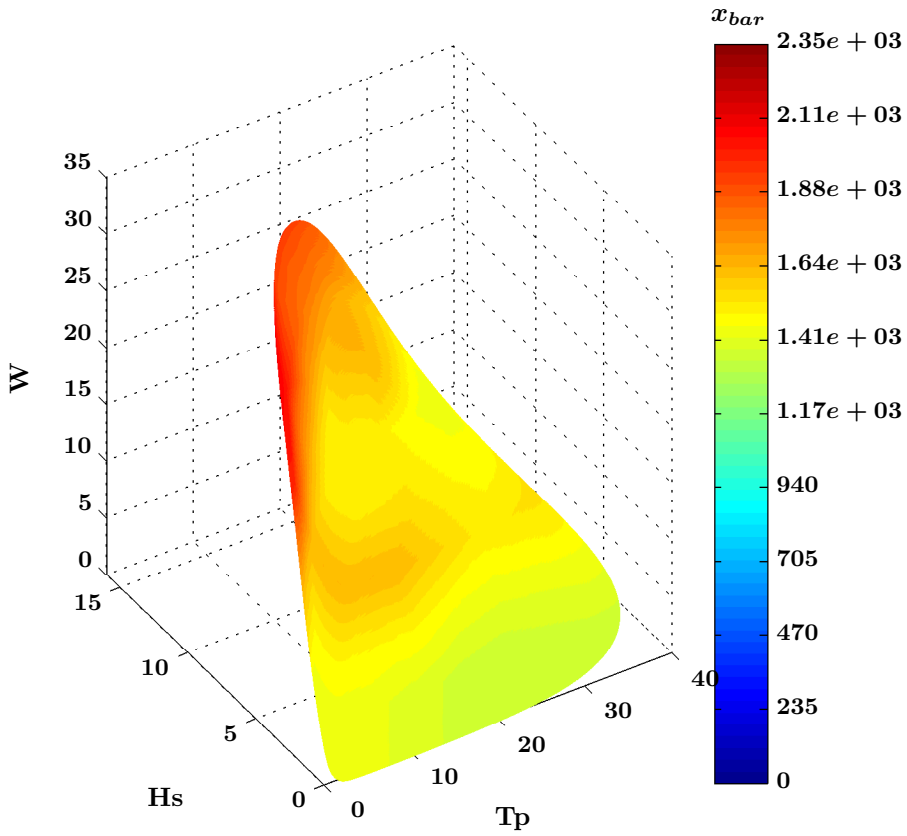

Figure 8.16: 100-year environmental contour surface with projected values of the mean response maxima, $\overline{X}_{3h}$.

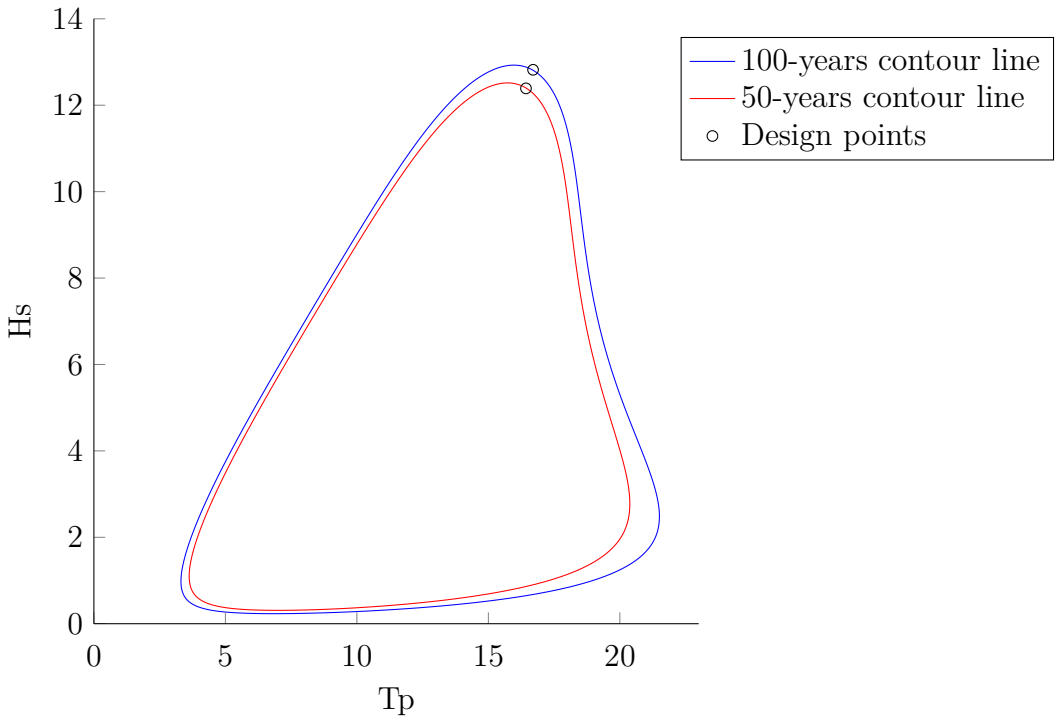

Figure 8.17: 50- and 100-year contour line with design points. Constant wind 22m/s

8.3.4 Response at Design Point

The environmental design point can be found for all of the three main mooring lines with the approach described in the preceding section. The parameter values at the design point and the values for the mean extreme response, $\overline{X_{3h}}$, are presented in Tables 8.2, 8.3 and 8.4.

Table 8.2: Environmental design point for mooring line 9.

Return period [years]	W	Hs	Tp	$\overline{X_{3h}}$
1	25.5	7.9	13.0	962
10	27.0	11.1	15.3	1059
50	27.3	12.6	16.7	1105
100	27.4	13.2	17.1	1131

Table 8.3: Environmental design point for mooring line 10.

Return period [years]	W	Hs	Tp	$\overline{X_{3h}}$
1	18.3	8.7	11.9	1993
10	22.0	11.3	15.7	2116
50	22.1	12.4	16.4	2349
100	22.1	12.8	16.7	2440

Table 8.4: Environmental design point for mooring line 11.

Return period [years]	W	Hs	Tp	$\overline{X_{3h}}$
1	19.1	9.3	13.5	1075
10	22.0	11.0	16.2	1133
50	22.0	11.8	17.2	1186
100	22.0	12.1	17.6	1206

From these tables it is seen that the largest mean extreme tension are found in mooring line 10. As mentioned before this is expected since the environmental loads are aligned with this line. By comparing the design points for mooring lines 9 and 11 it is seen that the design points occur for two different environmental conditions. This is surprising since the model is symmetric. This was also seen in the results of the long term analysis. Possible explanations for this have been discussed previously.

8.3.5 Detailed Analysis of Design Points

When the environmental design points are located for all important responses it is of interest to determine the short term distribution of the extreme response for these conditions. A detailed analysis of the design point can be carried out by doing a large number of simulations with the design point environmental parameters. In this work 40 realisations are simulated in the detail analysis. Based on this set of 40 simulations the Gumbel parameters are found

in the same manner as in Chapter 8.2.3. A Gumbel CDF is then obtained for the short term extreme response, X_{3h}, for the design point conditions, i.e. the design point distribution. By comparing this CDF to the extreme response value found in the long term analysis the corresponding percentile is found. The percentile value corresponds to the probability of not exceeding the extreme response value from the long term analysis in the design point distribution. The percentiles are only found for the 50- and 100-year cases for the main mooring lines. The other cases have not been included since the computational efforts required for each percentile value is extensive.

Table 8.5: Percentile in the design point extreme distribution corresponding to the true extreme response.

Percentiles		
Return period	50	100
Line 9	50.8%	44.8%
Line 10	69.5%	63.0%
Line 11	86.2%	84.5%

Some comments must be made concerning the presented percentile values. The percentile values are seen to span over a wide range, from 44.8% to 86.2%. It is seen that the percentile values are smaller for the 100-year cases than for the 50-year cases. This is not corresponding with the expectations for the percentile values. As it says in the introduction to this section the percentile levels are expected to increase with increasing return period. The reason for this behaviour is not really known but some suggestions will be discussed in the following Section 8.3.6.

The sensitivity of the percentile level is the subject of investigation in a study by Winterstein and Haver [9]. Here, a bootstrapping procedure has been carried out to investigate the variation of the percentile level. A Gumbel model is adopted as the true model for the three-hour maximum response values. The parameters are based on 24 model test runs. By reproducing 20 samples of size 24 with a Monte Carlo scheme it is here found that the true percentile level differs from 0.8 to 0.94 for the 20 samples. This shows that there is a significant uncertainty involved when estimating the true percentile level.

The estimation of percentile levels in this thesis is based on 40 simulations, but compared with the findings of Winterstein and Haver, even 40 simulations might be too few to obtain proper values for the percentile level.

8.3.6 Discussion of The Contour Line Method

It is of interest to compare the extreme response values found from the contour line analysis to the T-year response values found in the long term analysis. It is assumed that the T-year response found in the long term analysis is a good estimate of the correct T-year response value, and these values are therefore taken as the exact or true values. In Table 8.6 the response values from the contour line method are compared to those found in the long term

analysis, and the deviations between the two are presented. Negative values means that the response values from the contour line method are conservative, i.e. the contour line method overestimates the design values.

Table 8.6: Comparison of response values found at the environmental design point and with the long term analysis.

Line	Return period	Contour line method	Long Term Analysis	Deviation
9	50	1105	1091.0	-1.28%
	100	1131	1114.0	-1.50%
10	50	2349	2293.0	-2.39%
	100	2440	2390.0	-2.04%
11	50	1186	1157.0	-2.41%
	100	1206	1179.0	-2.24%

The largest deviation found in Table 8.6, is -2.41%. This means that the error by neglecting the short term variability in this case is small. To confirm this the Coefficient of Variation (COV), i.e. the ratio of s_{3h} and $\overline{X}_{3h}$ obtained from the long term analysis, is evaluated. For each of the analysed sea states a COV-value is obtained. For the main-mooring lines the maximum, minimum, average and the standard deviation of the COV-values are presented in Table 8.7.

Table 8.7: Representation of the COV for the mean maximum response, $\overline{X}_{3h}$, in the main-mooring lines.

Line	Maximum	Minimum	Average	Standard deviation
9	5.96%	0.23%	1.46%	1.12%
10	13.07%	0.32%	3.18%	2.65%
11	5.93%	0.20%	1.58%	1.19%

We see that the largest COV is found in mooring line 10 with a value of 13.07%. The largest mean value is also found for mooring line 10 with a value of 3.18%. It is noticed that the average values of the COV are small. This implies that the effect of neglecting the short term variability also will be small.

To elaborate the effect of the COV-value, on the short term variability, the Gumbel-PDF with parameters corresponding to a case with average COV-value is plotted in Figure 8.18a. It is seen from the figure that the PDF's range is between 2000kN and 2500kN. The median value of this distribution is 2163kN and the value corresponding to the 90%-percentile is 2265kN. This give an error of 4.7%. For the maximum case the median corresponds to a value of 2999kN, and the 90%-percentile corresponds to 3579kN. This is an error of 19.3%. The maximum case is plotted in Figure 8.18b.

Based on this it can be concluded that the tension in the main mooring lines is only slightly underestimated by the median value of the design point distribution. This is due to the apparently small short term variation in the system. This is in accordance with the importance factor presented previously. It must be emphasised that the under prediction

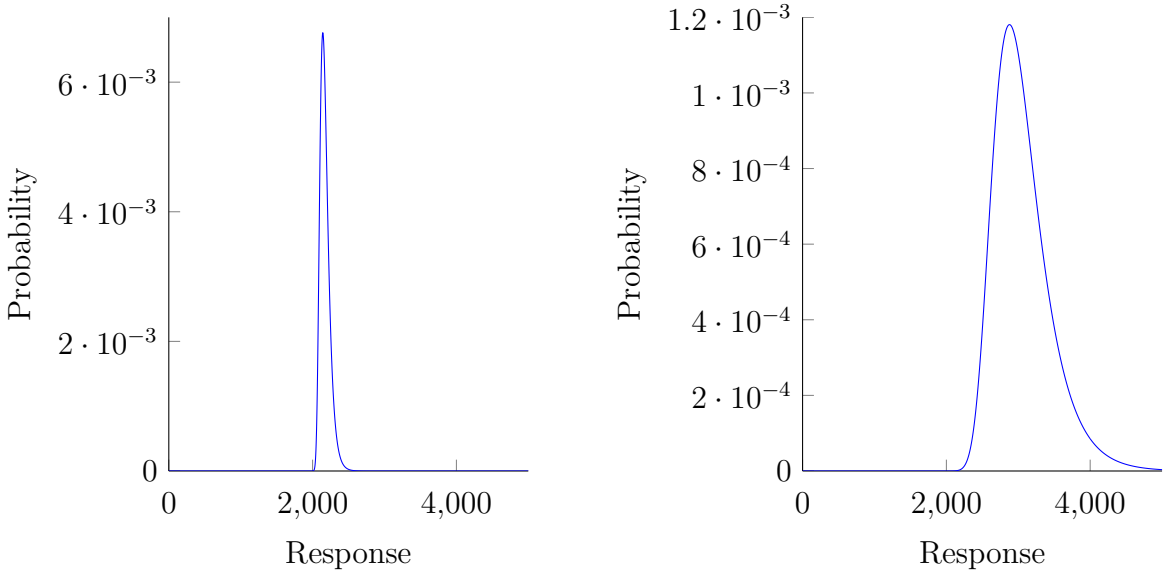

(a) Gumbel PDF with parameters corresponding to a mean value of the COV.

(b) Gumbel PDF with parameters corresponding to the maximum value of the COV.

Figure 8.18: Gumbel PDFs for two cases of different COV.

found for this case is smaller than what is suggested as general values by Haver [19]. A more thorough discussion of the contour line method's validity is therefore necessary.

For the contour line method to be fully trusted an important feature of the problem must be valid. This feature will be explained with reference to Figure 8.19. In this figure the mean extreme tension in mooring line 10, is plotted as a function of the mean wind velocity. The tension increases steadily from wind speeds of 0m/s to 17m/s. After this the tension decreases with increasing wind speeds until a wind speed value of 27m/s, before it again increases.

The observed behaviour of the mooring line tension in Figure 8.19 is due to the control system regulating the pitch on the wind turbine blades. As mention before in Chapter 4.5, the control system on Hywind Demo will optimise the pitch angle of the turbine blades with respect to maximising the electrical effect and minimising the structure's pitch motion. The sudden change in the tension line behaviour at wind speed 17m/s is caused by the change of operating regime in the control system.

With behaviour as seen in Figure 8.19, the design loads cannot be properly estimated from the contour line method. The problem arises since there is not a one-to-one relation in the function. This can be explained by a simple example.

Say that the contour line method shall be used to estimate the response value corresponding to a return period of 100-years for the process plotted in Figure 8.19. The 100-year combination is found to be the combination of the red line and a wind velocity of, say 24m/s. The 100-year design value would now be, according to the contour line method, the mean extreme environmental combination corresponding to this value in the figure, i.e. 1480kN. However, the tension peak is found to be 1660kN for a wind velocity of 17m/s. This

wind velocity only corresponds to the, 50-year return wind velocity. This means that the contour line method in this example would badly underestimate the 100-year return design load.

From Figure 8.19 it is also seen that the response process is not well modelled by the linear interpolation method used to obtain the curve. With a spline- or cubic-interpolation scheme the obtained curve would be continuous and thus be a better description of the problem. This implies that more wind conditions should have been included in the long term analysis. This has however no effect on the reason discussion of the contour line method.

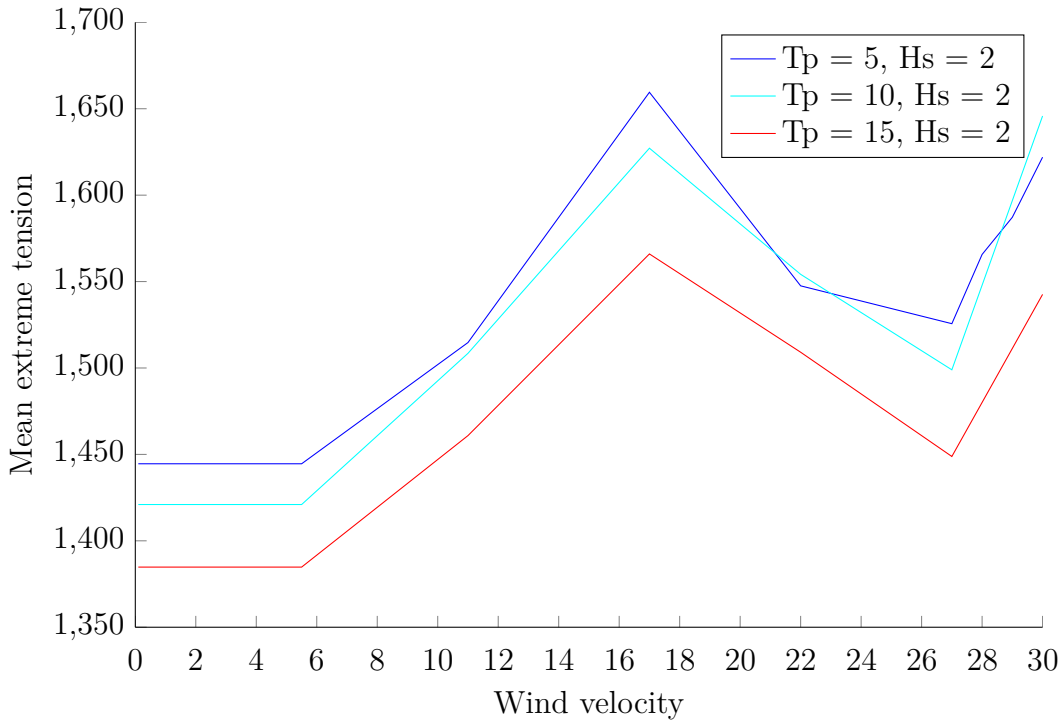

Figure 8.19: Tension in mooring line 10 as a function of mean wind velocity.

As a consequence of the discussed behaviour, application of the contour line method must said to be dubious. This is due to the non-monotonically increasing response history seen in Figure 8.19. This can be a possible explanation for the questionable percentile levels found for the mooring line tension. Even though the design tension value is only slightly underestimated by the extreme response median value, the reason discussion makes application of the environmental contour method doubtful for use on Hywind Demo. In general it must be advised to show extreme caution when applying the contour line method on any system where active control systems may affect the load properties.

9 Concluding Remarks

9.1 Conclusion

The extreme values of tension in the mooring lines on Hywind Demo are studied in this Master's thesis. To approach this problem a long term analysis is carried out and application of the contour line method is investigated. As a first step, a three-parameter environmental model has been further developed by calibrating it for the Hywind Demo location. The long term analysis and the contour line method both depend on proper environmental modelling so this is an important part of the thesis. The calibrated model shows good agreement with measurements of significant wave height from the Hywind Demo location.

Based on the calibrated environmental model the environmental contour surfaces are generated by means of the Rosenblatt transformation. When comparing contour surfaces for the two environmental models it is seen that the original model shows slightly worse weather conditions than the calibrated one. This is in accordance with expected behaviour.

A long term analysis for extreme response in a three hour period has been carried out. The analysis is based on 15 time-domain simulations for 172 different environmental conditions. Bootstrapping shows that 15 simulations for each environmental condition results in a rather wide range of possible response values. The long term design loads are calculated by solving the long term integral and by application of the inverse first order method. Good agreements are found when comparing the two approaches.

The environmental design point is defined as the combination of environmental parameters resulting in the worst short term extreme response. A detail analysis of the response at the design point gives a design point distribution. By comparing the median value of this distribution and the results from the long term analysis it is seen that the median value is slightly non-conservative estimate for the design response. For this to be true the short term response variation must be small. A thorough investigation of the statistical parameters in the short term distribution shows that this is in fact the case.

Unexpected values are obtained for the predicted percentile levels in the contour line method. To investigate this, the tension history is compared to the wind loading. It is found that the tension is not monotonically increasing with increasing wind velocities. For such cases, the design values can be severely underestimated by the contour line method. Based on this it is concluded that the environmental contour line method is not applicable to estimate design loads on Hywind Demo. In general it is advised to show extreme caution when applying the contour line method to structures with active control systems.

9.2 Recommendation for Further Work

An obvious drawback with this work is the lack of proper wind generation. The model used, describes uniform flow in the horizontal directions. It is expected that this will have a considerable impact on the results, especially regarding structural behaviour of the hull and tower. The effects on the response in the mooring lines are however expected to be small.

In later work it is recommended to use the direct link library available for combination with RIFLEX, to externally generate the wind field. It would also be of interest to further develop RIFLEX to include wind-structure interaction.

A linear interpolation scheme is used to generate the 3-dimensional response surfaces. In the Hs-Tp plane this seems to give a sufficient approximation, at least for environmental parameters within the 100-year contour. In the wind-plane the linear interpolation is found to be insufficient. Development of a 3-dimensional cubic interpolation scheme of scattered data in Matlab is therefore encouraged.

The response analysis in this work has been carried out with focus on the extreme tension in the mooring lines. More data are stored for each simulation, e.g. curvature in the tower and motions of the hull. As further work the long term analysis can be extended to include more responses.

During the life time of Hywind Demo considerable amounts of environmental- and response-data have been collected. It would be interesting to carry out a long term analysis based on these measurements and compare this to results from a long term analysis based on computer simulations.

Bibliography

[1] http://www.gtglobaltrader.com/news/britain-and-us-collaborate-floating-wind-turbines, des 2012.

[2] http://www.theengineer.co.uk/in-depth/the-big-story/wind-energy-gets-serial/1012449.article, des 2012.

[3] G. S. Baarholm, S. Haver, and O. D. Økland. Combining Contours of Significant Wave Height and Peak Period with Platform Response Distributions for Predicting Design Response. *Marine Structures*, 23(2):147 – 163, 2010.

[4] T.D. Hanson, B. Skaare, R. Yttervik, and F.G. Nielsen. Dynamic Response and Control of the Hywind Demo Floating Wind Turbine.

[5] T.D. Hanson, B. Skaare, and F.G. Nielsen. Importance of Control Strategies on Fatigue Life of Floating Wind Turbines. Proceeding of OMAE2007, 2007.

[6] T.D. Hanson, B. Skaare, R. Yttervik, F.G. Nielsen, and O. Havmøller. Comoparison of Measured Simulated Responses at the First Full Scale Floationg Wind Turbine Hywind.

[7] T. Hordvik. Design Analysis and Opimisation of Mooring System for Floating Wind Turbines. Master's thesis, NTNU, 2011.

[8] I. Moy. Parameter Sensitivity of Short-term Fatigue Damage of Spar-type Wind Turbine Tower. Master's thesis, NTNU, 2012.

[9] S. Haver and S. R. Winterstein. Environmental Contour Lines: A Method for Estimating Long Term Extremes by a Short Term Analysis. In *Society of Naval Architects and Marine Engineers*, pages 116–127, 2009.

[10] G. S. Baarholm and T. Moan. Application of Contour Line Method to Estimate Extreme Ship Hull Loads Considering Operational Restrictions. *Journal of Ship Research*, 2001.

[11] T. S. Meling, K. Johannessen, S. Haver, and K. Larsen. Mooring Analysis of a Semi-submersible by use of IFORM and Contour surfaces. In *Proceeding of ETCE/OMAE2000*. ASME, ASME, February 2000.

[12] K. Johannessen, T. S. Meling, and S. Haver. Joint Distribution for Wind and Waves in the Norhern North Sea. In *International Journal of Offshore and Polar Engineering*, volume 12. The international Society of Offshore and Polar Engineers, March 2002.

[13] M. Sathyajith. *Wind Energy Fundamentals*. Almas Schimmel, 2006.

[14] M. Rock and L. Parsons. Fact Sheet, Offshore Wind Energy. *Offshore Wind Energy*, 2010.

[15] EWEA. The European Offshore Wind Industry - key trends and statistics 1st half 2012. Technical report, EWEA, 2012.

[16] A.R. Henderson, B. Bulder, R. Huijsmans, J. Peeringa, J. Pierik, E. Snijders, M. van Hees, H. Wijnants, and M.J. Wolf. Feasibility study of floating windfarms in shallow offshore sites. *Wind Engineering*, 27(5):405 – 18, 2003.

[17] NORSOK Standard N-003 - Action and action effects, Sept. 2007.

[18] G. Gaudiosi J. Twidell, editor. *Offshore Wind Power*. Multi-science Publishing.

[19] S. K. Haver. Prediction of Characteristic Response for design purpose. 2011.

[20] O. M. Faltinsen. *Sea Loads on Ships and Offshore Structures*. Cambridge University, 1990.

[21] SIMO project team. SIMO - Theory Manual Version 3.7, 2010.

[22] RIFLEX User Manual.

[23] C. P. Sparks. *Fundamentals of Marine Riser Mechanics*. PennWell Corporation, 2007.

[24] M. Mathiesen E. Nygaard. *Hywind Metocean Design Basis*. Statiol ASA, Des 2008. Internal Statoil document.

[25] Det Norske Veritas. OFFSHORE STANDARD, DNV-OS-E301 - POSITIONING MOORING, 2010.

[26] P.A. Brodtkorb, P. Johannesson, G. Lindgren, I. Rychlik, J. Rydén, and E. Sjö. *WAFO - a Matlab Toolbox for the Analysis of Random Waves and Loads*, volume 3. 2000.

A Analysed Sea States

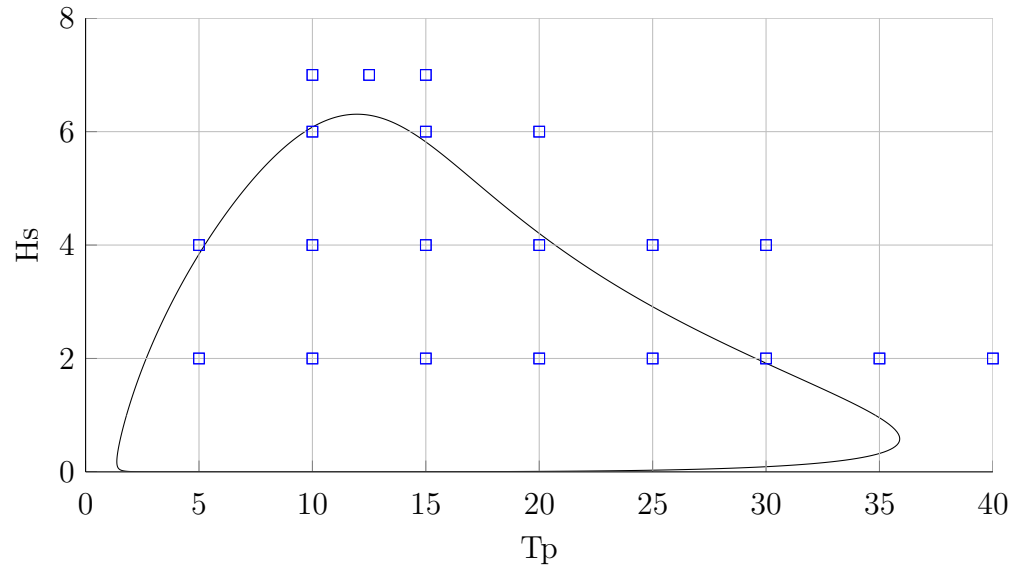

Figure A.1: Contour line for given wind speed 5m/s and selected analyses points.

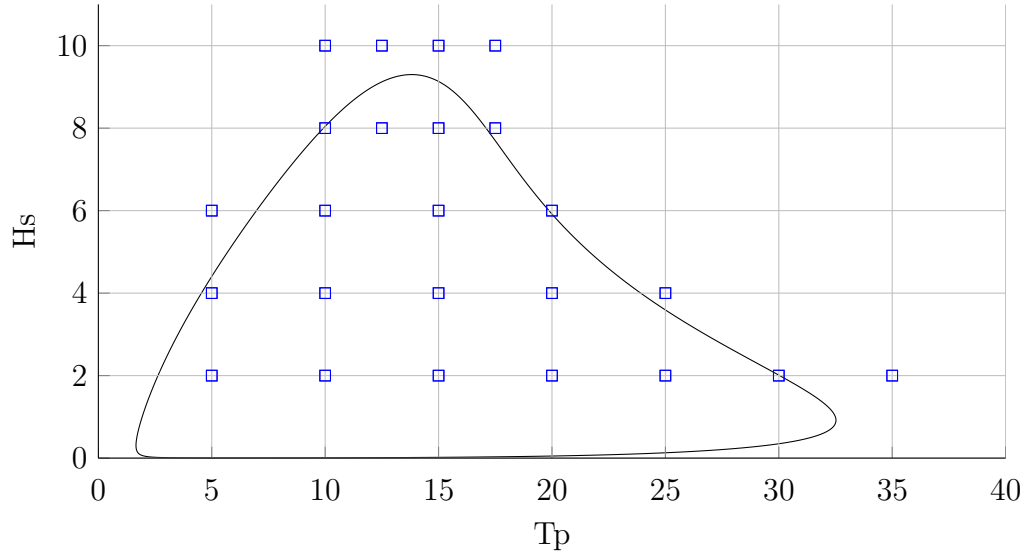

Figure A.2: Contour line for given wind speed 11m/s and selected analyses points.

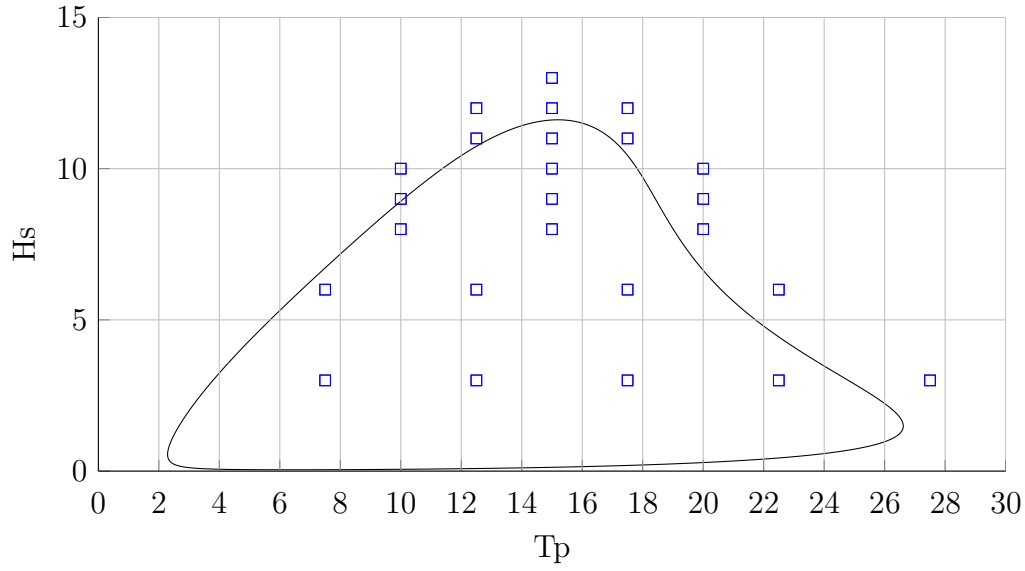

Figure A.3: Contour line for given wind speed 17m/s and selected analyses points.

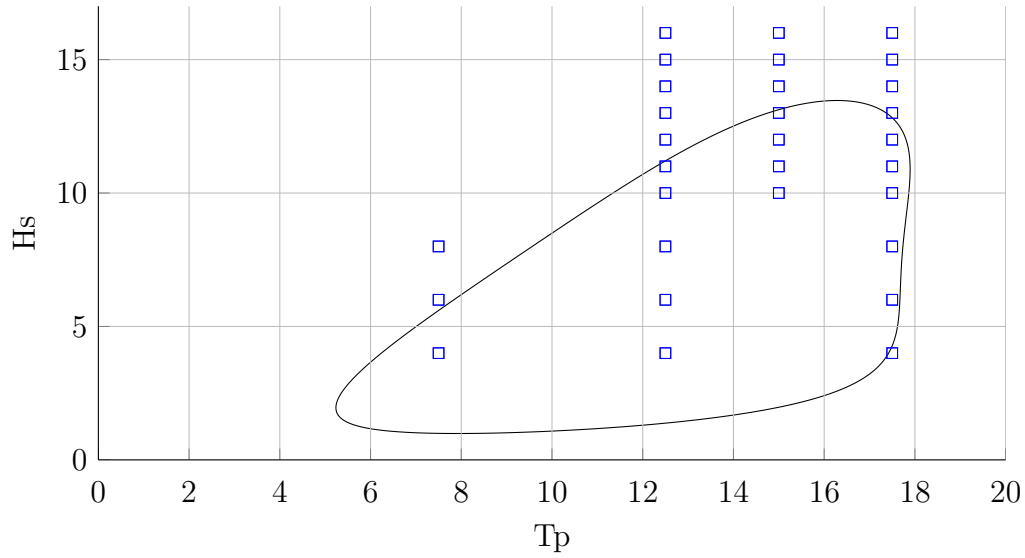

Figure A.4: Contour line for given wind speed 27m/s and selected analyses points.

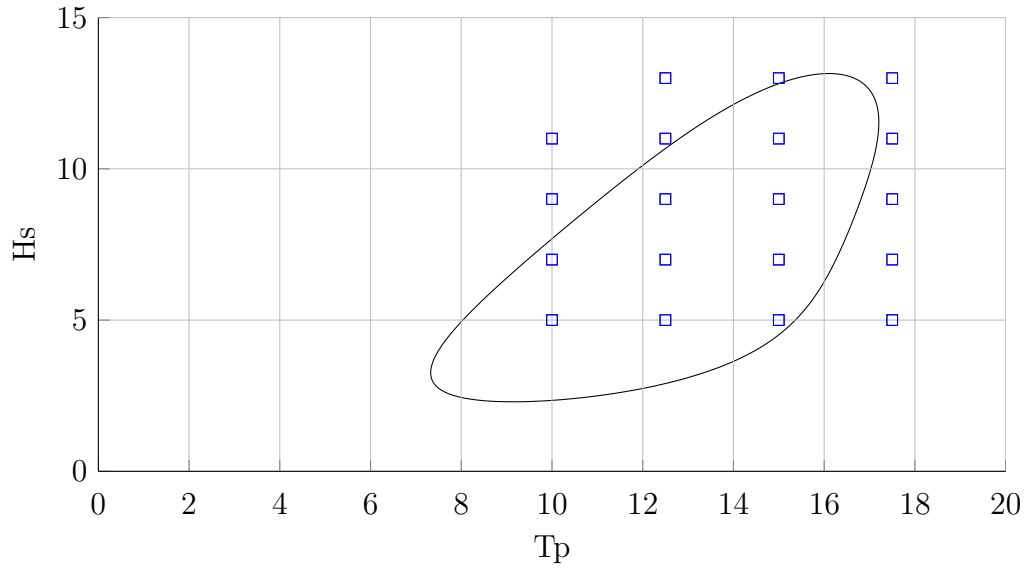

Figure A.5: Contour line for given wind speed 30m/s and selected analyses points.

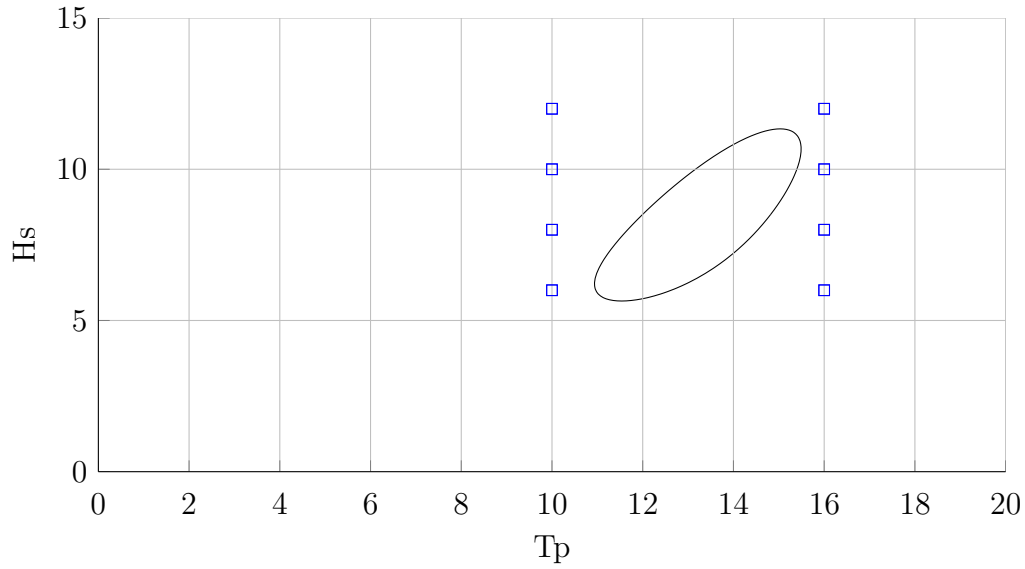

Figure A.6: Contour line for given wind speed 33m/s and selected analyses points.

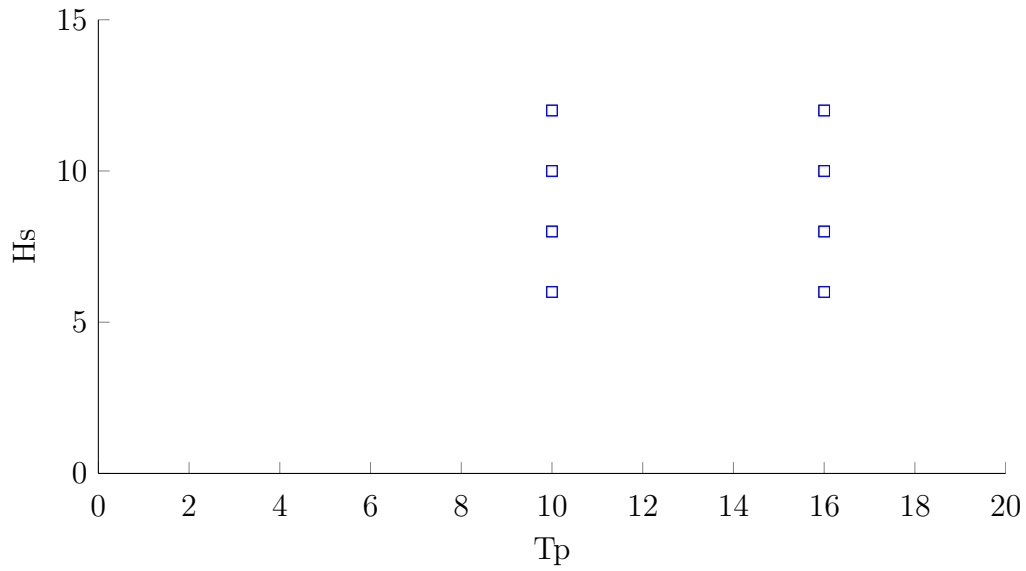

Figure A.7: Analyses points for wind speed 35m/s. The contour surface is non existing on mean wind speed 35m/s, but the points are included in the analyses to ensure that the contour surface is enclosed also with respect to the wind parameter.

B Convergence Study

Table B.1: Maximum deviation between the analyses in the convergence study.

Motion	Time-increment	Value	Deviation	Computer time [s]
Heave	0.05	0.0989	-21.13 %	239
	0.02	0.1165	-7.10 %	355
	0.01	0.1206	-3.83 %	731
	0.005	0.1254	Exact	1092
Sway	0.05	2.0748	19.70 %	239
	0.02	1.8612	7.38 %	355
	0.01	1.803	4.02 %	731
	0.005	1.7333	Exact	1092
Roll	0.05	0.0941	-53.85 %	239
	0.02	0.1652	-18.98 %	355
	0.01	0.1826	-10.45 %	731
	0.005	0.2039	Exact	1092

C Results of The Reliability Analysis

C.1 Long Term Formulation

Table C.1: Response values with return period 1-, 10-, 50-, and 100-years, for the mooring- and delta-lines.

Axial response [kN]					
Return periods		1	10	50	100
Line	9	959	1044	1091	1114
	10	1986	2130	2293	2390
	11	1071	1115	1157	1179
Delta line	3	629	701	755	777
	4	828	919	969	988
	5	1271	1391	1477	1515
	6	1075	1163	1259	1311
	7	835	872	896	906
	8	627	673	724	747

C.2 IFORM

Table C.2: 50- and 100-year return load ans importance factor in anchor line 9.

	Design point				Importance factor			
Return period	1	10	50	100	1	10	50	100
W	25.5	27.0	27.4	27.8	94.5 %	78.4 %	68.1 %	65.5 %
Hs	8.0	11.0	12.2	12.8	5.0 %	19.9 %	24.5 %	27.4 %
Tp	13.0	15.1	16.2	16.9	0.0 %	0.3 %	1.5 %	1.9 %
Response	962	1059	1115	1147	0.5 %	1.4 %	5.9 %	5.2 %

Table C.3: 50- and 100-year return load and importance factor in anchor line 10.

	Design point				Importance factor			
Return period	1	10	50	100	1	10	50	100
W	17.0	17.3	22.0	22.4	34.0 %	24.4 %	40.6 %	39.7 %
Hs	7.8	8.8	12.1	12.5	40.1 %	43.7 %	53.1 %	52.7 %
Tp	11.4	12.2	16.2	16.4	9.0 %	6.6 %	1.7 %	1.6 %
Response	2028	2154	2386	2498	17.0 %	25.3 %	4.5 %	6.0 %

Table C.4: 50- and 100-year return load and importance factor in anchor line 11.

	Design point				Importance factor			
Return period	1	10	50	100	1	10	50	100
W	17.4	22.0	22.1	22.0	36.1 %	48.6 %	41.1 %	38.1 %
Hs	8.4	11.0	11.1	11.6	48.4 %	45.0 %	42.7 %	43.2 %
Tp	12.7	15.9	16.9	17.1	1.3 %	4.1 %	8.1 %	9.4 %
Response	1083	1135	1197	1226	14.2 %	2.3 %	8.1 %	9.4 %

Table C.5: Design point and importance factor for the delta lines with return period 1 year.

Design point				
Line	W	Hs	Tp	Response
3	20.29	9.04	14.15	618.25
4	24.29	8.79	13.50	828.55
5	17.60	8.30	12.19	1317.19
6	5.50	1.20	12.27	1095.57
7	21.31	8.68	13.99	854.76
8	5.50	1.13	10.93	632.42

Importance factor				
Line	W	Hs	Tp	Response
3	54.5 %	38.7 %	1.1 %	5.6 %
4	85.4 %	13.8 %	0.0 %	0.8 %
5	35.9 %	46.6 %	4.8 %	12.7 %
6	0.6 %	0.1 %	9.5 %	89.8 %
7	61.7 %	27.0 %	1.3 %	10.0 %
8	0.6 %	0.3 %	7.7 %	91.4 %

Table C.6: Design point and importance factor for the delta lines with return period 10 years.

Design point				
Line	W	Hs	Tp	Response
3	24.44	11.06	15.62	698.41
4	26.95	11.06	14.73	934.55
5	17.35	9.18	12.72	1452.11
6	20.78	10.92	14.98	1175.11
7	22.01	10.98	15.11	896.30
8	25.92	11.02	15.84	665.76

Importance factor				
Line	W	Hs	Tp	Response
3	62.4 %	31.2 %	2.2 %	4.2 %
4	78.1 %	20.5 %	0.1 %	1.3 %
5	24.8 %	49.2 %	5.4 %	20.6 %
6	42.2 %	51.2 %	0.0 %	6.6 %
7	48.6 %	44.6 %	0.3 %	6.5 %
8	65.5 %	31.3 %	2.2 %	1.1 %

Table C.7: Design point and importance factor for the delta lines with return period 50-years.

Design point				
Line	W	Hs	Tp	Response
3	26.10	12.15	16.49	798
4	26.95	11.97	15.14	1044
5	22.01	12.14	16.01	1523
6	21.98	11.87	15.75	1387
7	20.60	11.04	14.12	930
8	25.16	11.88	17.23	763

Importance factor				
Line	W	Hs	Tp	Response
3	60.9 %	30.5 %	2.8 %	5.7 %
4	65.5 %	25.1 %	0.9 %	8.5 %
5	40.8 %	47.0 %	1.8 %	10.4 %
6	40.6 %	49.7 %	0.5 %	9.1 %
7	34.5 %	45.7 %	1.9 %	17.8 %
8	54.7 %	32.9 %	8.3 %	4.1 %

Table C.8: Design point and importance factor for the delta lines with return period 100-years.

Design point				
Line	W	Hs	Tp	Response
3	26.16	12.25	16.55	822
4	27.77	11.91	14.56	1055
5	17.01	9.65	12.74	1642
6	21.89	12.15	16.01	1439
7	20.30	10.93	13.92	936
8	24.67	12.26	17.37	794

Importance factor				
Line	W	Hs	Tp	Response
3	57.0 %	29.4 %	2.8 %	10.8 %
4	66.5 %	16.8 %	0.4 %	16.4 %
5	19.4 %	34.0 %	6.8 %	39.8 %
6	37.6 %	51.1 %	0.8 %	10.6 %
7	31.1 %	43.9 %	2.4 %	22.5 %
8	50.0 %	35.6 %	9.4 %	5.0 %

C.3 Comparison of The Long Term Approach and The IFORM

Table C.9: Percentage deviation between the long term integral and the IFORM analysis.

		Deviation			
Return period [year]		1	10	50	100
Line	9	0.31 %	1.44 %	2.20 %	2.96 %
	10	2.11 %	1.13 %	4.06 %	4.52 %
	11	1.12 %	1.79 %	3.46 %	3.99 %
Mean		1.18 %	1.45 %	3.24 %	3.82 %
Delta Line	3	-1.75 %	-0.43 %	5.70 %	5.79 %
	4	0.12 %	1.74 %	7.74 %	6.78 %
	5	3.62 %	4.39 %	3.11 %	8.38 %
	6	1.95 %	1.03 %	10.17 %	9.76 %
	7	2.40 %	2.75 %	3.79 %	3.31 %
	8	0.80 %	-3.90 %	5.39 %	6.29 %
Mean		1.19 %	0.93 %	5.98 %	6.72 %

D Digital Appendix

A digital appendix is attached to this work and is handed in as part of the thesis. The digital appendix includes two folders, one for the reliability analysis and one with the SIMA model.

D.1 Reliability Analysis

In the folder, "Appendix-1", are the Matlab routines containing the reliability analysis included. The files found in the "Appendix-1" are presented below with a short description.

post_pro.m	This is the main post processor. This routine reads the binary data from the RIFLEX-analyses and extracts the extreme maximum from each time-series. The computed values are stored in for_reg_full_2904.mat. This file is not possible to run.
for_reg_full_2904.mat	This mat-file contains the results of the post processor. The statistical parameters calculated for each sea state are store in this file for further use in the reliability analysis.
Main.m	This is the main file of the reliability analysis. This main-file calls the other routines as functions. The lines and return periods to run analysis for are given as input to this routine.
Make_dir.m	This routine organizes the results into folders.
Interpolation.m	The interpolation scheme are carried out in this routine and stored for use by the other routines.
Long_term.m	This routine carries out the long term integral and stores the results to an excel-file.
simps.m	This is a routine from the Matlab-file exchange doing numerical integration.
IFORM.m	This routine carry out the IFORM procedure and store the result to an excel-file.

Some additional files are also included in the folder. They are functions used for statistical computation and originate from the WAFO toolbox. WAFO is a toolbox containing Matlab routines for statistical analysis and simulation of random waves and loads. The toolbox is developed at the Center of Mathematics at Lund University and is a freely distribute software [26]. In this work WAFO is used to calculate statistical distributions and to perform mathematical operations like determining local turning points.

It is possible to run the reliability analysis in Matlab, from the included path. The analysis is started from the main file.

D.2 SIMA Model

The SIMA model is also included as a digital file in "Appendix-2". To open this file the latest version of SIMA is needed.

E Matlab

E.1 CDF-iteration

```
%CDFiter.m
%
%This routine is used to calibrate the environmental model.
clear all
clc
format shortg
%%
%INPUT
for i  = 1
%Parameters from Hywind Metocean data table 3.5
bettaHs = 1.192;
rhoHs = 1.612;
etaHs = 3.133;
alphaHs = 0.650;
tettaHs = 0.345;
a1 = 1.780;
a2 = 0.290;
a3 = 0.48;
b1 = 0.005;
b2 = 0.150;
b3 = 0.370;

%Wind parameters - Haver
gammaW_haver = 1.708;    %Shape
bettaW_haver = 8.426;    %Scale

%Wind parameters - Hywind
gammaW = 1.770; %Shape
bettaW = 8.078; %Scale

%Step size wind
k = 0.1;
%Range hs
n = 15;
%Range wind
m = 40;
%Step size hs
q = k*n/m;

%Interval hs:
hs = 0:0.02:15;
end

%%
%OUTPUT

%Set variable to enter while-loop
residual = 200;

%Environmental values
%Start value - a
```

```
a = 0.135;
%New value - a
a = 0.0647;
%Start value - b
b = 0.1;
%New value - b
b = 0.0927;
%Start value - c
c = 2.0;
%New value - c
c = 1.2132;
%Start value - d
d = 1.8;
%New value - d
d = 0.3912;
%Start value - e
e = 1.322;
%New value - e
e = 1.3113;

variable = a;
variable = variable - 0.007;
% if 1
while residual>0.001
count = 0;
increment = 0.0001;
    variable = variable + increment;
    d = variable;
    for i = 0:0.05:40
    count = count + 1;

    alphaH = c + a*i;
    bettaH = d + b*(i^e);

    F_pre(count,:) = wblcdf(hs,bettaH,alphaH)*wblpdf(i,bettaW,gammaW);

    end

%New distribution
F = trapz(F_pre)*(i/count);
%Original distribution
PHS = wblcdf(hs,rhoHs,bettaHs);
%Residual
res = F - PHS;
%Length of residual vector
l_r = length(res);
%Sum of squared residual
RES_ny = sum(res.^2);
%Store only the value giving the smallest residual
if RES_ny<residual
    A=a;
    B=b;
    C=c;
    D=d;
    E=e;
    residual = RES_ny;
end
```

```
109
110 RES = RES_ny;
111 %%
112 %Plot of the distribution with new parameters
113 plot(hs,F,hs,PHS)
114 title('CDF')
115 xlabel('Hs')
116 ylabel('Propability')
117 legend('Integrated','Model')
118 end
```

E.2 Contour Surfaces

```
1  %This routine calculates the contour surface of a wind and sea environment
2  %for a given return period.
3  clear all
4  clc
5  %Flags are used to manage the program, e.g. flag.plot = 1 asks the routine
6  %to plot figures.
7  flag.plot = 1;
8  flag.store = 1;
9  %%%%%%%%%%%%%%%%%%%%%%%%%%%%%%%%%%%%%%%%%%%%%%%%%%%%%%%%%%%%%%%%%%%%%%%%%%%%
10 %Start timer
11 tic
12 %Number of steps arround a sphere.
13 n = 250;
14 %Return period, [years]
15 R = 100;
16 %k-hour seastate, [hours]
17 k = 3;
18 %Number of k-hour seastates in the return period R
19 r = R*365*24/k;
20 %Probability of exceedance in an arbitrary k-hour period
21 p = 1/r;
22 %Radius in the normalized u-space, Reliability Index
23 betta = -norminv(p);
24 %%
25 %Wind parameters
26 gammaW = 1.770; %Shape
27 bettaW = 8.078; %Scale
28
29 %Parameters from Hywind Metocean data
30 bettaHs = 1.192;
31 rhoHs = 1.612;
32 etaHs = 3.133;
33 alphaHs = 0.650;
34 tettaHs = 0.345;
35 a1 = 1.780;
36 a2 = 0.290;
37 a3 = 0.48;
38 b1 = 0.005;
39 b2 = 0.150;
40 b3 = 0.370;
41
```

```
%Dummy conting variables used in the for-loop
count1 = 0;
count3 = 0;

%Looping around the surface of a sphere
for tetta = 0:pi/n:pi

    count1 = 1 + count1;
    count2 = 0;

    for phi = 0:pi/n:2*pi

        count2 = 1 + count2;
        count3 = 1 + count3;

        %Coordinates in the U-space
        u1 = betta * cos(tetta) * sin(phi);
        u2 = betta * sin(tetta) * sin(phi);
        u3 = betta * cos(phi);

        %Storing U-values
        U1(count1,count2) = u1;
        U2(count1,count2) = u2;
        U3(count1,count2) = u3;

        %Wind
        w = wblinv(normcdf(u1),bettaW,gammaW);

        %Wave height

        %Values for Johannessen's environmental model
%         alphaH = 2 + 0.135*w;
%         bettaH = 1.8 + 0.1*w^1.322;
        %Values for the calibrated environmental model
        alphaH = 1.2132 + 0.0647*w;
        bettaH = 0.3912 + 0.0927*w^1.3113;

        hs = wblinv(normcdf(u2),bettaH,alphaH);


        %Period

        %Peak period parameters
        mu = a1 + a2*(hs^a3);
        sigma = sqrt(b1 + b2 * exp(-b3*hs));

        t = logninv(normcdf(u3),mu,sigma);

        %Storing values
        W(count1,count2) = w;
        H(count1,count2) = hs;
        T(count1,count2) = t;


    end

end
```

```
99
100 contour = [T',H',W'];
101
102 %Set domain for the environmental parameters
103 h_axis = 0:0.5:15;
104 t_axis = 0:0.5:20;
105 w_axis = 0:0.5:40;
106 %%
107 %Plot
108 if flag.plot
109
110 w_elevation = 35; % Other wind values: 5.5 11 17 22 27 30
111 h = contour3(T',H',W',[w_elevation w_elevation],'k');
112
113 %Alternative plot
114 % contour3(T',H',W',[5.5 11 17 22 27 30])
115
116
117 %Alternative plot
118 %      figure('color','white');
119 %     c = W;
120 %     k = hypot(T,H)<1000;
121 %
122 %     plot3k({T(k)' H(k)' W(k)'},...
123 %         'ColorData',c,'ColorRange',[0 max(max(W))],'Marker',{'o',3},...
124 %         'Labels',{'','Tp','Hs','W','W'},...
125 %         'PlotProps',{'FontSize',12});
126 % view(-50,45)
127
128 title(['Analysed sea states' num2str(w_elevation)])
129 xlabel('Tp')
130 ylabel('Hs','rot',0)
131 zlabel('W','rot',0)
132 view(2)
133 hold on
134 longtermpoints(w_elevation);
135 axis([0 20 0 15])
136 hold off
137 end
138 %%
139 %Store the contour surface to mat-file
140 if flag.store
141     name = strcat('contour',num2str(R),num2str(n),'.mat');
142     filename3 = fullfile('D:\contour\',name);
143     if exist(filename3,'file')
144         delete(filename3)
145     end
146     matobj = matfile(filename3,'Writable',true);
147     matobj.H = H';
148     matobj.W = W';
149     matobj.T = T';
150 end
151
152 %End timer
153 toc
```

E.3 IFORM

```
function[MAT] = IFORM(flag,in)
%This routine performes the IFROM procedure
%%%%%%%%%%%%%%%%%%%%%%%%%%%%%%%%%%%%%%%%%%%%%%%%%%%%%%%%%%%%%%%%%%%%%%%%%%%%%%%
%Flags
flag_store = flag.store;
%Interpolation path
vq_path = in.target_path;%
%Target path
target_path = in.target_path;%
%Line to calculate:
line = in.line; %
%Type of response to evaluate:
response = in.response; %
%Load Gumbel parameters calculated by Interpolation.m
name = strcat(line,'_',response,'_','beta.mat');
matobj = matfile(fullfile(vq_path,name));
F_beta = matobj.F;

name = strcat(line,'_',response,'_','mu.mat');
matobj = matfile(fullfile(vq_path,name));
F_mu = matobj.F;

%Return period, [years]
R = in.return_period;
%k-hour seastate, [hours]
k = 3;
%Number of k-hour seastates in the return period R
r = R*365*24/k;
%Probability of exceedance in an arbitrary k-hour period
p = 1/r;
%Radius in the normalized u-space
betta = -norminv(p);
%Wind parameters
gammaW = 1.770; %Shape
bettaW = 8.078; %Scale

%Parameters from Hywind Metocean data
bettaHs = 1.192;
rhoHs = 1.612;
etaHs = 3.133;
alphaHs = 0.650;
tettaHs = 0.345;
a1 = 1.780;
a2 = 0.290;
a3 = 0.48;
b1 = 0.005;
b2 = 0.150;
b3 = 0.370;

%Dummy conting variables used in the for-loop
count1 = 0;
count4 = 0;
```

```
53
54 %Number of steps arround a sphere.
55 step = pi/8;
56 %Setting size of matrices
57 DP = zeros(1,4);
58 PEAK = 0;
59 %Iterate to find max response
60 for phi1 = step:step:2*pi;
61     disp(phi1)
62 for phi2 = 0:step:pi;
63 for phi3 = 0:step:pi;
64
65     %Angular step length arround the sphere
66     phi_step = 0.4*step;
67     %Inital values
68     res_last = -1;
69     res = 1;
70     go_direction = 1;
71     add = 0;
72     loop = 1;
73     count_red_1 = 0; count_red_2 = 0; count_red_3 = 0;
74     %Start iteration
75     while loop > 0
76
77         count4 = count4 + 1;
78
79         %Choise of step direction
80         if go_direction == 1
81             phi1 = phi1 + phi_step;
82         elseif go_direction == 2
83             phi2 = phi2 + phi_step;
84         elseif go_direction == 3
85             phi3 = phi3 + phi_step;
86         end
87
88         %Start position
89         u1 = betta * cos(phi1);
90         u2 = betta * sin(phi1) * cos(phi2);
91         u3 = betta * sin(phi1) * sin(phi2) * cos(phi3);
92         u4 = betta * sin(phi1) * sin(phi2) * sin(phi3);
93
94         %Wind
95         w = wblinv(normcdf(u1),bettaW,gammaW);
96
97         %Wave height
98         alphaH = 1.2132 + 0.0647*w;
99         bettaH = 0.3912 + 0.0927*w^1.3113;
100
101        hs = wblinv(normcdf(u2),bettaH,alphaH);
102
103        %Period
104        mu = a1 + a2*(hs^a3);
105        sigma = sqrt(b1 + b2 * exp(-b3*hs));
106
107        tp = logninv(normcdf(u3),mu,sigma);
108
109        %Response
```

```
110         BETA = F_beta(tp,hs,w);
111         MU = F_mu(tp,hs,w);
112 
113         res_ny = invgumb(normcdf(u4),BETA,MU);
114 
115         %Storing values
116         MAT(count4,:) = [w hs tp res_ny];
117 
118         %The following if-sentences decides whether the largeset response ...
                value
119         %is found or not. If not is the step size reduced and direction
120         %changed
121         if res_ny>res_last
122             res_last = res;
123             res = res_ny;
124             count_red = 0;
125         elseif res_ny≤res_last
126             if go_direction == 1
127                 phi1 = phi1 - phi_step;
128                 add = 1;
129                 count_red_1 = 1;
130             elseif go_direction == 2
131                 phi2 = phi2 - phi_step;
132                 add = 1;
133                 count_red_2 = 1;
134             elseif go_direction == 3
135                 phi3 = phi3 - phi_step;
136                 add = -2;
137                 count_red_3 = 1;
138             end
139         end
140 
141         go_direction = go_direction + add;
142         add = 0;
143 
144         %Enters if and only if STEP in all three directions results in
145         %smaller response.
146         if count_red_1 && count_red_2 && count_red_3
147             phi_step = phi_step/10;
148             count_red_1 = 0; count_red_2 = 0; count_red_3 = 0;
149             %If phi_step gets smaller than limit and no higher point can be
150             %reached, iteration stops.
151             if phi_step < 10e-5
152                 loop = -1;
153             end
154         end
155 
156         %Store peak-value for this startingpoint
157         if res_ny>DP(4)
158             DP = [w hs tp res_ny];
159         end
160 
161     end
162 %Store largest peak-value
163 if PEAK<res_ny
164 PEAK = res_ny;
165 display(PEAK)
```

```
 U_w = u1; U_hs = u2; U_tp = u3; U_res = u4;
end
end
end
end

%%
%Computation of new reliability index
beta_dp = sqrt(U_w^2 + U_hs^2 + U_tp^2); iform.beta_dp = beta_dp;
p_dp = normcdf(-beta_dp);
r_dp = 1/p_dp;
R_dp = r_dp/365/8; iform.R_dp = R_dp;
%Computation of importance factor
imp_factor = [U_w^2/betta^2 U_hs^2/betta^2 U_tp^2/betta^2 U_res^2/betta^2];
iform.imp_factor = imp_factor;
iform.MAT = MAT;

B{1,1} = 'Variable'; B{1,2} = 'Design point';
B{2,1} = 'W'; B{2,2} = DP(1);
B{3,1} = 'Hs'; B{3,2} = DP(2);
B{4,1} = 'Tp'; B{4,2} = DP(3);
B{5,1} = 'Response'; B{5,2} = DP(4);

B{1,4} = 'Importance factor'; B{2,4} = imp_factor(1); B{3,4} = imp_factor(2);
B{4,4} = imp_factor(3); B{5,4} = imp_factor(4);

B{7,1} = 'Return period'; B{7,2} = R;
B{8,1} = 'New return period'; B{8,2} = R_dp;
%%
%Storing results to file
if flag_store
    name2 = strcat('IFORM2','.mat');
    filename = fullfile(target_path,name2);
    matobj = matfile(filename,'Writable',true);
    matobj.IFORM = iform;
    filename = strcat('IFORM Design Point.xls');
    xlswrite(filename, B);
    movefile(filename,target_path)
end
```

E.4 Monte Carlo Wind Scaling

```
clear all
clc
%Input
for i  = 1
%Parameters from Hywind Metocean data table 3.5
bettaHs = 1.192;
rhoHs = 1.612;
etaHs = 3.133;
alphaHs = 0.650;
tettaHs = 0.345;
a1 = 1.780;
a2 = 0.290;
```

```
a3 = 0.48;
b1 = 0.005;
b2 = 0.150;
b3 = 0.370;

%Wind parameters - Haver
gammaW_haver = 1.708;    %Shape
bettaW_haver = 8.426;    %Scale

%Wind parameters - Hywind
gammaW = 1.770; %Shape
bettaW = 10.541; %Scale

%Step size wind
k = 0.1;
%length hs
n = 15;
%length wind
m = 40;
%Step size hs
q = k*n/m;

%Interval Hs
hs = 0:0.02:15;
end
%%
for i = 1:1000;
    r = rand();
    w = wblinv(r,bettaW,gammaW);
    ww = w/((65/10)^(1/7));
    WW(i) = ww;
end

A = createFit1(WW);

bettaW = A.a; %Shape
gammaW = A.b; %Scale

w = 0:0.1:40;
W = wblpdf(w,bettaW,gammaW);

WW = wblpdf(w,bettaW_haver,gammaW_haver);

plot(w,W,w,WW,'r');
legend('Hywind','Haver')
title('Wind-distribution')
xlabel('Wind velocity')
ylabel('Probability')
```